Aus der Klinik und Poliklinik für Radioonkologie, Cyberknife-und Strahlentherapie
der Universität zu Köln
Kommissarischer Direktor: Dr. Johannes Rosenbrock

The Effect of Prescription Dose and Dose Fractionation on the Abscopal Effect in a Mouse Model of Non-small Cell Lung Cancer

Inaugural-Dissertation zur Erlangung der Doktorwürde
der Medizinischen Fakultät
der Universität zu Köln

vorgelegt von
Jiali Cai
aus Hennan, China

promoviert am 27.September 2023

Gedruckt mit Genehmigung der Medizinischen Fakultät der Universität zu Köln

2023

Dekan: Universitätsprofessor Dr. med. G. R. Fink
1. Gutachter: Privatdozent Dr. med. J. M. G. A. Herter
2. Gutachterin: Universitätsprofessorin PhD C. M. Niessen

Erklärung

Ich erkläre hiermit, dass ich die vorliegende Dissertationsschrift ohne unzulässige Hilfe Dritter und ohne Benutzung anderer als der angegebenen Hilfsmittel angefertigt habe; die aus fremden Quellen direkt oder indirekt übernommenen Gedanken sind als solche kenntlich gemacht.

Bei der Auswahl und Auswertung des Materials sowie bei der Herstellung des Manuskriptes habe ich Unterstützungsleistungen von folgenden Personen erhalten:

Privatdozent Dr. med. J. M. G. A. Herter
Dr. Mayer
Dr. Kiljan
Postdoktorandin Gökcen Gözüm

Weitere Personen waren an der Erstellung der vorliegenden Arbeit nicht beteiligt. Insbesondere habe ich nicht die Hilfe einer Promotionsberaterin/eines Promotionsberaters in Anspruch genommen.

Die Dissertationsschrift wurde von mir bisher weder im Inland noch im Ausland in gleicher oder ähnlicher Form einer anderen Prüfungsbehörde vorgelegt.

Die in dieser Arbeit angegebenen Experimente sind nach entsprechender Anleitung durch PD Dr. med Jan Herter von mir Selbst ausgeführt worden.

Für den Strahlentherapie-Teil möchte ich Dr. Mayer und ihr Team für ihre Unterstützung bei der Bereitstellung von Positionierungs- und Bestrahlungsplanungsdiensten danken.

Die verbleibenden Teile der Experimente wurden vollständig von mir persönlich durchgeführt, einschließlich der Bewertung der Tiere, chirurgischer Eingriffe an den Tieren (Blutentnahme aus dem Herzen, Entnahme verschiedener Organe, Gefrieren von experimentellen Proben, etc.), Einzelzellpräparation, Zellkultur, Zellinjektion, Durchführung von Durchflusszytometrie-Färbungen und Speicherung der Durchflussdaten. Die Daten stammen ausschließlich aus den objektiven Ergebnissen der Experimente, wurden von mir persönlich gesammelt und von mir unter Verwendung entsprechender Software analysiert.

Bei Schwierigkeiten während der Datenanalyse erhielt ich Anleitung von PD Dr. med Jan Herter, Dr. Kiljan und der Postdoktorandin Gökcen Gözüm.

Dritte haben von mir weder unmittelbar noch mittelbar geldwerte Leistungen für Arbeiten erhalten, die im Zusammenhang mit dem Inhalt der vorgelegten Dissertationsschrift stehen.

Erklärung zur guten wissenschaftlichen Praxis:

Ich erkläre hiermit, dass ich die Ordnung zur Sicherung guter wissenschaftlicher Praxis und zum Umgang mit wissenschaftlichem Fehlverhalten (Amtliche Mitteilung der Universität zu Köln AM 132/2020) der Universität zu Köln gelesen habe und verpflichte mich hiermit, die dort genannten Vorgaben bei allen wissenschaftlichen Tätigkeiten zu beachten und umzusetzen.

Köln, den 14.02.2023

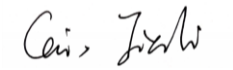

Unterschrift: .....

Acknowledgements

First of all, I would like to thank Dr. PD. Jan Hutt, M.D. and Ph.D. I would like to thank Dr. Grit Herter-Sprie for providing me with the opportunity to conduct my doctoral thesis in their laboratory. I greatly value the time and energy you spent supervising and teaching me so diligently. In addition, I would like to thank my colleagues Martha Kiljan, Gökcen Gözüm, Olta Ibruli, Li-na Niu, Isabelle Heßelman, Lea Wißkirchen, Luca Lichius, Sylvia Müller, and my former colleagues Dr. Sabrina Weil and Yağmur Sahbaz for helping me complete the experimental room work. I would like to thank our senior scientists for my training and education and for their careful management of the daily work in the laboratory. He always guided me during experimental work and discussed the latest research.

Thanks to Olta and Lina for their selfless help early in the morning and late at night, I no longer feel cold when I conduct experiments in winter.

Special thanks to Marimel Mayer and her team for their selfless help and professional guidance, so that I do not need to worry about the operation of the radiotherapy equipment in the radiotherapy experiment.

Special thanks to Jan who always comes up with new ideas when my experiments don't go well. He always taught me generously, shared his comprehensive knowledge with me, and taught me how to critically analyze the work of scientists. I am grateful to Jane and Gert for sharing their thoughts about science and life.

Last but not least, I want to thank my parents. Without their unwavering faith and unconditional support, I would never have had the opportunity to complete my doctoral thesis.

The completion of a doctoral thesis is not an end but a summary of one's own experiments. It is a starting point for my future scientific research work. I am grateful for the professional and non-professional things I learned during this journey. I have spent countless cold nights mired in self-doubt, and I have also hidden in my apartment and burst into tears. If I can look back over the years, I hope that in the future I will be able to smile and be calm when I look back on my life.

Widmung

TABLE OF CONTENTS

LIST OF ABBREVIATIONS

ANOVA	Analysis of variance
APC	Allophycocyanin
BED	Biological effective dose
CD	Cluster of differentiation
CTLA-4	Cytotoxic T-lymphocyte antigen 4
DC	Dendritic cell
DMEM	Dulbecco‘s modified Eagle‘s medium
DMSO	Dimethyl sulfoxide
DNA	Deoxyribonucleic acid
ECM	Extracellular matrix
EOMES	Eomesoderin
EpCAM	Epithelial cell adhesion molecule
FACS	Flow cytometry
FBS	Fetal bovine serum
FDA	Food and Drug Administration
FSC-A	Forward scatter area
FSC-H	Forward scatter height
FSC-W	Forward scatter width
FoxP3	Forkhead box P3
GATA-3	GATA-binding protein 3
GEMM	Genetically Engineered Mouse Model
GFP	Green fluorescent protein
Gy	Gray
HDRT	High-dose radiotherapy
ICD	Immunogenic cell death
ICIs	Immune checkpoint inhibitors
IFN-γ	Interferon gamma
IL	Interleukin
L	Liter
Ly	Lymphocyte antigen
Ly6C	Lymphocyte antigen 6 complex, locus C
Ly6G	Lymphocyte antigen 6 complex, locus G
mg	Milligram

mL	Milliliter
MDSC	Myeloid-derived suppressor cell
MHC	Major histocompatibility complex
N	Average division number
NFAT	Nuclear factor of activated T cell
NK	Natural killer
NSCLC	Non-small cell lung cancer
Nur77	Nuclear receptor 4A1
PBS	Phosphate buffered saline
PD	Progressive disease
PD-1	Programmed cell death 1
PD-L1	Programmed cell death ligand 1
PD-L2	Programmed cell death ligand 2
PS	Performance status
RORγt	RAR-related orphan receptor gamma
RPMI	Roswell park memorial institute medium
RT	Radiotherapy
SABR	Stereotactic ablative radiotherapy
SBRT	Stereotactic body radiation therapy
SCLC	Small cell lung cancer
TAM	Tumor-associated macrophages
T-bet	T cell-specific T-box transcription
TCR	T cell receptor
Tg	Transgenic
Th	T-helper cell
Th1	Type 1 helper T cell
Th2	Type 2 helper T cell
Th17	Type 17 helper T cell
TILs	Tumor-infiltrating lymphocytes
TIM-3	T-cell immunoglobulin and mucin-domain containing 3
TMB	Tumor mutational burden
TME	Tumor microenvironment
TNA	Tumor neoantigens
TP53	Tumor protein 53
TNF-β	Tumor necrosis factor-beta
Treg	Regulatory T cell

U	Units
WT	Wild type
µg	Microgram
µl	Microliter
µM	Micromolar

1. ZUSAMMENFASSUNG

Lungenkrebs ist weltweit einer der häufigsten und tödlichsten bösartigen Tumore, wobei der nicht-kleinzellige Lungenkrebs der häufigste Subtyp ist. Neben der Operation und der Chemotherapie ist die Strahlentherapie zu einem der grundlegenden Ansätze für die Behandlung von Lungenkrebs geworden, die bei etwa 60-70 % der Patienten zum Einsatz kommt. Insbesondere bei Tumoren, die schwer zugänglich sind, in kritische Funktionsbereiche eindringen oder nicht operativ entfernt werden können, ist die Strahlentherapie unverzichtbar geworden. Nicht-kleinzelliges Lungenkarzinom hat eine relativ hohe Rate an Fernmetastasen (etwa 57 %), und die Strahlentherapie kann den direkten Tod von Tumorzellen herbeiführen, die Tumornekrose fördern, Tumorantigene freisetzen und das Immunsystem aktivieren, wodurch die Mikroumgebung des Tumors verändert und die Antitumorimmunität gefördert wird. Die Beobachtung des Abszesseffekts in einigen Fällen deutet darauf hin, dass die Strahlentherapie zusätzlich zu ihrer lokalen therapeutischen Wirkung auch eine systemische Antitumorwirkung hat. Auch die Kombination von Immun-Checkpoint-Inhibitoren mit einer Strahlentherapie kann nachweislich den Abskopierungseffekt auslösen. Der Mechanismus ist jedoch nach wie vor unklar, und es fehlt an geeigneten Tiermodellen zur Untersuchung des Abskopeffekts, was den Bedarf an Tiermodellen zum besseren Verständnis dieses Phänomens unterstreicht, das ein großes klinisches Potenzial hat.

In dieser Studie wurden Tiermodelle von Tumoren und Metastasen erstellt, indem nicht-kleinzellige Lungenkrebszellen (KP-Zelllinie) in die Flanken immunkompetenter Mäuse geimpft und spezifische Strahlentherapieschemata auf der Grundlage der biologisch wirksamen Dosis (BED) festgelegt wurden. Die Strahlentherapie zielte auf den Tumor auf einer Seite der Maus (den Primärtumor), gefolgt von einer PD-1-Antikörperinjektion zur Immuntherapie. Die Tumorvolumina wurden aufgezeichnet, und es wurden Wachstumskurven erstellt. Mit Hilfe der Durchflusszytometrie wurden Veränderungen bei Leukozyten, CD4+ T-Zellen, CD8+ T-Zellen und die Expression von Tumorzelloberflächenantikörpern in sekundären Tumorherden analysiert. Im Vergleich zur Kontrolle und zur Immuntherapie allein hemmte die Strahlentherapie in Kombination mit der Immuntherapie unter demselben Schema das Wachstum der Sekundärtumore. Das Bestrahlungsschema 8,7Gyx5F war beim Vergleich des Sekundärtumorwachstums wirksamer als das 24Gyx1F-Schema. Eine durchflusszytometrische Analyse der immunologischen Mikroumgebung im Sekundärtumorgewebe zeigte eine erhöhte Infiltration von Leukozyten, CD4+ T-Zellen und CD8+ T-Zellen sowie eine erhöhte Expression von PD-L1 und EpCAM bei Mäusen, die eine 8,7Gyx5F-Strahlentherapie in Kombination mit einer PD-1-Behandlung erhielten. Eine kontinuierliche fraktionierte Strahlentherapie war bei der Kontrolle von Sekundärtumoren wirksamer als eine einzelne Strahlendosis im Vergleich zu einer Strahlentherapie mit der

gleichen BED. Wenn das Strahlentherapieschema konsistent war, zeigte die kombinierte Behandlung aus Strahlen- und Immuntherapie eine bessere Tumorkontrolle als die Strahlentherapie allein. Die Mäuse dieser Gruppe wiesen eine verstärkte Infiltration von Immunzellen auf, was auf eine antitumorale Immunaktivität hinweist. Diese Studie liefert wichtige experimentelle Grundlagen für die klinische Umsetzung der kombinierten Strahlen- und Immuntherapie und bietet erste Einblicke in den Mechanismus der strahleninduzierten abskopischen Effekte. Für eine umfassende Bewertung der klinischen Aussichten dieser kombinierten Behandlungsstrategie ist jedoch eine weitere Optimierung der Versuchsprotokolle und der Datenanalyse erforderlich.

2. ABSTRACT

Lung cancer is one of the most prevalent and deadliest malignant tumors worldwide, with non-small cell lung cancer being the most common subtype. Besides surgery and chemotherapy, radiotherapy has become one of the fundamental approaches for lung cancer treatment, with approximately 60%–70% of patients requiring it. Radiotherapy has become indispensable, particularly for tumors that are difficult to access, invade critical functional areas, or cannot be surgically removed. Non-small cell lung cancer has a relatively high rate of distant metastasis (around 57%), and radiotherapy can induce direct tumor cell death, promote tumor necrosis, release tumor antigens, and activate the immune system, thereby altering the tumor microenvironment and promoting antitumor immunity. The observation of the abscopal effect in some cases suggests that radiotherapy has a systemic antitumor effect in addition to its local therapeutic effect. The combination of immune checkpoint inhibitors with radiotherapy has been demonstrated to cause the abscopal effect as well. However, the mechanism remains unclear, and suitable animal models for studying the abscopal effect are lacking, emphasizing the need for animal models to better understand this phenomenon, which holds significant clinical promise.

This study established animal models of tumors and metastases by inoculating the NSCLC Genetically Engineered Mouse Model (GEMM) [$Kras^{G12D}Tp53^{-/-}$(KP)] cells into immunocompetent mice flanks and determined specific radiotherapy regimens based on the biologically effective dose (BED) values. Radiotherapy targeted the tumor on one side of the mouse (the primary tumor), followed by PD-1 antibody injection for immunotherapy. Tumor volumes were recorded, and growth curves were obtained. The study employed flow cytometry to examine alterations in leukocytes, CD4+ T cells, CD8+ T cells, and the expression of tumor cell surface antibodies in secondary tumor foci. Compared to control and immunotherapy alone, radiotherapy combined with immunotherapy under the same regimen inhibited the growth of secondary tumors. The 8.7Gyx5F radiotherapy schedule was more effective than the 24Gyx1F schedule when comparing secondary tumor growth. Flow cytometry analysis of the immune microenvironment in secondary tumor tissues showed increased infiltration of leukocytes, CD4+ T cells, and CD8+ T cells, along with increased expression of PD-L1 and EpCAM in mice receiving 8.7Gyx5F radiotherapy combined with PD-1 treatment. Continuous fractionated radiotherapy was more effective than a single dose of radiation in controlling secondary tumors compared to radiotherapy with the same BED. When the radiotherapy regimen was consistent, the combined treatment of radiotherapy and immunotherapy showed better tumor control than radiotherapy alone. Mice in this group exhibited enhanced infiltration of immune cells, indicating antitumor immune activity. This study provides important experimental groundwork for the clinical translation of combined radiotherapy and immunotherapy and offers initial

insights into the mechanism of radiation-induced abscopal effects. However, further optimization of experimental protocols and data analysis is needed for a comprehensive assessment of the clinical prospects of this combined treatment strategy.

3. INTRODUCTION

3.1 Lung Cancer

Lung cancer is a malignant tumor of the bronchial mucous membrane or lung glands. Before the age of 75, an individual's lifetime cancer death risk is roughly 20%. In 2021, cancer caused approximately 10 million deaths globally, making it the leading cause worldwide[1]. With 2.21 million new cases, lung cancer came in second on the list of cancer diagnoses in 2020. Lung cancer was the main cause of contributor to fatalities caused by cancer in 2020 (World Health Organization, 2022). Based on morphology, immunohistochemistry, and molecular markers, lung cancer is categorized into two primary types: small cell lung cancer (SCLC) and non-small cell lung cancer (NSCLC)[2].

3.1.1. Risk Factors and Symptoms

Smoking remains the most critical risk factors critical lung cancer. Additional factors linked to the chance of developing lung cancer include a history of secondhand smoke (2.7% percent of new cases, or approximately 6400 cases in 2022), asbestos, radon, organic chemicals, radiation, air pollution, occupational exposure and family history[3,4].

Lung cancer has very complex clinical manifestations. In general, the early symptoms of lung cancer are usually mild or uncomfortable. However, the manifestations of central lung cancer manifest earlier and are severe[5]. Common symptoms of lung cancer include cough, blood in the sputum, or hemoptysis, difficulty in breathing, hoarseness and chest pain[6,7].

3.1.2. Classification of the Non-small Cell Lung Cancer and Staging

NSCLC comprises about 80% of all lung cancers. It is often categorized into three histological groups: adenocarcinoma (AD), squamous cell carcinoma (SCC), and large cell carcinoma (LCC). Other distinguished types are adenosquamous carcinoma, carcinoid sarcoma, and unclassified cancers[4,5].

Present-day therapeutic staging of lung cancer is determined by the eighth edition of the AJCC/TNM staging system for NSCLC, which was implemented in the United States on January 1st, 2018[10]. The guidelines are derived from the International Association for the Study of Lung Cancer (IASLC) 2016 proposal to revise TNM staging[11].

Table 1. Eighth edition guidelines of AJCC/TNM staging of NSCLC: definition of T, N, and M

Table was taken/edited from Detterbeck et al., 2018[12].

T (primary tumor)	
T0	No primary tumor
Tis	Carcinoma in situ (squamous or adenocarcinoma)
T1	Tumor ≤3 cm
T1mi	Minimally invasive adenocarcinoma
T1a	Superficial spreading tumor in central airways*
T1a	Tumor ≤1 cm
T1b	Tumor >1 but ≤2 cm
T1c	Tumor >2 but ≤3 cm
T2	Tumor >3 but ≤5 cm or tumor involving: visceral pleura,† main bronchus (not carina), atelectasis to hilum†
T2a	Tumor >3 but ≤4 cm
T2b	Tumor >4 but ≤5 cm
T3	Tumor >5 but ≤7 cm or invading chest wall, pericardium, phrenic nerve; or separate tumor nodule(s) in the same lobe
T4	Tumor >7 cm or tumor invading: mediastinum, diaphragm, heart, great vessels, recurrent laryngeal nerve, carina, trachea, esophagus, spine; or tumor nodule(s) in a different ipsilateral lobe
N (regional lymph nodes)	
N0	No regional node metastasis
N1	Metastasis in ipsilateral pulmonary or hilar nodes
N2	Metastasis in ipsilateral mediastinal or subcarinal nodes
N3	Metastasis in contralateral mediastinal, hilar, or supraclavicular nodes
M (distant metastasis)	
M0	No distant metastasis
M1a	Malignant pleural or pericardial effusion‡ or pleural or pericardial nodules or separate tumor nodule(s) in a contralateral lobe
M1b	Single extrathoracic metastasis
M1c	Multiple extrathoracic metastases (1 or >1 organ)

*Superficial spreading tumor of any size but confined to the tracheal or bronchial wall. †Atelectasis or obstructive pneumonitis extending to hilum; such tumors are classified as T2a if >3 and ≤4 cm, T2b if >4 and ≤5 cm. ‡Pleural effusions are excluded that are cytologically negative, nonbloody, transudative, and clinically judged not to be due to cancer.

Table 2. TNM staging of lung cancer based on eighth edition guidelines of the AJCC/TNM staging system for NSCLC

Table was taken/edited from Lababede et al., 2018[13].

Stage group		
Stage 0		TisN0M0
Stage Ⅰ	Stage ⅠA	T1N0M0
	Stage ⅠB	T2aN0M0
Stage Ⅱ	Stage ⅡA	T2bN0M0
	Stage ⅡB	T (1–2) N1M0 T3N0M0
Stage Ⅲ	Stage ⅢA	T (1–2) N2M0 T3N1M0 T4N (0–1) M0
	Stage ⅢB	T (1–2) N3M0 T (3–4) N2M0
	Stage ⅢC	T (3–4) N3M0
Stage Ⅳ	Stage ⅣA	Any T, Any N, M1a, b
	Stage ⅣB	Any T, Any N, M1c

3.1.3. Treatment Options for Non-small Cell Lung Cancer

The treatment of NSCLC requires different treatment options contingent upon the individual's physiological state, cancer histopathology, molecular classification, degree of infiltration, and

growth rate. Treatment options for NSCLC need to be discussed and developed by a multidisciplinary team (MDT). Current NSCLC treatments include surgical resection, radiotherapy (RT), chemotherapy, and immunotherapy as monotherapy or combination therapy[8]. These novel therapies have improved the survival rate among patients diagnosed with NSCLC.

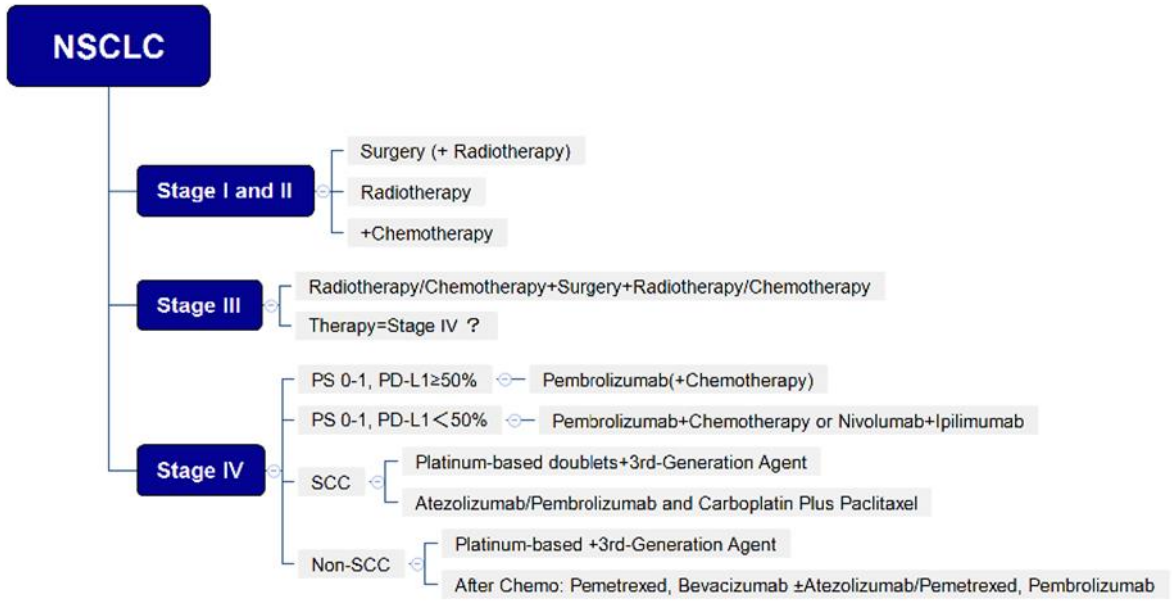

Figure 1. Current treatment options for NSCLC

Figure was taken/edited/adapted from Daniel et al., 2022[8].

Surgery remains the primary option for treating stage I and II NSCLC[14]. For NSCLC staged as stage IIIA, the choice of surgery needs to be evaluated based on more refined staging criteria, as stage IIIA is a non-homogeneous group, coupled with the fact that many patients may be unresectable[15,16]. According to treatment guidelines, some individuals with stage IV NSCLC are advised to have surgical procedures. However, the available evidence is limited. At the same time, for patients with mediastinal lymph node malignancy or locally progressed tumors in stage IV, surgery should be recommended more rarely due to its limited benefits[17].

Radiotherapy (RT) can be used at any stage of NSCLC[18,19]. Stereotactic body radiotherapy (SBRT) is a viable treatment choice for individuals with early-stage NSCLC who are not suitable candidates for surgical intervention[20]. For the locally advanced NSCLC, radiotherapy can be used as a curative treatment that, combined with chemotherapy, provides a better treatment option for patients[21]. RT can be a local treatment of limited recurrence and metastases and palliative care (pain relief, relief of compression obstruction, and other needs) in advanced patients with incurable extensive metastases[22–24].

Chemotherapy significantly affects the management of NSCLC. However, not all NSCLC patients require chemotherapy. It is generally accepted that chemotherapy is mostly used for locally advanced NSCLC and metastatic cases[25]. Postoperative adjuvant chemotherapy is also used as a means of consolidation after surgery[26–28]. Besides, clinical data have shown that neoadjuvant chemotherapy can provide good therapeutic effects for NSCLC patients[29,30].

Immunotherapy is a method of treatment that activates the immune system of the patient to find and attack cancer cells[31]. Immunotherapy can achieve this by enhancing or increasing the natural defenses of the host to recognize and eliminate cancer cells[32]. Alternatively, artificially synthesized molecules may be used to activate the immune system to identify and eliminate tumor cells[33].

The treatment of NSCLC should be complex treatment[34]. The choice of comprehensive therapy needs to be carried out after the patient's performance status (PS) assessment[35]. The MDT must consider several aspects to decide the best-personalized treatment strategy. In general, systemic therapy (encompasses targeted therapy and immunotherapy), clinical trials, and palliative care will be the treatments of choice, according to the disease's extension and the patient's health status[36].

3.2 Abscopal Effect

W.H. Mole first described the abscopal effect in 1953[37], where the prefix Ab meant “position away from” and scopos described “a mark or target for shooting at.”[38] It refers to observing an overall effect on the spread of cancer to other body parts following a localized treatment of one of the tumors[39,40]. The most obvious proof of this effect is the significant reduction of both primary and metastatic tumors after RT. While the abscopal effect is rare in solid tumors[41]. Several clinical case reports have indicated the abscopal effect in the treatment of melanoma[42], renal cell carcinoma[43], breast cancer[44], hepatocellular carcinoma[45], and other metastatic solid tumors[46] many years after it was initially referred to.

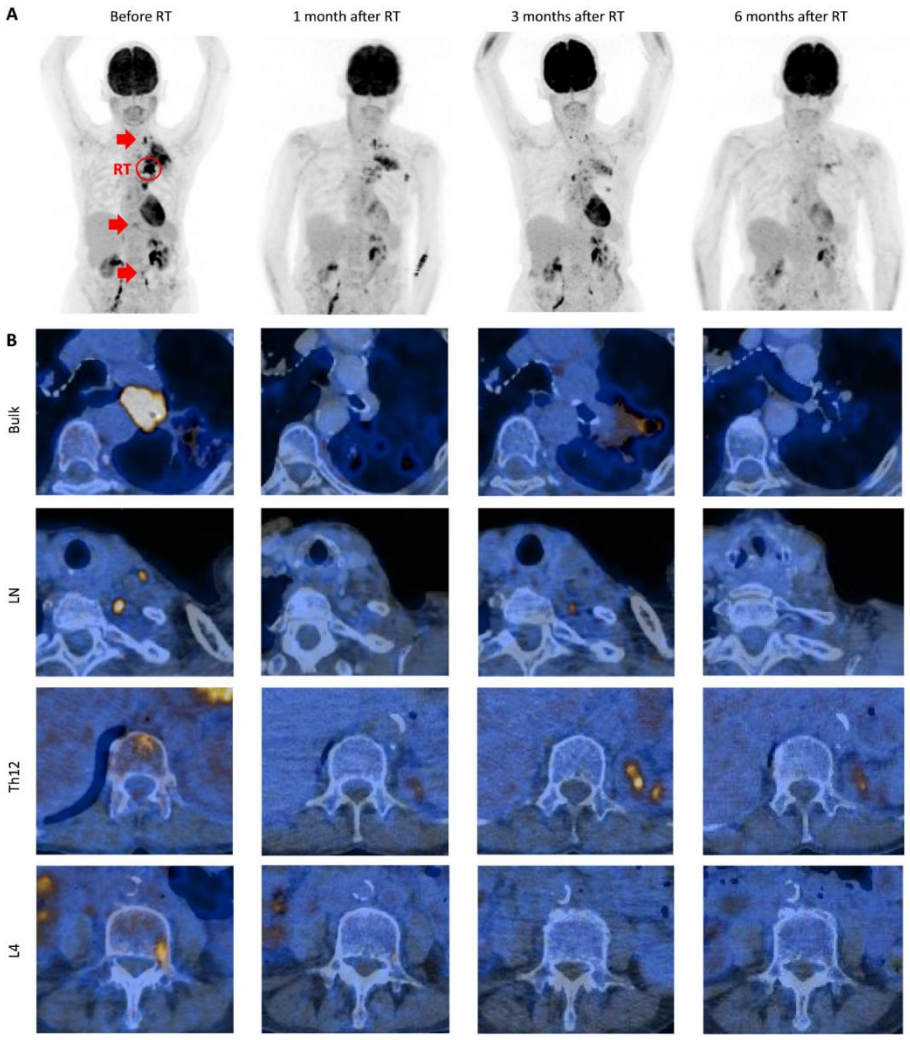

Figure 2. True abscopal effect in a patient with metastatic non-small cell lung cancer

The figure was adapted from Vilinovszki et al., 2021[40].

3.2.1. Abscopal Effect as a Potential Treatment for Cancer

The abscopal effect is a novel approach to tumor treatment method[47]. The benefits of the abscopal effect were considered to be used to enhance treatment efficiency[48,49] and decrease the occurrence of metastases among individuals undergoing local RT for primary tumors[50,51].

According to the National Comprehensive Cancer Network (NCCN) guidelines, most cancer patients can benefit from systemic therapy[52,53]. Nevertheless, systemic treatment may cause serious adverse reactions in patients, and severe discomfort may also affect the psychological well-being of many patients prior to, during, and subsequent to the medical intervention. Although the abscopal effect cannot replace systemic therapy, it will enhance the efficacy of systematic treatment and the optimize the patients' experience[54–56].

In radiation oncology, the abscopal effect of RT has been described as tumor regression in non-irradiated lesions[57], indicating that local tumor treatment can have systemic effects[58]. With the development of RT and immunotherapy techniques, increasing clinical evidence further supports the objective existence of the abscopal effect[59,60]. Due to the particularity of the abscopal effect, the abscopal effect as a treatment can be much better with fewer side effects[59]. Therefore, an improved understanding of the abscopal effect in clinical applications will help support precision medicine to improve the quality of lifestyle of patients[61], and increase the RT and immunotherapy efficacy[62,63]. This also proves that the use of the abscopal effect to treat tumors has become an active area of cancer research[64].

3.2.2. Potential Mechanisms of the Abscopal Effect

Many scholars have conducted various studies to understand how the abscopal effect occurs. The purpose is to clearly understand how to trigger the abscopal effect and transform the abscopal effect into one of the clinical treatment options. However, the precise underlying process responsible for the abscopal effect remains unclear.

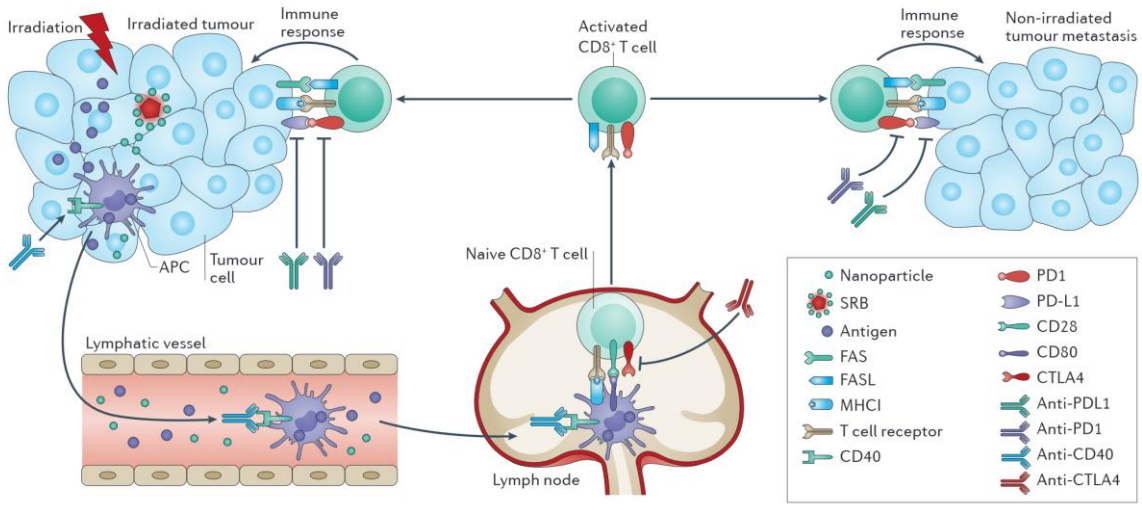

Figure 3. Potential mechanism of the abscopal effect
The figure was adapted from Ngwa et al., 2018[60]

Azami et al. reported that RT alone can trigger abscopal effects[65]. However, the abscopal effect caused by RT monotherapy triggers are still rare. With the rise of immunotherapy, more cases of the abscopal effect have been observed in clinical treatments. Franzese et al. reviewed that anticancer medications can affect the immune response of the host and the immunogenicity characteristic of cancerous cells. RT and immunotherapy interact and synergize to cause the abscopal effect, tumor xenogenesis, and immunogenic cell death (ICD)[66]. Therefore, tumor immunity was thought to play an essential role in generating the abscopal effect[67]. Muro et al. reported a case about an advanced gastric cancer and brain metastases patient subjected to

RT and anti-PD-1(Programmed Death-1) demonstrated successfully inducing the abscopal effect[68].

The abscopal effect may be associated with the in situ vaccine response elicited by RT[69]. Newly generated antitumor immune responses have been observed post-RT in murine models and some patients[70]. Regional RT induces tumor cell death, releasing immunogenic factors through ICD[71], and produces antitumor immunity via the release of damage-associated molecular[72–77].

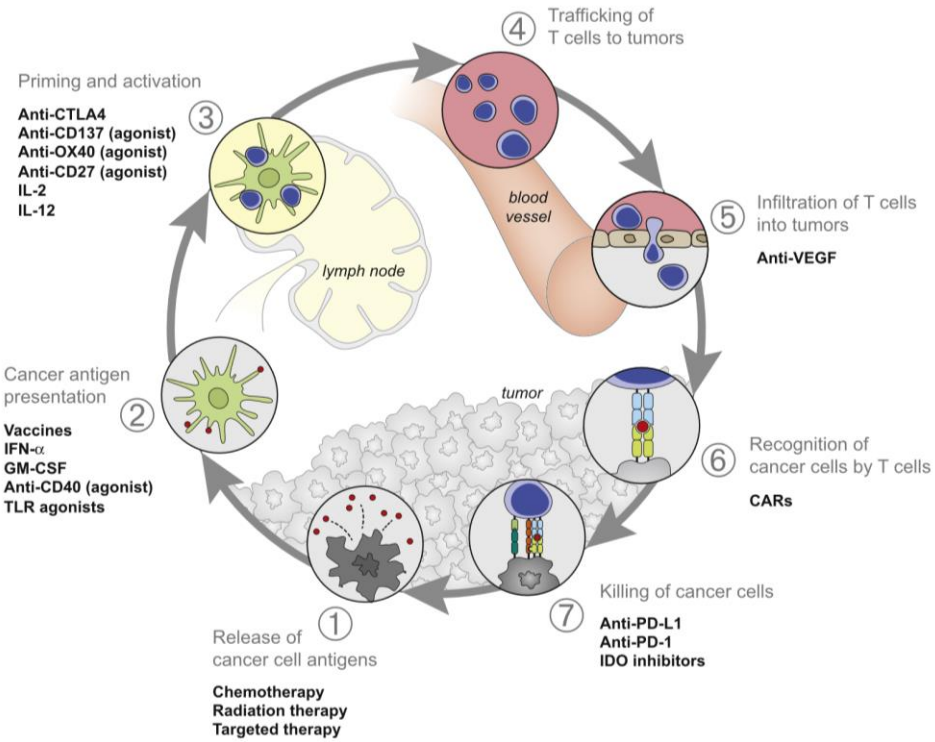

Figure 4. Therapies that might affect the cancer-immunity cycle

The figure was adapted from Chen and Mellman, 2013[78]

The tumor microenvironment (TME) was a factor in the response to cancer immunotherapy. Immune markers often serve as prognostic indicators of individual survival, regardless of the specific treatment. RT is commonly administered to individuals with cancer because of its ability to kill cancer cells directly. By encouraging the recruitment and functioning of effector T cells, RT can influence TME, and the abscopal effect was also associated with RT-induced remodeling of TME[79,80]. Chemokines may be induced to recruit effector T cells, effectively transforming the tumor into an "inflammatory" tissue vulnerable to T-cell attack[23]. Therefore, RT may have pro-inflammatory response in stromal cells and cancer cells in the TME[81,82].

3.2.3. Radiotherapy and the Abscopal Effect

RT has become one of the three primary treatments for malignant tumors. Approximately 50% of cancer cases worldwide are treated with RT, and more than 70% of patients with malignant tumors need RT at some stage of their treatment[83]. RT has enhanced the ability to locally manage tumors and increase the overall survival rate for many people with cancerous growths[84–89]. RT demonstrates superior outcomes in achieving localized tumor control while minimizing adverse effects[90].

RT generally kills cancer cells through both direct and indirect effects[91–95]. Direct effect via high-energy X-rays, gamma rays, or neutron beams to kill tumor cells[96], those rays can directly damage double-stranded DNA[97,98]. Indirect effect means that RT on water molecules in cancer cells to form oxygen free radicals. The large number of free radicals released can kill cancer cells[99]. The degree of the killing induced by RT is positively associated with the rate at which cells grow but inversely correlated with the level of cell differentiation[100]. The killing efficiency of radiation on tumor cells is higher than on normal tissue cells because of the lower growth rate and differentiation degree of cancer cells.

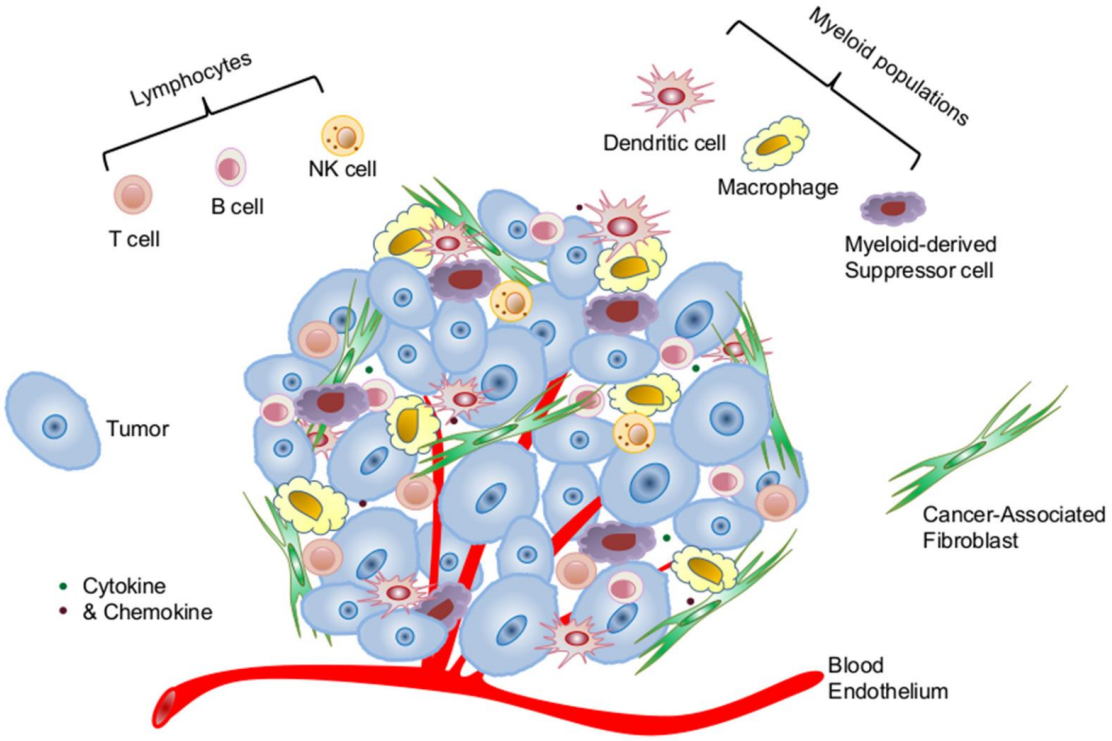

Figure 5. Cellular constituents of the tumor microenvironment that shape tumor immunological landscape
The figure was adapted from Cui and Guo, 2016[101]

RT can change the way tumor cells interact with their surrounding environment and activate immune responses, which is one of the potential mechanisms for the abscopal effects[102,103]. The TME is an important mediator of response to local and systemic RT[104,105]. TME refers to the components surrounding tumors, such as surrounding blood vessels, immune cells, fibroblasts, signaling molecules, and extracellular matrix (ECM)[106,107]. Immune cells in the TME will influence the proliferation and development of tumor cells. Recent research has increasingly emphasized the impacts of RT on the TME[108,109].

RT not only directly destroys malignant cells but also activates immunological responses[110], thereby inhibiting the growth of cancer cells located beyond the region exposed to radiation[111]. The generation of the abscopal effect is closely related to this[112,113]. RT can extend the scope of immunotherapy to non-immunogenic tumors[114]. For individuals who develop immunity to immune checkpoint inhibitors (ICI), RT may still be an effective treatment[115]. Multiple ongoing clinical trials are assessing the effectiveness of RT combined with ICIs[116,117].

The target cells, triggers, and mechanisms of action of the abscopal effects remain unclear[38]. Combination treatment strategies often produce more significant the abscopal effects than RT alone[64]. From 1969 to 2014, only 46 cases reported the abscopal effects caused by RT alone, and the concurrent use of RT with immunotherapy has the potential to improve abscopal effect[118]. This treatment approach is consistent with precision medicine and provides significant benefits at a lower cost[119].

3.2.4. Immunotherapy and the Abscopal Effect

In the last few decades, immunotherapy has become essential for treating some types of cancer[120]. Six main types of immunotherapies are at present being utilized in cancer therapy[121]:

Table 3. Types of cancer immunotherapy

Types of cancer immunotherapy	
Checkpoint inhibitors	Checkpoint inhibitors are a type of immunotherapy that block different checkpoint proteins. These drugs basically take the 'brakes' off the immune system, which helps it recognize and attack cancer cells.
Chimeric antigen receptor (CAR) T-cell therapy	CAR T-cell therapy is a type of adoptive cell transfer. This therapy takes some T-cells from a patient's blood, mixes themwith a special virus that teaches T-cells how to attach to tumor cells, and then gives the cells back to the patient so they can find, attach to, and kill cancer.
Cytokines	Cytokines are a group of proteins that are found naturally in the body. They help to boost the immune system. Manufactured versions of these proteins are a cancer treatment. This treatment uses cytokines (small proteins that carry messages between cells) to stimulate the immune cells to attack cancer.
Oncolytic viruses	This treatment uses viruses modified in a lab to infect and kill certain tumor cells.
Monoclonal antibodies (mAbs or MoAbs)	These are manufactured versions of immune system proteins. mAbs can be very useful in treating cancer because they can be designed to attack a particular part of a cancer cell.
Cancer vaccines	Unlike vaccines to prevent disease, cancer treatment vaccines are for people who already have cancer. These vaccines are mainly available as part of clinical trials. Vaccines are substances put into the body to start an immune response against certain diseases. We usually think of them as being given to healthy people to help prevent infections. But some vaccines can help prevent or treat cancer.

The advancement of precision medicine, particularly in personalized medicine and cancer treatment, has witnessed significant progress in recent years[122]. Immunotherapy, either as a standalone approach or in conjunction with conventional modalities like RT and chemotherapy, has emerged as the conventional therapeutic regimen for numerous cancers, exhibiting noteworthy success[123]. Among the immunotherapeutic strategies, Immune checkpoint inhibitors (ICI) represent a pivotal category[124]. As a type of antitumor immunotherapy, ICI exerts its effects by boosting anticancer effects through the targeted modulation of immunologic receptors on the surface of T cells[125]. The advent of ipilimumab in 2011 marked a pivotal milestone, as ICIs distinguished unique therapeutic option[126] because they had long-lasting effects with low toxicity profile[127]. In contrast to conventional treatment approaches, ICIs reinvigorate the host immune system[128]. These immune checkpoints can inhibit and stimulate related pathways to affect immune cell activity[129].

The most popular immunotherapeutic medications during the previous decade have been antibodies that specifically bind to immunological inhibitory receptors, like CTLA-4, PD-1, and PD-L[130]. Researchers have discovered a multitude of novel immune checkpoint targets, including lymphocyte activation gene 3 (LAG-3), T cell immunoglobulin and mucin-domain containing protein 3 (TIM-3)[131]. The US Food and Drug Administration (FDA) has approved three ICI classes for therapeutic purposes for various cancers: PD-1 inhibitors (Nivolumab, Pembrolizumab, and Cemiplimab), PD-L1 inhibitors (Atezolimumab, Durvalumab, and Avelumab), and CTLA-4 inhibitors (Ipilimumab)[132].

3.2.4.1 PD-1 and Its Role in Immunotherapy

PD-1 is an inhibitory receptor critical in programmed death signaling, exerting regulatory control over T-cell-mediated responses[133]. Its involvement includes the reduction of cytokines and modulation of the CD28 co-stimulatory signaling pathway, resulting in the suppression of cell proliferation[134]. Within the TME, PD-1 expression is discernible across various immune cell types, encompassing activated monocytes, DCs, NK cells, T cells, and B cells[135].

PD-1 has two ligands, PD-L1 and PD-L2[136], which play crucial roles. PD-L1, present in both tumor cells and immune cells, has been identified as a biomarker that can predict the efficacy of anti-PD-1/PD-L1 antibodies in treating individuals with various forms of cancer[137]. Also referred to as B7-H1 or CD274, PD-L1 assumes a pivotal role in suppressing the cancer-immunity cycle by attaching to negative regulators of T-cell activation[138]. Consequently, the ligation of PD-L1 impedes the migration and proliferation of T cells, therefore constraining tumor cell death (Figure 6)[139]. Tumor cells evade immune detection by using the PD-1/PD-L1 pathway, thereby reducing cellular immune responses[140]. This multifaceted interplay underscores the significance of the PD-1/PD-L1 axis in shaping immune responses within the context of cancer immunotherapy[141].

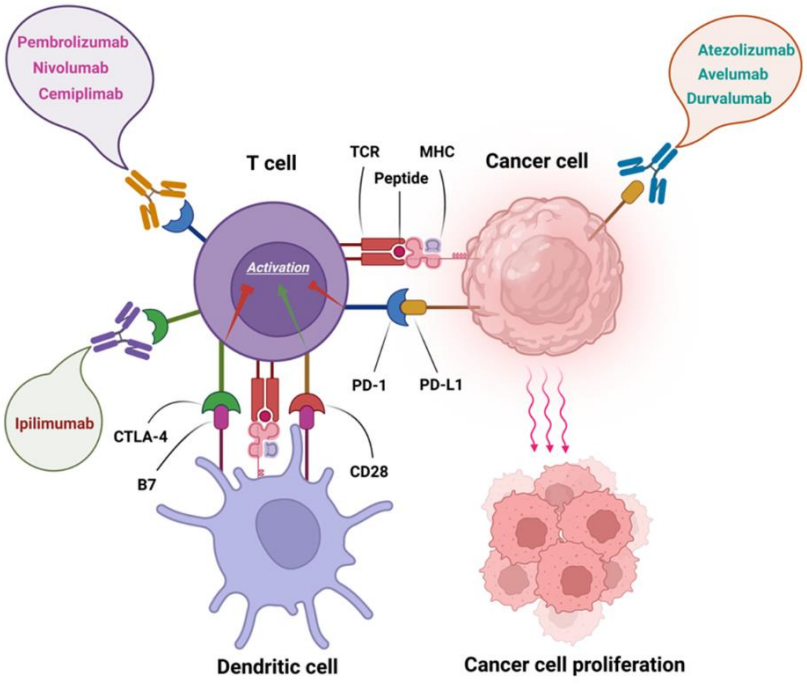

Figure 6. Immune checkpoint inhibitors approved by US FDA.
Taken from Shiravand et al., 2022[142].

3.2.4.2 Clinical Applications of PD-1/PD-L1 Inhibitors

Immunotherapy has shown significant effectiveness in cancer treatment, particularly with the clinical utilization of PD-1/PD-L1 antibodies[143–147]. This therapeutic approach has markedly prolonged survival rates among patients afflicted with melanoma, lung, and liver cancers[148–150]. While RT was traditionally regarded as a localized treatment modality, combining immunotherapy and RT is no longer just a local treatment method for malignant tumors and has become an integral part of systemic cancer treatment.

Pembrolizumab

Pembrolizumab, a PD-1 inhibitor, has gained attention for its effectiveness in treating various cancers, including rare and in late-stage ones. Clinical trials have demonstrated its ability to improve survival rates among patients with melanoma[151], NSCLC[152,153], and other malignancies[154–156]. The drug works by blocking the association between PD-1 and PD-L1/PD-L2, thereby enhancing the immune response against tumor cells[157,158].

Cemiplimab

Cemiplimab, another PD-1 inhibitor, is recommended by the 2020 European multidisciplinary guidelines and NCCN as a first-line treatment for cancer patients[159–161]. It has shown significant anticancer properties in individuals with metastatic cutaneous squamous cell carcinoma and has a favorable safety profile[162]. Cemiplimab works similarly to pembrolizumab, enhancing T cell activity by inhibiting the PD-1 pathway.

Atezolizumab

Atezolizumab is a monoclonal antibody that targets PD-L1[163]. The FDA has approved it for adjuvant therapy for individuals with stage II and IIIA NSCLC following surgery and chemotherapy[164]. In the randomized phase II trial, Atezolizumab has shown a statistically significant improvement in mortality among individuals with recurrent NSCLC tumors that express an intermediate or high level of PD-L1[165,166]. Atezolizumab inhibits the interaction between PD-L1 and PD-1, which enhances the killing of tumors by T cells[167].

Avelumab

Avelumab is another PD-L1 inhibitor that attaches directly to PD-L1, preventing its interaction with PD-1 and enabling a robust T cell-mediated antitumor response[168]. The FDA determined that Avelumab is a breakthrough antitumor medicine with a good safety profile[169].

Durvalumab

Durvalumab binds specificity to PD-L1 and inhibits its interactions with PD-1 and CD80[170]. This dual inhibition amplifies the immune system's ability to detect and attack cancer cells. Durvalumab has shown antitumor effects in certain types of tumors[171–173]. Its approval and usage are based on clinical trials showing improved patient outcomes and manageable safety profiles.

3.2.4.3 Synergistic Protential of Radiotherapy and PD-1 Inhibitors in Inducing the Abscopal Effect

Increasing cases of the abscopal effect of local RT has been documented since the clinical implementation of ICIs[174]. Several trials and cases have documented a relatively low overall incidence of the abscopal effect when RT only. This limited efficacy may be related to the inherent inadequacy of RT in overcoming the immunological resistance inherent to malignant tumors. Given the capacity of immunotherapy to remodel adaptive immune cell responses, the synergistic combination of RT and immunotherapy holds promise for augmenting antitumor immune responses and increasing the likelihood of eliciting the abscopal effect[175–177].

Theelen et al., the compiled results of two Pembro-RT studies[178,179] showed that the abscopal effect objective response rate in the PD-1 monoclonal antibody combined with the RT group was more significant than in the PD-1 monotherapy group. SBRT is also called stereotactic ablative radiation therapy[180]. Recently, numerous clinical cases have been reported highlighting the abscopal effects after SBRT conjunction with anti-PD-1/PD-L1 therapy[181–185].

Tumor cells show upregulation of PD-L1 expression, which leads to the activation of T lymphocytes and their subsequent death through PD-1 ligation, thereby inhibiting the recognition and eliminating tumor cells[186,187]. Although many studies have used animal models to confirm that RT combined with PD-1 can stimulate the abscopal effect, translating of these findings to clinical applications remains a formidable challenge in cancer research. Engert et al. (NCT03480334) conducted a clinical experiment, the researchers hypothesized that local RT induces an immunogenic effect, which in combination with Nivolumab may synergize and promote enhanced systemic (i.e., abscopal effect) response, then provide patients may have the possibility of a better survival benefit; the study is still ongoing. Several ongoing clinical trials based on PD-1 inhibitors induced the abscopal effect including NCT03480334, NCT04873440, and NCT05435053.

Table 4. Ongoing trials about the abscopal effect from clinicaltrials.gov

Table was taken from Zhang, 2020[188].

NCT number	Hospital/ Institute	Status	Study Title	Conditions	Interventions	Phase	Outcome Measures
NCT03480334	Cologne University Hospital	Recruiting	Abscopal Effect of Radiotherapy and Nivolumab in Relapsed Hodgkin Lymphoma After Anti-PD1 Therapy	Classical Hodgkin Lymphoma	Nivolumab plus radiotherapy	2	Abscopal response rate
NCT04238169	Xinqiao Hospital of Chongqing	Not yet recruiting	Clinical Trial Assessing the Efficacy of Abscopal Effect Induced by SBRT and Immunotherapy in Advanced NSCLC	Non-Small-Cell Lung Cancer Stage IV	Drug: Bevacizumab Drug: Toripalimab	2	Objective response rate Objective response of non-target lesion Progression-free survival (PFS)
NCT04168320	KABEG Klinikum Klagenfurt, Institute for Radiation Oncology	Recruiting	SBRT-based PArtial Tumor Irradiation of HYpoxic Segment	Unresectable Malignant Solid Neoplasm	Radiation: SBRT-PATHY (SBRT-based PArtial Tumor irradiation targeting HYpoxic segment	1	Bystander and abscopal effects Overall survival Progression-free survival
NCT03396471	Mayo Clinic; MD Anderson Cancer Center	Recruiting	Study of Pembrolizumab and Concurrent Radiation in Patients With Previously Treated Carcinoma of Unknown Primary	Carcinoma, Unspecified Site	Drug: Pembrolizumab Radiation: External Beam Radiation Therapy	2	Abscopal Response Rate Response Rate Assess Adverse Events
NCT04245514	Kantonsspital Aarau Aarau, Switzerland	Recruiting	Multimodality Treatment in Stage III Non-small Cell Lung Cancer (NSCLC)	Non-small Cell Lung Cancer	Drug: Durvalumab Radiation: Radiotherapy	2	Event-free survival (EFS) at 12 months Event-free survival (EFS) Recurrence-free survival (RFS) after R0 resection
NCT03993678	Kantonsspital Graubünden Chur, Switzerland	Recruiting	Intratumoral Injection of IP-001 Following Thermal Ablation in Patients With Advanced Solid Tumors.	Advanced Solid Tumors	Drug: IP-001 Device: Thermal Ablation	1-2	Toxicity and tumor control

Because of the occurrence of clinically observable the abscopal effect is rare, prospective studies with big sample sizes and prolonged follow-up periods are needed. The clinical efficacy and target beneficiary populations of abscopal effects in the context of combined RT plus immune checkpoints need to be conducted in future studies before the abscopal effects can be used in clinical treatments[189].

3.3 Immune Cells Composition of the Tumor Microenvironment

The TME encompassed the neighboring milieu where tumor cells reside, comprising nearby blood vessels, immune cells, fibroblasts, as we know well, while including various signaling molecules, and extracellular matrix[190].

Immune cells are critical components of theTME[191]. In general, the immune cells associated with tumors can be categorized into two groups: immune cells that work against the tumor and immune cells that support tumor growth[192]. The immune cells that counteract tumors mostly consist of effector T cells (including CD8+ cytotoxic lymphocytes and effector CD4+ T lymphocytes), natural killer cells (NK cells), dendritic cells (DCs), M1-polarized macrophages and N1-polarized neutrophils[193]. The immune cells that primarily promote tumor growth are regulatory T (Treg) cells and myeloid-derived suppressor cells (MDSCs)[194].

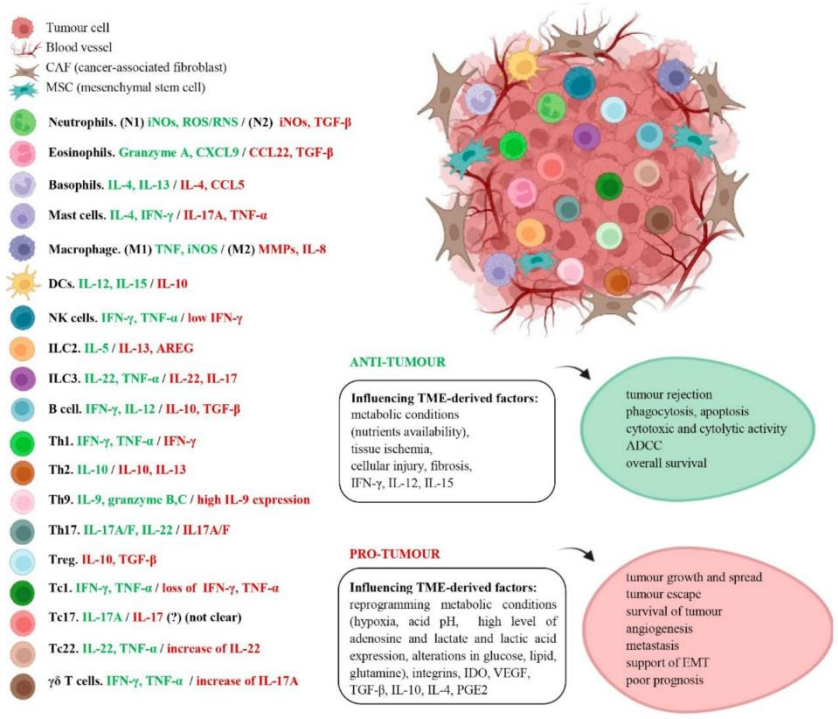

Figure 7. Immune cells composition of the tumor microenvironment
Taken from Peña-Romero and Orenes-Piñero, 2022[195].

3.3.1. Role of T Cells in the Tumor Microenvironment

T cells are an important class of immune cells. Under normal circumstances, the T cell population and their subsets is relatively stable in the surrounding tissues[196]. T cells in spleen, lymph nodes, and peripheral blood account for approximately 30%, 75% and 60% to 80% of immune cells, respectively. Changes in the total amount and proportion of T cells or their subpopulations are indicative of immune abnormalities linked to the occurrence and development of certain diseases[197].

With highly heterogeneous cell populations, T cells can be classified into distinct groups and subsets, mainly based on the composition of the T cell receptor (TCR) double peptide chain, the expression of surface CD molecules, and the functional characteristics of γδ T cells.

According to the composition of the TCR double peptide chain, it can classification includes αβ T cells and γδ T cells[198]. αβ T cells are the primary T cells in the adaptive immune response, accounting for 90% to 95% of T lymphocytes in peripheral blood. These cells have a CD3+ CD2+ CD4+ CD8- (or CD4- CD8+) phenotype[199]. γδ T cells are one type of lymphocyte that is innate and can be categorized into different functional groups, including primary/naive T cells (Tn), effector T lymphocytes (Te), helper T cells (Th), memory T cells (Tm), Treg cells and cytotoxic T cells (Tc)[200].

Mature T cells can be categorized as CD4+CD8- or CD4-CD8+ cells based on the presence of CD4 and CD8 molecules[201]. According to the CD45 molecular isoforms on the cell surface, CD4+ cells can be classified into two subtypes: CD45RA+ and CD45RO+ T cells, which are the essential characteristics of naive T cells and memory T cells, respectively[202].

3.3.1.1 Role of CD8+ T Cells in the Tumor Microenvironment

As the main lymphocytes, CD8+ T cells are essential in antitumor immune responses. These cells inhibit tumor growth and destroy the spread of cancer by directly identifying and eliminating malignant cells[203]. CD8+ T cells are considered an indicator of cancer regression[204], and activation is initiated through T cell receptor (TCR) binding to antigenic peptides produced by major histocompatibility complex class I molecules (MHC-I)[205]. Once activated, they proliferate and differentiate into effector CD8+ cytotoxic T lymphocytes (CTL)[206], which target infected cells and ultimately eliminate tumor cells (Figure 8).

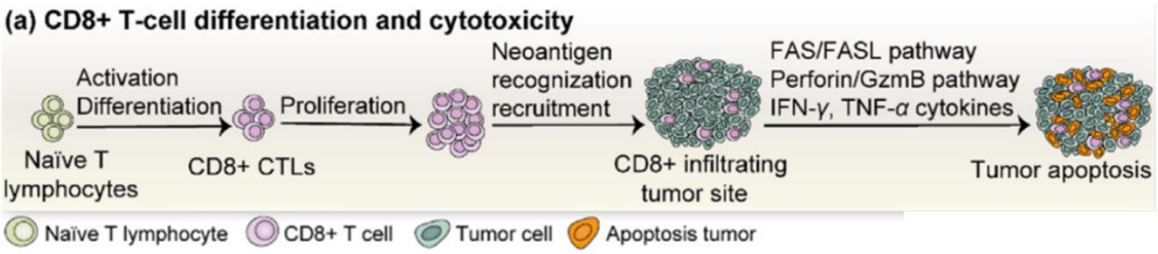

Figure 8. Infiltration of CD8+ T cells into tumors
Taken from Xie et al., 2021[207].

Immune checkpoints are crucial in regulating CD8+ T cell activation and serve as the key signaling axis for controlling the exhaustion of tumor-specific CD8+ T cells[208–210]. There is a positive association between the quantity and distribution of CD8+ T lymphocytes at the location of tumors and the clinical diagnosis of multiple types of tumors and patient prognosis[211]. However, during the process of tumor metastasis, the efficacy of CD8+ T lymphocytes is easily damaged[212], and their concentration, especially the concentration of CTL, is extremely responsive to inflammatory factors that either promote or suppress the TME[213].

Overall, CD8+ T cells protect normal host tissues, inhibit virus-infected cells, and destroy tumor cells[214]. However, tumor dynamic interactions are complex, immune responses in the TME are suppressed, and tumors progress through local invasion and distant metastasis. Tumor-associated stromal cells and immune cells jointly shape the TME[215], impairing the recruitment, activation, and cytotoxicity of CD8+ T lymphocytes (Figure 9). Therefore, an in-depth study of the interplay among CD8+ T lymphocytes and the TME has crucial clinical value for developing new antitumor immunotherapies[216].

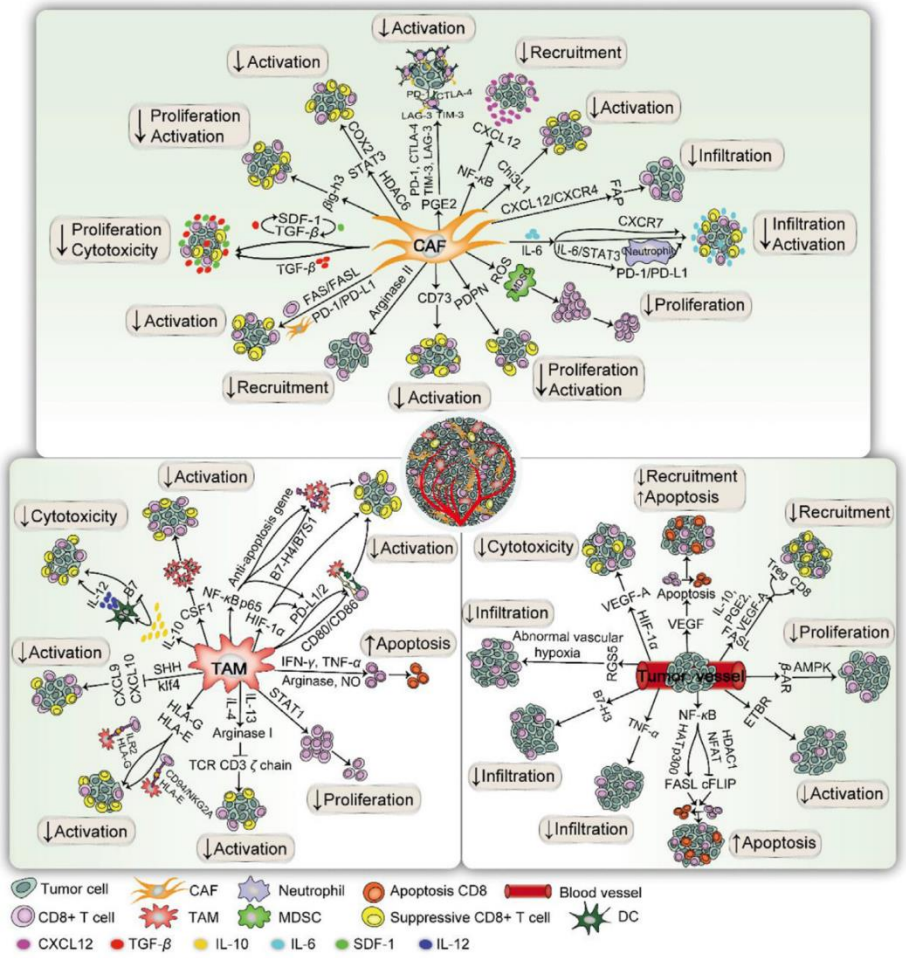

Figure 9. Suppressive immunization regulation of CD8+ T cells with stromal cells in the TME
Taken from Xie et al., 2021[207].

3.3.1.2 Role of CD4+T Cells in Tumor Microenvironment

CD4+ T cells referred to as helper T lymphocytes (Th cells), serve as central coordinators in immune responses and significantly affect the amplification and regulation of cellular immune responses[217]. Its activation signal initially comes from the interaction of the TCR and MHCII-antigen peptide complex[218]. Naive CD4+ T lymphocytes (Th0) were distinguished into multiple subgroups, comprising Th1, Th2, Th17, Tfh, and Treg[219], each with unique functions in the TME (Figure 10). These Th lymphocytes play a key role in promoting an efficient imuune response against tumors, regulating adaptive immune responses, and influencing the TME, and are considered potential targets for immunotherapy[220].

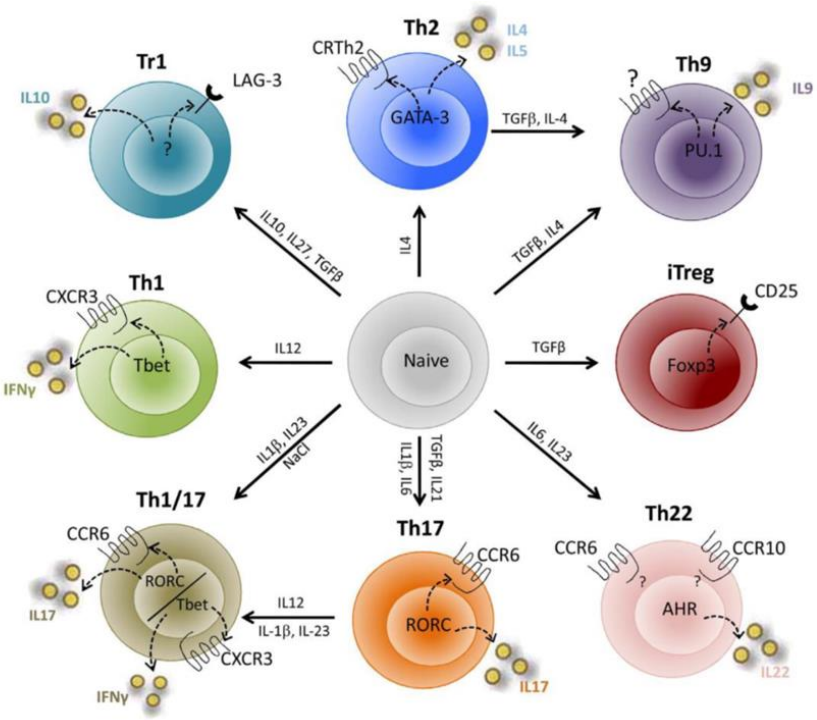

Figure 10. CD4+ T cell subsets
Taken from Belikov, 2016[221].

Th1 releases cytokines, including IFN-γ, interleukin (IL)-2, and TNF-β[222], which are crucial for stimulating CD8+ T lymphocytes and inhibiting tumor development. However, the immunosuppressive properties of the TME may impede the transformation of Th0 cells into Th1 cells[223,224]. In contrast, Th2 releases IL-4, IL-5, IL-10, IL-13, and other cytokines, inhibiting the differentiation of Th0 cells into Th1 cells and promoting tumor-associated macrophages (TAMs) and immunosuppressive cell proliferation and differentiation[225]. The TME immunosuppression determines the drift of Th1/Th2 ratio onto Th2 cells within the tissues of

cancer. Therefore, the Th1/Th2 ratio is also commonly used to predict the efficacy of antitumor drugs and tumor prognosis[226].

Tregs are a discrete subgroup of the CD4+ T lymphocytes family that exhibit distinctive phenotypes and functions. Treg cells provide immunosuppressive effects to counteract aberrant immunological responses resulting from excessive activation of autoreactive T lymphocytes to maintain autoimmune tolerance and immune homeostasis[227]. Conversely, Treg cells suppress the activity of CD8+ T lymphocytes in the TME by releasing inhibitory substances such as IL-10 and TGF-β, and influencing the development of DCs[228]. Further, it induces immune evasion by tumors and thus emerges as a promising focus for medical treatment. It reported that the through anti-CTLA-antibody inhibition of Tregs can enhance the killing function of effector T lymphocytes and improve antitumor efficacy[229,230].

The TME exhibited a substantial rise in the proportion of Th17 cells. Th17 secretes cytokines like IL-17F, IL-21, IL-22, and IFN-γ, inhibiting tumor growth and proliferation through antitumor angiogenesis and attracting and activating CD8+ T cells[231]. Th17 not only has antitumor effects but also has tumor-promoting effects[232]. Promote tumor development and proliferation by releasing immunosuppressive substances, like IL-10. Therefore, the function of Th17 in the TME needs to be explored further[233,234].

Th9 cells exhibit better antitumor properties than Th1 and Th17[235–243], but may also promote tumor growth[244]. Th22 cells play major functions in mucosal defense, tissue repair, and wound healing, but their overexpression may lead to tumor growth[245].

Overall, subsets of CD4+ T lymphocytes exhibit distinct functional roles in tumor tissues, with some promoting immune responses against tumors and others supporting tumor development. Their interactions are regulated by multiple factors in the TME, which is vital to better understanding and developing novel anticancer immunotherapies[246].

3.3.2. Role of B Cells in the Tumor Microenvironment

B cells, as specialized immune cells, have the responsibility of producing antibodies, antigen presentation, and cytokine secretion[247], play a pivotal role in tumorigenesis[248]. They tend to accumulate at tumor margins, particularly in adjacent lymph nodes close to the TME[249]. Although fewer B cells infiltrate the TME compared to T cells, they can still exert pro- and antitumor roles[250].

Traditionally viewed B cell as having predominantly tumor-promoting functions[251]. B cells were thought to facilitate the expansion and advancement through the production of immune complexes[252] and antitumor antibodies[253,254]. In human studies, tumors with high B cell infiltration are linked to poor outcomes and heightened invasiveness[255,256]. Similar to Tregs, Breg cells stimulate tumor invasion[257] by producing IL-10 and TGF-β cytokines that promote the immunosuppressive phenotype of macrophages, neutrophils, and cytotoxic T cells[258].

However, further studies in recent years have found that B cells also have antitumor immune effects[259] (Figure 11). An analysis of 69 existing studies found that more than half reported that B cell infiltration was associated with a positive patient prognosis[260]. B cells can cluster around tumor margins, forming intricate tumor-associated immunological aggregates, for example, tumor-associated tertiary lymphoid structures (TLS)[261]. The formation of TLS contributed by B cells facilitates the maturation and subtype switching of B cells that are specific to tumors, and they also play a role in the formation of T cell responses that are unique to tumors[262]. TLS composition varies according to tumor stage and origin, and its presence has prognostic implications for various cancers[263]. B cells be considered crucial cancer predictors[260], engage in antigen-specific interactions with T cells, notably within TLS and tumor-infiltrating lymphocyte populations[264]. Their antigen presentation to CD4+ and CD8+ T cells and generates antigen-specific immune responses in the TME[265,266].

The various immunotherapy modalities are based on the dual function of B cells in TME[267–270].

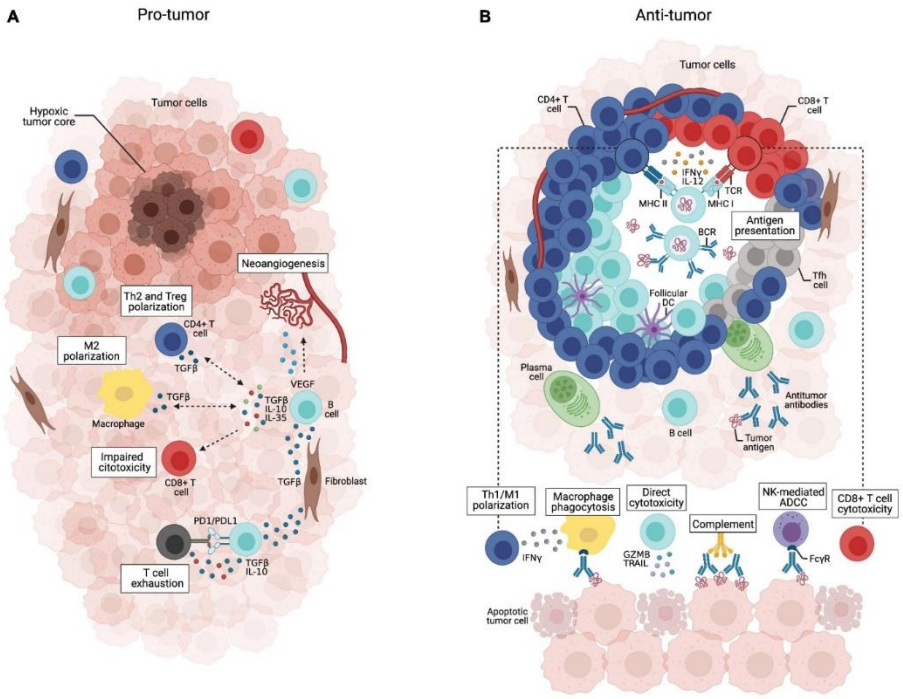

Figure 11. Dual role of tumor-infiltrating B cells

Ttaken from Kinker, 2021[265].

3.3.3. Role of NK cells in Tumor Microenvironment

Discovered in 1973, NK cells are lymphocyte-like cytotoxic innate immune cells[271], essential to innate immunity, with a natural capacity to eliminate tumor cells and infected cells[272–274]. Functionally, NK cells participate in the process of cellular-mediated tumor cell elimination or secreting inflammatory cytokines[275]. Unlike T and B cells, NK cells may recognize and kill target cells without specific antigen-sensitizing signals[276].

In addition, Street et al.[277] found the cytotoxic effect of NK cells plays a vital role in inhibiting tumor growth. Imai et al.[278] evaluated the cytotoxicity of NK cells in the peripheral blood of tumor patients and revealed that tumor metastasis is closely related to low activity NK cells. The degree of NK cells infiltration in the malignancy region influences the effect of immunotherapy[279,280], and the recruitment of targeted NK cells to the malignancy can effectively improve the antitumor immune response[281]. NK cells also contribute significantly to enhancing the antitumor ability of others immune cells. Specifically, NK cells generate a range of pro-inflammatory cytokines, such as IFN-γ, GM-CSGF, TNF, etc[282,283].

NK cell activity can be determined by regulating the negative signals induced by inhibitory receptors on the surface of NK cells or positive signals delivered by activating receptors[284]. MHC I molecules on the surface of normal cells can attach to the inhibiting receptors located on the surface of NK cells[285], thereby controlling the killing function of NK cells[286–288]. Surface receptors that have an inhibitory function on NK cells are usually dominant under normal physiological conditions. However, when tumors appear in the body, the activation signal induced by the activation receptor is stronger than the inhibition receptor's, prompting NK cells to play a cytotoxic role[289–292].

The effector function of NK cells is determined due to the existence of activation and inhibitory receptors on their cell surface[293]. Changes in the presentation of corresponding ligands on the surface of malignant cells also affect the balance of the receptor signals and the activation of NK cells[294–296]. NK cells are the main defense against malignant cells. They are very effective in eliminating circulating malignant cells but less efficient in TME[297].

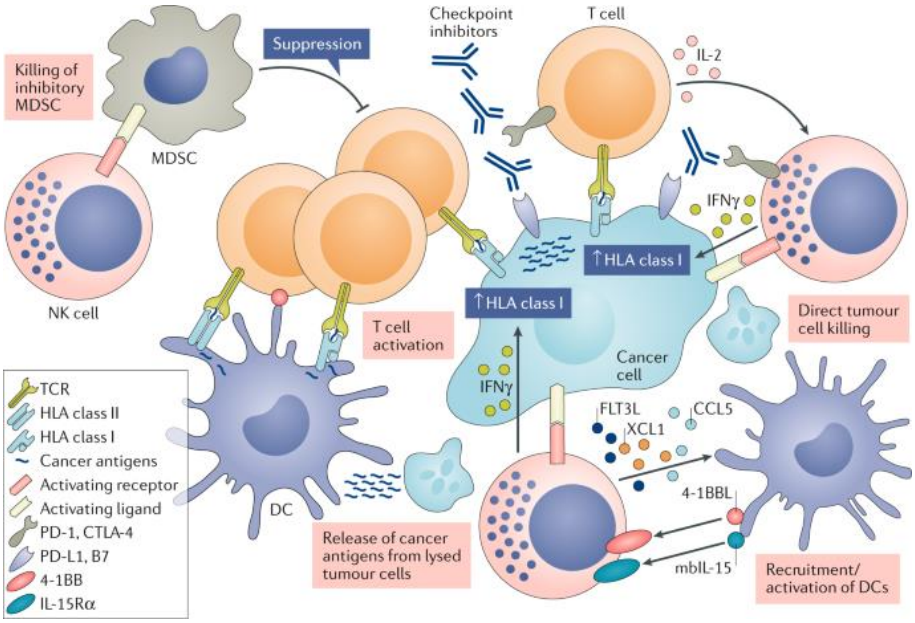

Figure 12. NK cells for cancer immunotherapy
Taken from Shimasaki et al., 2020[297]

3.3.4. Granulocytes and Neutrophils

Granulocytes are a type of white blood cells, including neutrophils, eosinophils, and basophils[298]. Their cytoplasm contains enzymatic granules. The function of each kind of granulocyte is unique. Within that group, neutrophils are the most prevalent form of granulocyte in the body, accounting for two-thirds of all white blood cells, accounting for approximately 40% to 60%[299,300]. Neutrophils are crucial in fighting infections and maintaining immunological balance. In the TME, tumor-associated neutrophils (TANs) are also involved in complex antitumor and pro-tumor processes[301–303].

Neutrophils with antitumor effects are called "N1" TANs, whereas those with protumor effects are referred to as "N2" TANs. TME affects the equilibrium of N1 and N2 subsets through secretion of various cytokines[304–306]. TANs engage with other lymphocytes inside the TME and modulate their function[307]. In mice with 4T1 tumors, N2 TANs inhibited the ability of NK cell to eliminate tumor cells, thereby promoting malignant metastasis[308]. In contrast, N1 TANs produce chemokines that recruit CD8+ T cells to the TME[309,310]. They release cytokines to stimulate cytotoxic CD8+ T lymphocytes, promoting antitumor effects[311,312].

Neutrophils could contribute to the abscopal effect. Takeshima et al.,[313] study showed the TANs recruited by RT cause sterile inflammation, ultimately activating tumor-specific cytotoxic T lymphocytes, recruiting them to the location of the malignancy, and causing malignancy

regression. This is also consistent with the research conclusion of Faraoni et al.,[314] that TANs affect the appearance of the abscopal effect. Although the above studies indicate that neutrophils might have a beneficial impact on the abscopal effect, it is also important to note that neutrophils may participate in immunosuppression[315] under certain circumstances, negatively impacting the abscopal effect.

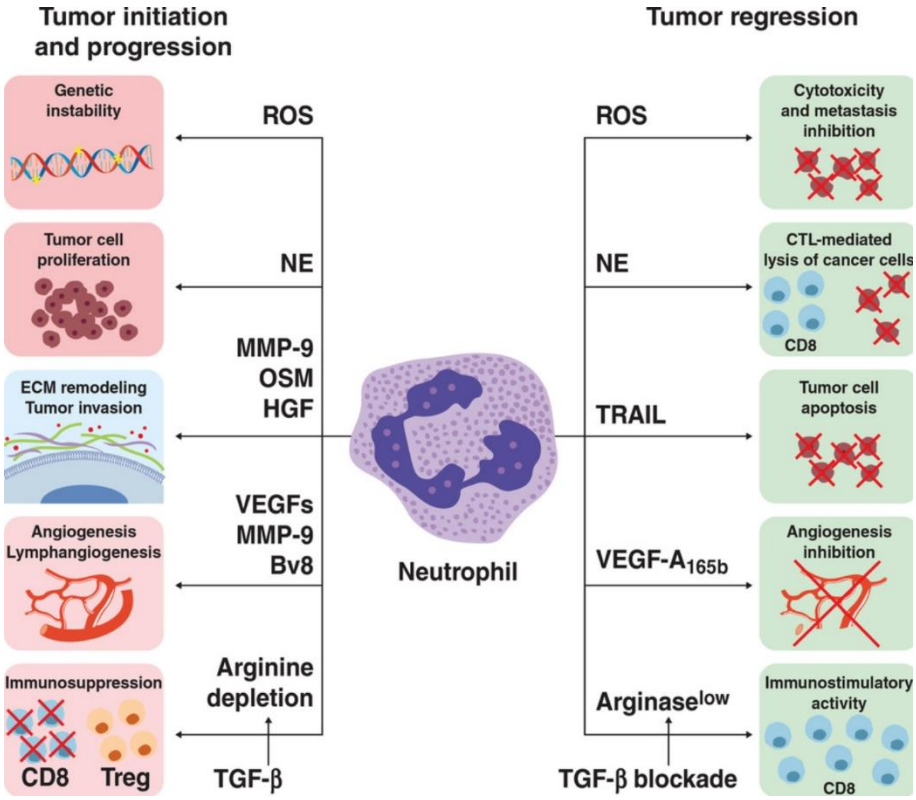

Figure 13. Dual role of neutrophils in cancer-related inflammation
Taken from Galdiero et al., 2018[312]

3.4 Aim of the Thesis

Cancer remains a significant disease that seriously threatens human health. In NSCLC, RT is a crucial treatment. Approximately 60%-70% of NSCLC individuals obtain RT while undergoing treatment.

With the continuous advancement of technology and comprehensive RT, the status of high-dose radiotherapy (HDRT) is gradually rising. HDRT may direct malignant cell death, increase tumor necrosis, generate tumor antigens, stimulate the immune system, and transform the TME from an immune desert state to an inflamed state with immune cell infiltration[316]. The abscopal effect observed in rare HDRT cases can extend local therapeutic effects to systemic antitumor effects. Although immune checkpoint blockade improves the survival rate of locally

advanced and metastatic NSCLC, majority individuals be unsuccessful in demonstrate an optimal reaction to anti-PD-1/anti-PD-L1 monoclonal antibodies.

With the rise of immunotherapy, reports of the abscopal effects have gradually increased. Therefore, therapies that induce the abscopal effects may positively impact treating patients with advanced metastatic malignancies. Nevertheless, the specific mechanism of the abscopal effect remains uncertain. Therefore, establishing the abscopal effect animal models will provide an experimental platform for in-depth research of the molecular mechanisms underlying the abscopal effects, which is expected to improve existing treatment options or develop new treatments. The objectives of the present investigation are:

1. To study the therapeutic effect of RT combined with anti-PD-1 therapy on tumor-bearing mice;

2. To study the impact of different RT doses on treatment based on similar BED;

3. To explore the link between the induction of the abscopal effect and the dosage.

4. MATERIAL AND METHODS

4.1 Materials

4.1.1. Chemicals and Solutions

Product	**Company**
ACK lysis buffer	Gibco
Brefeldin A	BioLegend
CD8a Microbeads	Miltenyi Biotec
DMEM (1x)	Gibco
DMSO	ITW Reagents
DPBS (1x) (w/o Ca and Mg)	Gibco
DPBS (1x) (with Ca and Mg)	Gibco
Ethanol	Carlroth
FBS	Gibco
Heparin	BBraun
IL-2	BioLegend
Isoflurane	Piramal
Ketamine	Zoetic Inc.
L-Glutamine	Lonza/Bioyzm
LS MACS column	Miltenyi Biotec
NEAA	Gibco
Penicillin/Streptomycin	Lonza/Bioyzm
Percoll	
PBS (10x)	Invitrogen
RPMI (1x)	Gibco
Tag it-Violet	Invitrogen
True-Nuclear Transcription Factor Buffer Set	BioLegend
Trypan blue solution	Sigma
0.5% Trypsin-EDTA Solution 10X	Sigma
Xylazine	Bayer
Zombie NIR	BioLegend
β-Mercaptoethanol	Sigma

4.1.2. Buffers and Media

Buffer or Media	**Ingredients**	**Conc./Volume**
Cell culture medium	DMEM	445 mL
	FBS	10%
	Penicillin/Streptomycin	1%
cDMEM	DMEM	417 mL
	FBS	10%
	L-glutamine	1%
	NEAA	6 mL
	Sodium pyruvate	6 mL
	Sodium bicarbonate	6 mL
	Penicillin/Streptomycin	1%
	β-Mercaptoethanol	0.00168%
Dissociation buffer	RPMI	439 mL
	FBS	10%
	Penicillin/Streptomycin	1%
	Collagenase Ⅳ	(1:1000)
	Dnase I	(1:100)
	Brefeldin	(1:1000)
MACS buffer	BSA	0.5%
	EDTA	2 mM
	DPBS (w/o Ca and Mg)	
Grinding buffer	DPBS (with Ca and Mg)	480 mL
	FBS	2%
	L-glutamine	5 mL
	Penicillin/Streptomycin	1%

4.1.3. Antibodies

Product	Conjugate(s)	Clone	Company
Flow cytometry			
Nur77	FITC(Alexa Fluor™ 488)	12.14	eBioscience
CD4	PerCP/Cy5.5	GK15	BioLegend
CD49b	PE	DX5	BioLegend
CD3	PE	17A2	BioLegend
Foxp3	PE	150D	BioLegend
PD-L2 (CD273)	PE	TY25	BioLegend
Eomes	PE	X4-83	BD Biosciences
Ly6C	PE/Dazzle594	HK1.4	BioLegend
CD107a	PE/Dazzle594	1D4B	BioLegend
PD-1 (CD279)	PE/Dazzle594	29F.1A12	BioLegend
PD-L1	PE/Dazzle594	10F.9G2	BioLegend
CD103	PE/Cy7	2E7	BioLegend
CD62L	PE/Cy7	MEL-14	BioLegend
CD8	PE/Cy7	53-6.7	BioLegend
T-bet	PE/Cy7	4B10	BioLegend
NKp46	APC	29A1.4	BioLegend
CD8a	APC	53-6.7	BioLegend
CTLA-4	APC	UC10-4B9	BioLegend
Ep-CAM	APC	G8.8	BioLegend
RORγt	APC(Alexa Fluor® 647)	Q31-378	BD Biosciences
CD45	Alexa-700	30-F11	BioLegend
Ly6G	BV421	1A8	BioLegend
CD69	BV421	H1.2F3	BioLegend
Ki-67	BV421	16A8	BioLegend
GATA3	BV421	16E10A23	BioLegend
CD19	BV510	6D5	BioLegend
CD8a	BV510	53-6.7	BioLegend
CD25	BV510	PC61	BioLegend
CD11c	BV605	N418	BioLegend
CD134 (OX-40)	BV605	OX-86	BioLegend
TIM-3	BV605	RMT3-23	BioLegend

CD11b	BV650	M1/70	BioLegend
CD44	BV650	IM7	BioLegend
LAG-3	BV650	C9B7W	BioLegend
IFN-γ	BV650	XMG1.2	BioLegend
Isotype control			
Mouse IgG1, kappa	FITC (Alexa Fluor™ 488)	P3.6.2.8.1	eBioscience
Mouse IgG1, κ	PE	MOPC-21	BioLegend
Rat IgG2a, κ	PE	RTK2758	BioLegend
Rat IgG2a, κ	PE/Dazzle594	RTK2758	BioLegend
Rat IgG2b, κ	PE/Dazzle594	RTK4530	BioLegend
Armenian Hamster IgG	APC	HTK888	BioLegend
Armenian Hamster IgG	BV421	HTK888	BioLegend
Rat IgG1, κ	BV605	RTK2071	BioLegend
Rat IgG2a, κ	BV605	RTK2758	BioLegend
Rat IgG1, κ	BV650	RTK2071	BioLegend

4.1.4. Laboratory Equipment

Device	**Company**
Cytoflex S	Beckman Coulter
Cell culture centrifuge	HERMLE Labortechnik GmbH
Cell culture incubator	Axon Labortechnik GmbH
Lab centrifuge	HERMLE Labortechnik GmbH
TrueBeam STx	Varian

4.1.5. Software

Flow cytometry data analysis: CytExpert 2.3

Statistics and graphs: GraphPad PRISM, version 8.0.2

Bibliography: Zotero 6.0.8

4.2 Methods

4.2.1. Animal Experiments

The animal studies were conducted at the Security Level 1 (S1) facility. The animal experiments were designed under the German Animal Protection Act of the Cologne Government (Animal Experiment License number 81-02.04.2017.A511) and complied with the ethics committee requirements. The mice were kept in different groups of up to 5 per cage, following a 12-hour cycle of darkness and light. The food and bedding were completely sanitized. Experimental mice were scored daily and written down the score sheet.

4.2.1.1 Mouse Strains and Cell Line

Nur77 mice [C57BL/6-Tg(Nr4a1-EGFP/cre)820Khog/J] were purchased from Jackson Laboratory (strain#:016617) in this study. These mice have been genetically modified to carry green fluorescent protein fusion (GFP) protein driven by the Nur77 promoter. The experimental animals of the Nur77 line were obtained from heterozygous breeding. The cell line used in the murine flank tumor model is derived from the NSCLC Genetically Engineered Mouse Model (GEMM) [$Kras^{G12D}Tp53^{-/-}$(KP)].

4.2.1.2 Tumor Inoculation and Preparation

Tumor cells cell culture and preparation

All tumor cell lines were cultured in Dulbecco's modified Eagle's medium (DMEM; Gibco), supplemented with 10% fetal calf serum (Gibco) and 1% Penicillin/Streptomycin (Lonza). Cells were maintained at 37°C and 5% CO_2 in a humidified incubator and passaged every 3–4 days (1:10–1:20 dilution). The routine passage was performed by rinsing with phosphate-buffered saline (PBS), then incubating in 10 mL of 0.05% trypsin EDTA (Gibco) at 37°C and 5% CO_2 for 5–8 minutes, removing of cells, and centrifugating them at 500 g for 5 minutes. Cell pellets were resuspended in 10 mL fresh complete media and divided into a new Petri dish. Cells utilized for tests were kept in the log phase of growth for a minimum of 24 hours before to usage. Before inoculation, cells were washed with PBS, collected using trypsin-EDTA, subjected to centrifugation at 500 g for 5 minutes, and then suspended in fresh media. The cell count was determined using trypan blue and a hemocytometer. The counted cells were resuspended in the suitable volume of PBS to achieve the desired experiment density of $1x10^6$ cells/100 µL. The prepared cells were kept on ice before injection.

Flank tumor inoculation

The experimental mouse was placed in the anesthesia induction box connected with isoflurane. While administering the anesthesia, the oxygen flow was set at 1 L/min (the oxygen flow was reduced or increased appropriately based on the experience), and isoflurane was adjusted to the concentration of approximately 4%–5%; Isoflurane was set at a concentration of 2% to 3% when the respiratory mask was connected for sustaining the anesthesia. When the spontaneous movement of the inter tendon reflex of the mouse, the mouse was taken out of the anesthesia induction box and placed under the continuous anesthesia device. Approximately $1x10^6$ KP cells were subcutaneously injected into bilateral flanks at a dose of 100 µl per side. After subcutaneous injection, the mouse was disconnected from the continuous anesthesia and observed on the open heating plate until it recovered from anesthesia.

4.2.1.3 Tumor Irradiation

Measurement of tumor volume

A vernier caliper was used for measuring the tumor volume. It was calculated according to the formula $\mathbf{Tumor\ volume} = \frac{\mathbf{length} * (\mathbf{width})^{\mathbf{2}}}{\mathbf{2}}$ and was expressed in mm^3. The tumor volumes were measured every two days. The treatment plan was carried out when the tumor volume reached 100–200 mm^3.

Radiotherapy

Approximately $1x10^6$ cells were injected into bilateral flanks subcutaneously on day 0, as previously explained in section 4.2.1.2. After the tumor volume reached 100–200 mm^3 (18–21 days), mice were irradiated on one side of the tumor. During radiation, mice were anesthetized with ketamine (100 mg/kg) and xylazine (10 mg/kg), with a maximum injection volume of 250 µl/mouse. The mice were fixed on the operating table after the appropriate depth of anesthesia was reached. Their eyes were protected from drying by applying a small amount of eye cream. The exact position of the tumor was located with the assistance of a medical physicist, and separate experimental groups were irradiated with 24Gyx1F, 8.7Gyx5F, 8Gyx3F, 5Gyx5F, and 2Gyx5F dosages. Mice were irradiated with a TrueBeam STx machine with 9 MeV electrons, a source-to-surface distance of 100 cm, and an electron tube for 6 x 6 cm^2 fields with a cut-out of 2 cm diameter. The light field was focused on the tumor with a 5-8 mm margin to avoid scatter radiation, and all other regions were shielded. RT lasted approximately 3–5 minutes. After RT, the mice were placed on a heating pad in a quiet environment until they were fully awake. These experimental animals were transported back to room S1 in the animal facility.

4.2.1.4 Anti-PD1 Immunotherapy

Anti-PD-1 immunotherapy

When the tumor volume reached 100–200 mm^3, the mice in the experimental group intraperitoneally received anti-PD-1 immunotherapy (150 μl/mouse). The mice who were treated with RT combined with immunotherapy received anti-PD-1 injections three times per week-starting from 6 hours after RT until the animal experiment was terminated. These experimental animals were transported back to room S1 in the animal facility.

4.2.2. Organs Isolation

Preparation

Items: Clean surgical instruments, dissecting forceps, dissecting scissors, 6 cm petri dish, 1.5 mL tube, 0.5 mL syringe, 20 mL syringe, 27G needle, ice box, beaker, and aluminum foil.

Reagents: Isoflurane, PBS buffer (without calcium and magnesium), PBS buffer (with calcium and magnesium), heparin, and 20% sucrose solution.

The experiment procedure

4.2.2.1 Cardiac Perfusion

Mice were euthanized with isoflurane in sterile conditions and fixed on the operation table after confirming that breathing had stopped. The heart was fully exposed for cardiac perfusion using clean surgical instruments. A 27G needle was used to puncture the left ventricle of the heart, then inserted into the ascending aorta, and fixed it. The needle was connected with a 20 mL syringe containing PBS buffer (without calcium and magnesium). Surgical scissors were used to open the right atrial appendage and simultaneously push the syringe for cardiac perfusion. The perfusion process was stopped when the color of the lungs and liver of the mice became pale.

4.2.2.2 Target Organ Extraction:

1. Apical blood collection

The apical blood sampling of mice was carried out before the heart perfusion. After fully exposing the heart, a 0.5 mL syringe (without the dead space) was used to puncture the right ventricle of the mouse to collect apical blood. After extracting the apical blood (150–200 μL), the syringe was pulled out, and slowly injected the blood sample was transferred into a 1.5 mL tube coated with heparin. The collected blood samples were stored in the ice box until further experiments were performed.

2. Lymph nodes

Lymph nodes were collected after the cardiac perfusion. To collect the axillary lymph nodes and inguinal lymph nodes on both sides of the mouse, surgical instruments were used to fully expose the lymph nodes of the target mouse to the surgical field. The whole operation was gently performed to ensure that the integrity of the lymph nodes was not damaged while collecting them. The collected lymph nodes were placed in a 6 cm Petri dish containing PBS buffer (without calcium and magnesium), sealed with paraffin film, and placed in the ice box.

3. Tumors

Tumors were dissected entirely after cardiac perfusion. The abdominal costal tumor skin and mucosa were separated with surgical instruments, and the tumor was completely exposed to the surgical field. The tumor was dissected and separated from connective tissue along the boundary of the tumor using surgical scissors and tweezers and placed in 6 cm Petri dishes containing PBS buffer (with calcium and magnesium) in the ice box.

4. Spleen

The spleen was also harvested after cardiac perfusion. The abdominal cavity of the mouse was opened, and mice were fixed on the operating table to expose the surgical field of vision. The spleen is located on the left side of the mice. The stomach was pulled and separated from the intact spleen using surgical tweezers. The spleen was then put into a 6 cm Petri dish containing PBS buffer (without calcium and magnesium), sealed with paraffin film, and preserved in the ice box.

4.2.3. Isolation of Immune Cells

4.2.3.1 Isolation of Immune Cells from Tumors

Initially, tumor weights were determined and recorded in milligrams. Tumors were dissected into small fragments and put into a 50 mL conical tube filled with tumor dissociation buffer and DNase I (final concentration: 50 μg/mL), Collagenase IV (1:1000) and Brefeldin (1:100) (100

mg use 1 mL). The tumor samples were incubated at 37°C for 45–60 minutes on a rocker for sufficient dissociation. After digestion, tumor samples were filtered through a 70 µm cell strainer. Undigested tumor samples were grinded with a syringe plunger and rinsed with RPMI + 10% FBS buffer. The cell pellet was collected by centrifugation at 500 g for 5 minutes at 4°C. Later the pellet was resuspended in 1 mL of ACK lysis buffer and incubated at room temperature (21–23°C) for 5 minutes to remove red blood cells. After the incubation, cells were washed with PBS buffer (calcium and magnesium free). The washed cell pellet was resuspended in 30% Percoll solution, and the cells were purified by density gradient separation by centrifuging at 1800 g 20°C for 25–30 minutes. The cell pellet was obtained from the second centrifugation step, the supernatant was removed, and fresh 1 mL of PBS buffer (without calcium and magnesium) was added to resuspend the cells.

4.2.3.2 Isolation of Immune Cells from Spleen

The spleen was removed from the ice box and weight was recorded in milligrams. Then, it was placed into a 70 µm cell strainer, ground by a syringe plunger, and rinsed with PBS buffer from the filter. The spleen cell pellet was collected after centrifugation at 500 g for 5 minutes at 4°C, resuspended in 1 mL of ACK lysis buffer, and incubated at room temperature (21–23°C) for 5 minutes to remove red blood cells. After incubation, PBS buffer was used for lysis termination and washing. The spleen sample was washed with PBS buffer (without calcium and magnesium) at least 2 times, using the centrifuge at 500 g for 5 minutes at 4°C. Then, the supernatant was removed and fresh 5 mL PBS buffer (without calcium and magnesium) was added to the cell pellet to resuspend the cells.

4.2.3.3 Isolation of Immune Cells from Blood

The blood samples were placed in a 37°C water bath or a room temperature shaker for at least 15 minutes, and then 500 µl ACK lysate was added to lyse red blood cells. After incubation at room temperature for 5 minutes, the process was terminated by adding PBS buffer (without calcium and magnesium). The blood samples were washed two times with PBS buffer (without calcium and magnesium) by centrifugation at 400 g for 5 minutes. After removing the supernatant, fresh 600 µl PBS buffer (without calcium and magnesium) was added to resuspend the cells.

4.2.3.4 Isolation of Immune Cells from Lymph Nodes

Dissected lymph nodes samples were placed on the rough surface of the sliding glass. Lymph node grinding buffer (30 µl) was added to the sliding glass, and the rough surfaces of the two glass slides were ground against each other. The cells were washed from the rough surface of the slide into a 70 µm cell strainer using lymph node grinding buffer and collected into a 15 mL conical tube after filtration. The lymph node cell pellet was collected by centrifuging at 4°C for 5 minutes at 350 g. After removing the cell pellet supernatant, a fresh 600 µl PBS buffer (without calcium and magnesium) was added to resuspend the cell pellet.

4.2.4. Flow Cytometry Analysis

Staining

1. Surface staining

The single-cell suspensions were prepared by extracting the cells from different tissues (obtaining cell pellet by centrifugation) and resuspending them in 100 µl PBS buffer (without calcium and magnesium). Samples were stained with Zombie NIR (1:500) and surface staining antibodies (1:200) according to the already labeled groups and incubated at 4°C for 20 minutes. Next, samples were rinsed twice with PBS (without calcium and magnesium). The cell pellets of samples that did not require intracellular staining were fixed with 1% formalin. For intracellular staining, cell pellets were fixed with 1x transcription factor fix solution, and all samples that were resuspended in the fixatives were incubated overnight at 4°C. The samples that did not require intracellular staining were washed twice after overnight incubation with PBS (without calcium and magnesium), and 200 µl PBS (without calcium and magnesium) was used to resuspend cells before the flow cytometry measurements.

2. Intracellular staining

The cell samples were washed after overnight incubation with 1x Perm buffer, the cell pellet was resuspended in 100 µl of 1x Perm buffer, and 1 µl of the corresponding type of fluorescent antibodies (Nur77, Foxp-3, Ki-64, T-bet, RORγt, GATA3, and Eomes) were added. The samples were incubated at room temperature for 30 minutes while being shielded from light and then washed with 1x Perm and PBS buffer (centrifugation at 500 g and 4°C for 5 minutes). After washing, added 200 µl PBS buffer (without calcium and magnesium) was added to resuspend the cells before flow cytometry measurements.

Flow cytometry measurements

All samples were placed in the flow cytometer for measurement and data collection. The total sample to be taken was set at 500,000 cells or 200 µl volume. The flow cytometry data were analyzed using the CytExpert 2.3 software.

4.2.5. Statistical Analyses

Flow cytometry data were analyzed using CytExpert 2.3, and statistical analyses were conducted using GraphPad Prism 8.0.2 software. Data were reported the mean ± SD unless specified otherwise stated. Means for independent data were compared using either one-way or two-way ANOVA, followed by post hoc tests such as Tukey's, Dunnett's, or Sidak's tests to account for multiple comparisons. For mean tumor growth curves, significance was determined between treatment arms via one-way ANOVA or unpaired t-test. P-value of <0.05 was considered statistically significant. All P-values are reported as: *$p \leqslant 0.05$, **$p \leqslant 0.01$, ***$p \leqslant 0.001$, and ****$p \leqslant 0.0001$.

5. RESULTS

5.1 *In vivo* Radiotherapy Set-up and Delivery Procedure

The tumor-bearing mice were anesthetized and fixed on the bed of the RT equipment in a prone position to fully expose the tumors and irradiate them. The laser was used for positioning the beam, and electron beam RT was performed under optical guidance. The energy used for the treatment was 9 MeV, a source-to-surface distance of 100 cm, and the electron tube for 6 x 6 cm² fields with a cut-out 2 cm diameter. The light field was focused on the tumor with a 5–8 mm margin to avoid scatter radiation, and all regions were shielded.

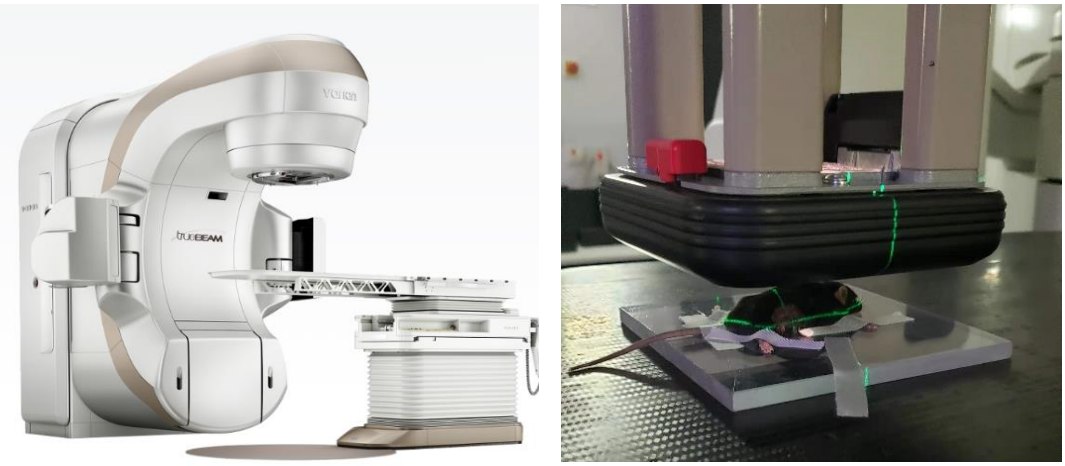

Figure 14 (Figure 5.1). Radiotherapy set up. Radiotherapy equipment TrueBeam STx machine (Left). Mice were anesthetized in the prone position, fixed on the bed, and received electron beam radiotherapy with 9 MeV energy after laser localization under optical guidance (Right).

5.2 Administration of Radiotherapy with or without Anti-PD-1 Therapy to Tumor-bearing Mice

The cell line used in the murine flank tumor model is derived from the NSCLC Genetically Engineered Mouse Model (GEMM) [$Kras^{G12D}Tp53^{-/-}$(KP)]. The mice inoculated with KP cells were divided into groups and treated with specific combinations (RT, immunotherapy, or both) to compare and evaluate the therapeutic efficacy of RT and immunotherapy in mice with flank tumors. Treatment was started when the tumors reached 100–200 mm³ in size and the particular day was recorded as Day 0 to ensure easy tumor localization and administration of RT. The tumor volumes were measured and recorded every two days using calipers. According to our experimental set-up, mice received different fractions and doses of RT (1 fraction of 24Gy and 5 fractions of 8.7Gy). The RT treatment doses were based on similar BED calculations, which were evaluated and confirmed by the radiotherapist and the radiation

technologist. A control group was set up that received only anti-PD-1 intraperitoneal injection to evaluate the effect of anti-PD-1 monotherapy. Further, an untreated control group that did not receive any treatment was set up. In the group that received RT, the primary tumor (located on one side) was treated with RT. The secondary tumor (located on the other side) was not directly irradiated and was investigated for the abscopal effect (Figure 5.2A). Data were normalized for tumor volume at the start of treatment to better compare related treatment outcomes.

The mouse group that received 8.7Gyx5F radiation dose combined with anti-PD-1 immunotherapy treatment exhibited smaller tumor volumes than the untreated control group and group received monotherapy with anti-PD-1 (Figure 5.2B above). However, statistically significant differences were observed only in comparison with the anti-PD-1 monotherapy group. In the mouse group that received only 8.7Gyx5F RT dose, tumor control was seen over time and tumor progression was observed in the untreated control group and group received monotherapy with anti-PD-1; however, statistically significant differences were not observed (Figure 5.2B above). Next, the primary and secondary tumors within the group that received 8.7Gyx5F RT combined with anti-PD-1 immunotherapy were compared, the tumor volume was statistically significant ($p = 0.0059$). However, no significant distinction was seen in the between-group comparison in the mouse group that received only 8.7Gyx5F RT (Figure 5.2B above).

The results of the mouse group that received 24Gyx1F RT showed that combining of anti-PD-1 immunotherapy with RT could relatively control the tumor progression over time. However, there is no significant difference in the statistical analysis results (Figure 5.2B below). Furthermore, the between-group comparisons of primary and secondary tumors in the groups that received 24Gyx1F RT combined with anti-PD-1 immunotherapy and 24Gyx1F RT alone indicated statistically significant differences (p values were 0.0375 and 0.0163, respectively; Figure 5.2B below).

Since the RT regimens for 8.7Gyx5F and 24Gyx1F were calculated based on the same BED and segmented accordingly, their therapeutic effects were expected to be similar. The results also confirmed that the same BED with different segmentation schemes was feasible. In the between-group comparison, the control of the primary tumor that received direct RT was better than that of the secondary tumor. However, no significant difference was found in the 8.7Gyx5F RT only group.

A.

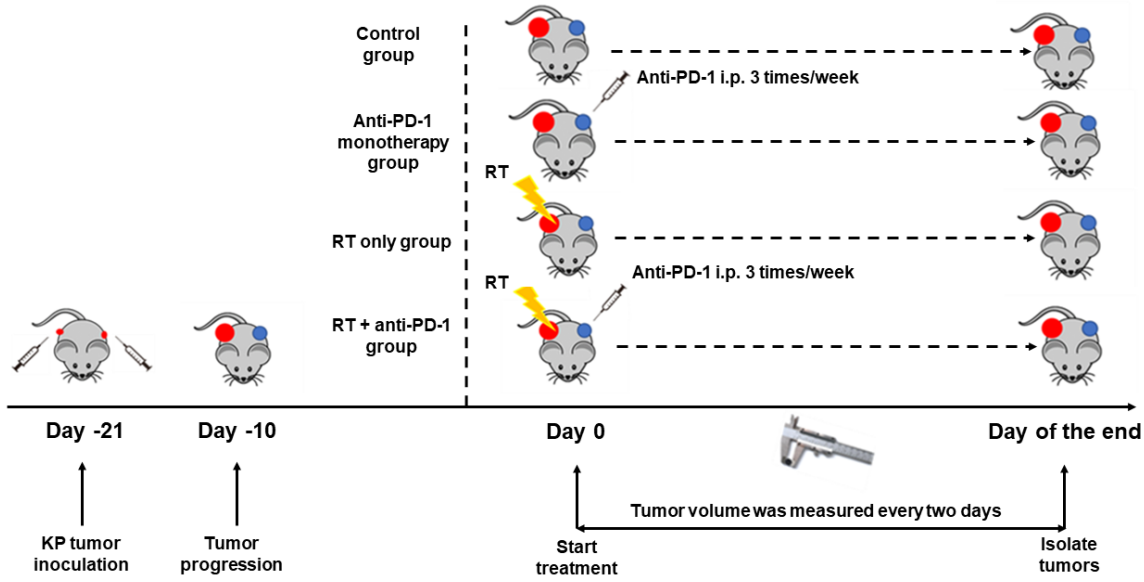

B.

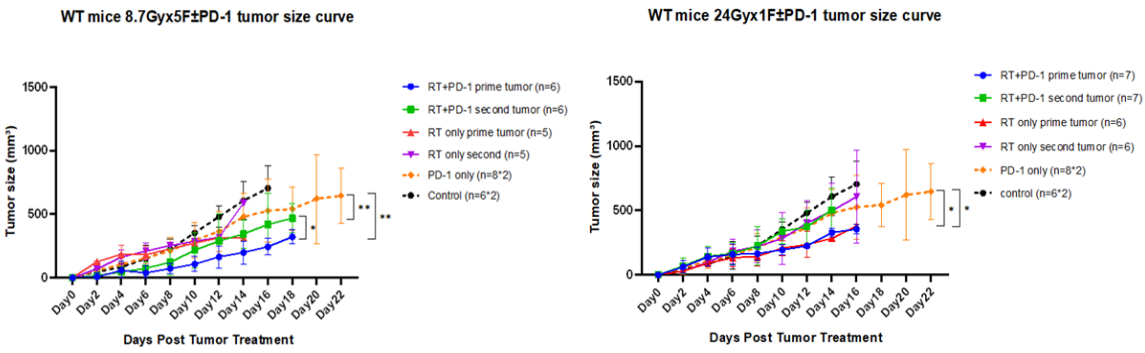

Figure 15 (Figure 5.2). Comparison of different radiation doses based on similar BED control in mice bearing flank tumors. (A) Mice experiment scheme. KP cells were inoculated flank tumor in the wild-type mice ($1x10^6$ cells/side), and tumor growth was measured with a vernier caliper every 2 days. Based on different treatment schemes, mice were divided into diverse groups. Data are representatives of different groups (n = 5–10). (B left) 8.7Gyx5F radiotherapy administered with or without anti-PD-1 treatment. (B right) 24Gyx1F radiotherapy administered with or without anti-PD-1 treatment. P values were determined by one tailed unpaired t test for pairwise comparison and one-way ANOVA with Tukey's post-test for time-associated comparison among multiple groups. *p≤0.05, **p≤0.01, ***p≤0.001, and ****p≤0.0001.

5.3 Evaluation of the Abscopal Effects of Combined Radiotherapy and Immunotherapy Treatment

The RT groups based on similar BED were simultaneously compared with the untreated control and anti-PD-1 monotherapy groups to further investigate whether RT with or without immunotherapy could induce the abscopal effect. The growth curves of tumor volume and tumor growth rate were recorded.

In comparison to the volume of the tumor in the untreated control group, the secondary tumor volume in tumor-bearing mice was relatively controlled for progression over time in all the treatment groups. However, statistical analysis revealed that compared with the ani-PD-1 monotherapy group, the secondary tumor volume significantly decreased in the group that received 8.7Gyx5F RT combined with anti-PD-1 treatment (p = 0.0018).

For comparisons of tumor growth rates, data from all groups of tumor-bearing mice could not be obtained because secondary tumors were not relatively controlled for progression over time. For example, the group receiving only 24Gyx1F radiation showed much rapid tumor progress, and the growth rate even exceeded the untreated control group. However, a statistically significant difference in secondary tumor volume was observed between the group receiving 8.7Gyx5F radiation dose combined with anti-PD-1 therapy and the group receiving only anti-PD-1 monotherapy (p = 0.0013). The tumor growth rates were calculated and plotted based on tumor volume at the start of treatment (Figure 5.3B).

While comparing RT with or without anti-PD-1 therapy depending on different fractions of similar BED, although tumor volumes were controlled by treatment over time, statistically significant differences were not observed among most groups. However, a different conclusion was obtained from comparing the tumor volumes after normalizing the tumor growth rate.

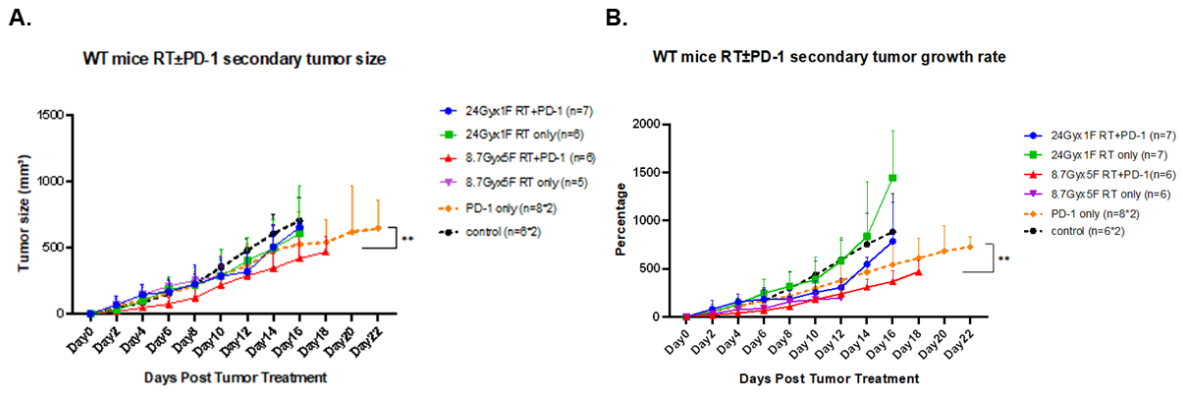

Figure 16 (Figure 5.3). Tumor burden in different mouse groups: secondary tumor size curves and growth rate curve after radiotherapy with or without anti-PD-1 immunotherapy. (A) KP cells were inoculated flank tumor in wild-type mice ($1x10^6$ cells/side), and tumor growth was measured with a vernier caliper every 2 days. Secondary tumor is the one that was not irradiated directly. (B) KP cells were inoculated flank tumor in wild-type mice ($1x10^6$ cells/side), and tumor growth was measured with a vernier caliper every 2 days. Secondary tumor is the one that was not irradiated directly. Tumor growth rates were normalized by comparing tumor volumes to those at the start of treatment. Data are representatives of different groups (n = 5–10). P values were determined by one-way ANOVA with Tukey's post-test for time-associated comparison among multiple groups. *p≤0.05, **p≤0.01, ***p≤0.001, and ****p≤0.0001.

5.4 Analysis of Cell Death and Expression of Cell Surface Antibodies in Secondary Tumor Tissues

Flow cytometry was performed to quantitatively compare cell death and cell surface antibody expression in secondary tumor tissues. Exclude adhesions and cellular debris based on forward scatter area (FSC-A) versus side scatter (SSA) and height (FSC-H) and ignore adhesions and cells by gating on Zombie NIR positive cells for dead cell fragments. The living cell population with CD45+ surface expression was selected to label leukocytes. Since the cells detected by this channels setting are derived from single cell suspensions prepared from tumor tissue, CD45- surface expression is defined as tumor cells. After labeling tumor cells was complete, EpCAM, PD-L1, and PD-L2 surface expression was assessed in all tumor cells (Figure 5.4A).

The impact of tumor weight and necrosis was excluded by considering only the quantitative comparison of cell counts. Flow cytometry-based analysis revealed that the living cell counts in the treatment groups were lower than those in the untreated control group, except for the counts in the 8.7Gyx5F RT combined with anti-PD-1 immunotherapy group. Nevertheless, the disparity did not reach statistical significance (Figure 5.4B). Notably, in the 8.7Gyx5F RT group treated with a combination of anti-PD-1 immunotherapy, the living cell count of the secondary tumor tissue was significantly different from the that in the treatment group receiving only 8.7Gyx5F RT ($p = 0.0035$). Although radiation regimens of 8.7Gyx5F and 24Gyx1F RT had the same BED, a statistically significant difference was also observed in viable cell counts in the secondary tumor after two different radiation doses ($p = 0.0176$). The difference in living cell counts between the 8.7Gyx5F RT combined with anti-PD-1 immunotherapy group and the anti-PD-1 monotherapy group was statistically significant ($p = 0.0009$; Figure 5.4B).

The flow cytometry-based quantitative analysis of tumor cells and leukocytes in the secondary tumor yielded similar results. Notably, leukocyte counts were significantly different between the 8.7Gyx5F RT combined with anti-PD-1 immunotherapy and the untreated control groups ($p = 0.0017$; Figure 5.4B).

Furthermore, the presentation of specific antibodies on the surface of secondary tumor cells in different treatment groups was analyzed by flow cytometry. In all RT groups, the expression of EpCAM and PD-L1 on tumor cells did not significantly change compared with that in the untreated group (Fig. 5.4C). Conversely, the expression of PD-L2 was dramatically reduced in treated groups compared to the untreated group ($p \leqslant 0.0001$; Figure 5.4C).

A. Gating strategy to identify tumor cells and tumor cell surface antibody expression

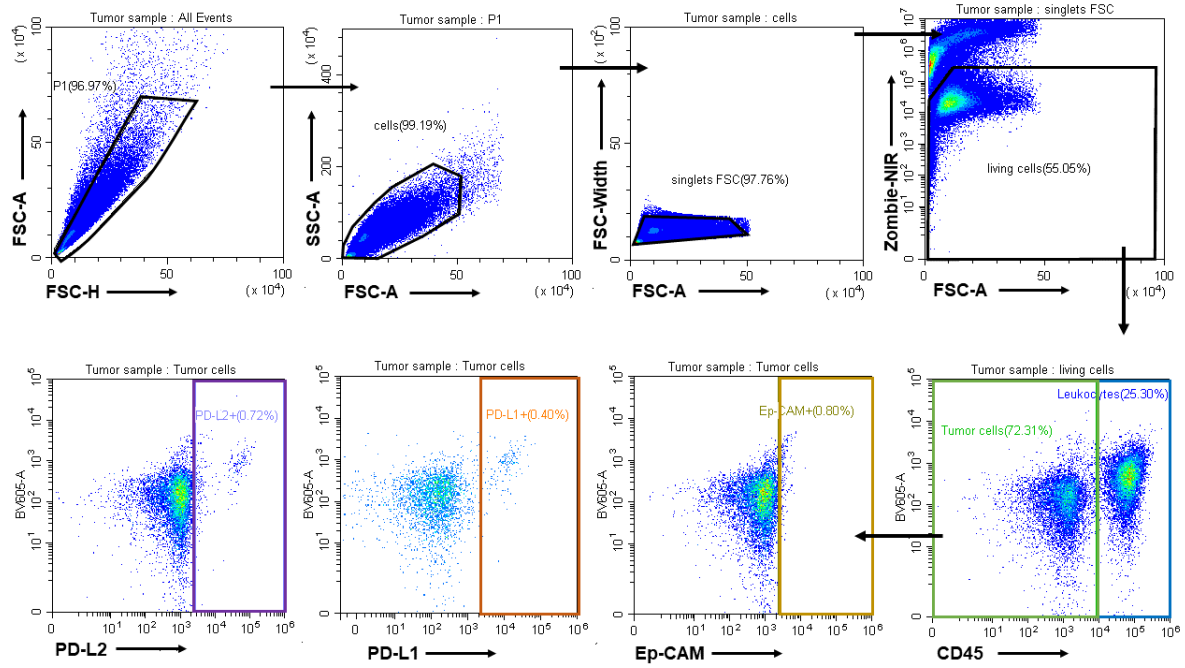

B.

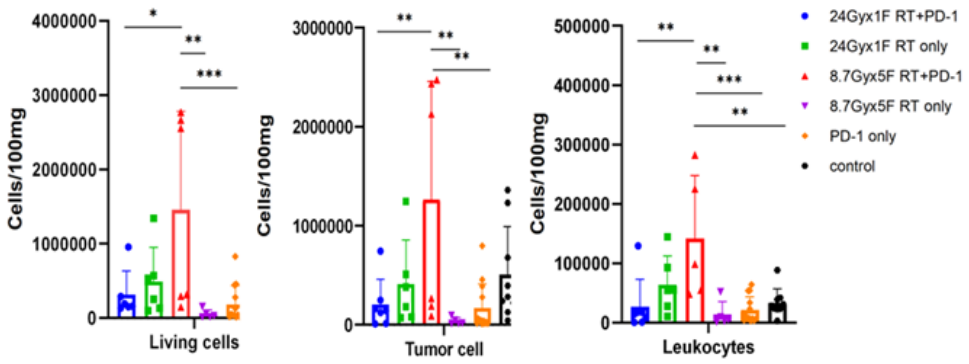

C.

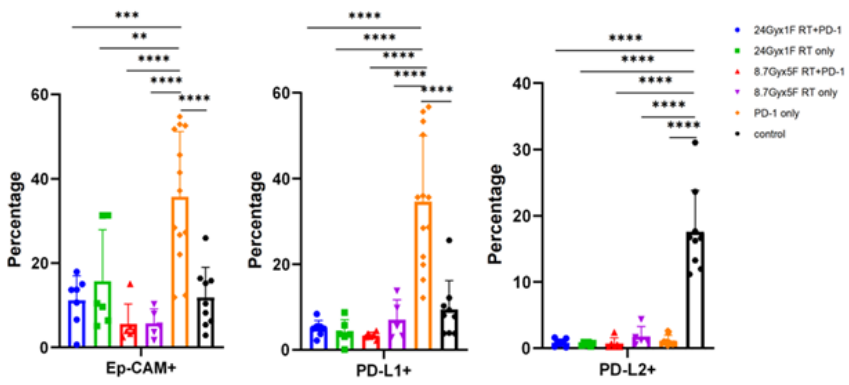

Figure 17 (Figure 5.4). Flow cytometric gating strategy and analysis to identify tumor cells surface antibodies of interest. (A) Quantification of representative flow cytometry staining of tumor cells and corresponding cell number (B) percentages of tumor cells showing EpCAM, PD-L1, and PD-L2 expression (C) in the secondary tumor after treatment (n = 5-10 mice/group). P values were determined by one-way ANOVA with Tukey's post-test for time-associated comparison among multiple groups. *p≤0.05, **p≤0.01, ***p≤0.001, and ****p≤0.0001.

Although there was not a noticeable statistical distinction among the groups that received the same irradiated dose with or without anti-PD-1 immunotherapy, a comparative analysis was performed between all the groups that received RT and those that received anti-PD-1 monotherapy. The results indicated that the expressions of EpCAM and PD-L1 in tumor cells from the groups that received RT were statistically different from those in the group receiving anti-PD-1 monotherapy (Figure 5.4C).

5.5 Analysis of Immune Cell Expression in Secondary Tumors

Next, using flow cytometry to evaluate different therapies that might induce changes in the immune infiltration into the tumor, tumor samples from different treated groups were analyzed for immune cell populations. Cellular debris was excluded depended on FSC-A versus SSA and doublets by FSC-H versus FSC-A. Exclusion of deceased cells were achieved by applying a gating strategy that specifically targeted cells that did not exhibit Zombie NIR fluorescence. All immune cells were identified by CD45+ surface expression and CD4 and CD8 surface markers were used to distinguish CD4+ T and CD8+ T subpopulations of T cells. CD8+ T cells are cytotoxic immune cells, using the Emoes+ marker to label the activated CD8+ T cells. CD4+ Th cells offer auxiliary functions to other cells of the immune system, particularly antigen-presenting cells during their activation and maturation. There are distinct subpopulations of CD4+ Th cells, including Th1, Th2, and Th17. Each subtype was differentiated from common CD4+ cells by specific cytokines as they showed distinct transcription factor and cytokine profiles. To identify Th cell subsets, T-bet+, GATA-3+, and RORγt+ markers were used for Th1, Th2, and Th17, respectively (Figure 5.5A).

Based on the flow cytometry results, I calculated the corresponding cell numbers and quantified the absolute cell numbers in addition to percentage comparisons. Notably, our results showed that the CD4+ T cell count in the secondary tumor of the 8.7Gyx5F RT combined with the anti-PD-1 immunotherapy group was markedly greater than the level noticed in the control group. No statistically significant differences were found in the CD8+ T cell counts in the secondary tumors from all the treatment groups (Figure 5.5B).

A. Gating strategy to identify cells expression

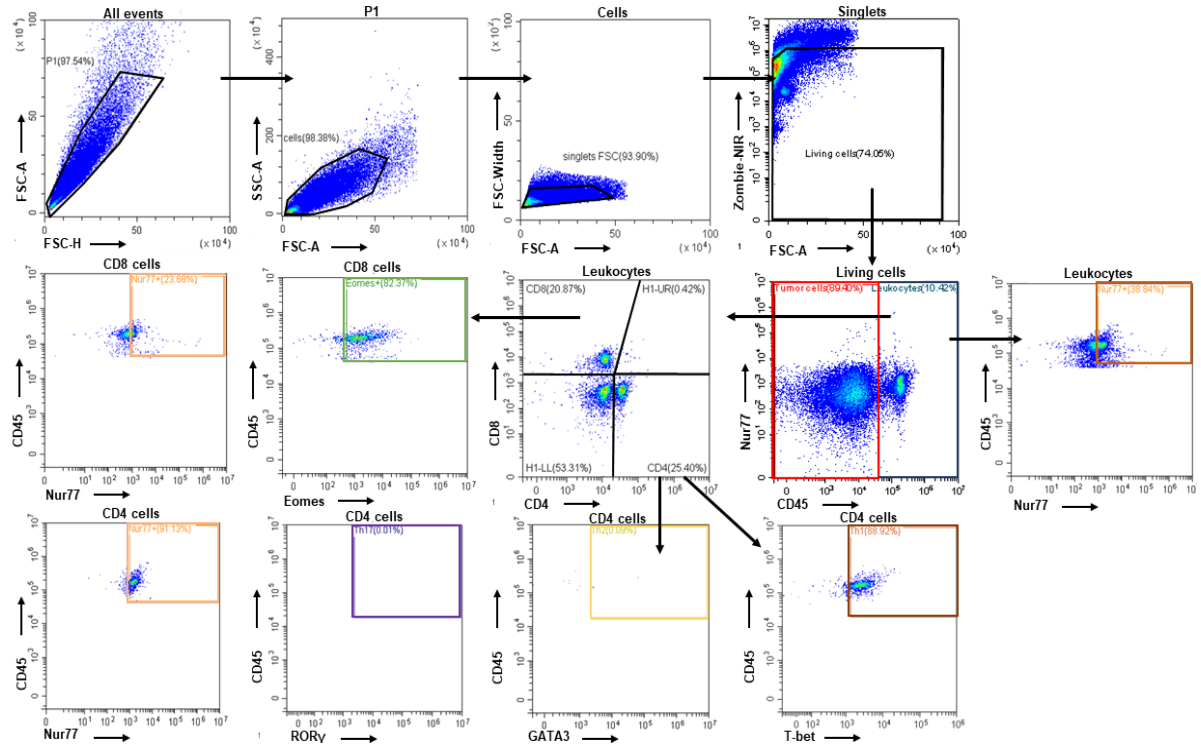

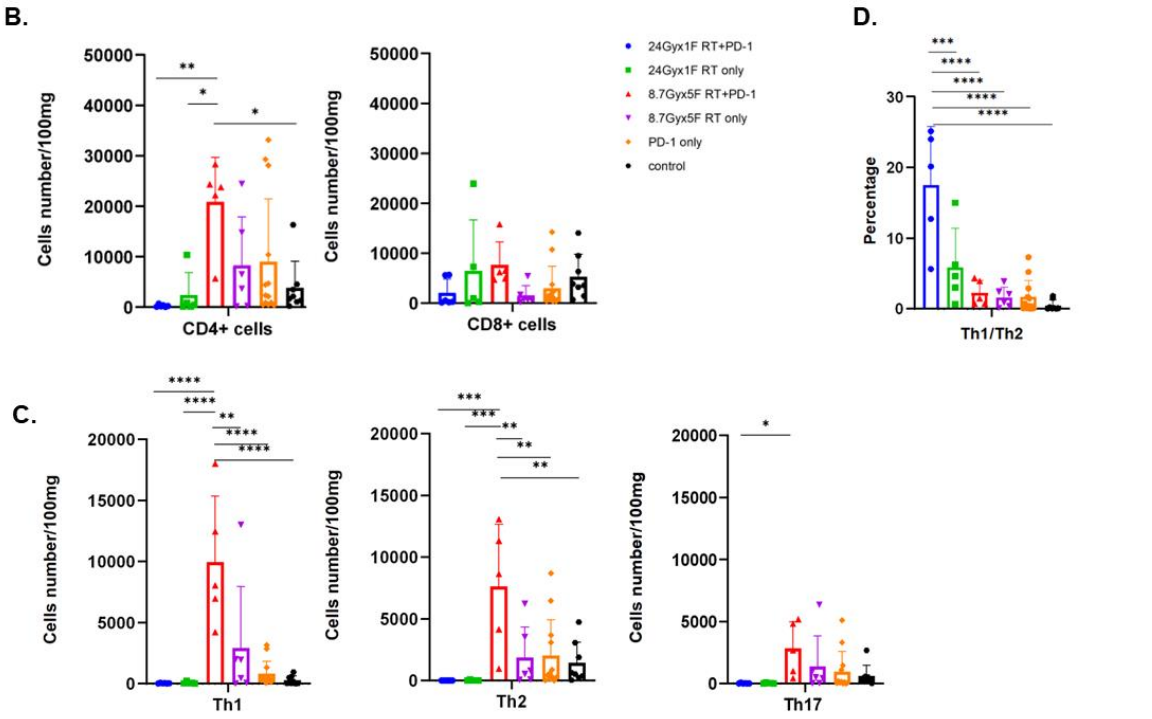

Figure 18 (Figure 5.5). Flow cytometry gating strategy and analysis to identify specific intracellular transcription factors of the immune cells. (A) Representative quantitative flow cytometry staining of CD4+ T cells and CD8+ T cells (B) and identifying Th1, Th2 and Th17 cells (C) Next, compared the Th1/Th2 ratio (D) in the secondary tumor after treatment (n = 5–10 mice/group). P values were determined by one-way ANOVA with Tukey's post-test for time-associated comparison among multiple groups. *p≤0.05, **p≤0.01, ***p≤0.001, and ****p≤0.0001.

The differences in the absolute numbers of different subpopulations of Th cells were further compared. The results revealed that the 8.7Gyx5F RT combined with the anti-PD-1 immunotherapy group had significantly higher Th1 and Th2 counts than those in other groups. However, when Th17 cell counts were analyzed, significant differences were found only in the 8.7Gyx5F RT combined with the anti-PD-1 immunotherapy group and the 24Gyx1F RT combined with the anti-PD-1 immunotherapy group (Figure 5.5C).

The value of Th1/Th2 drift is the ratio of T cell Th1/Th2 subtypes. It is crucial to acknowledge that the significance of Th1/Th2 drift is not absolute, but dynamic and can change with time and treatment. Th1/Th2 drift values need to be evaluated in a changing environment to understand the immune response better. Further, Th1/Th2 cell populations were analyzed in the non-irradiated tumors from different treatment groups. The Th1/Th2 value in the 24Gyx1F RT combined with the anti-PD-1 immunotherapy group was higher than that in the other groups, and the disparity was statistically significant (Figure 5.5D).

6. DISCUSSION

6.1 Mechanism of the Abscopal Effect is Still an Unsolved Question

RT is a highly prevalent modality for the treatment of malignancies, and the reports on radiation-induced the abscopal effects dates back to 1953[37]. In recent years, with the rise in immunotherapy-based cancer treatments, several clinical case reports on the abscopal effect have been presented, and efforts are underway to clarify the molecular mechanism of this phenomenon to reasonably utilize this effect to formulate personalized treatment plans for patients. Currently, mice are most commonly used to construct animal models and to explore the mechanism of the abscopal effect by combining RT and immunotherapy. The method involves the inoculation of tumor-inducing cells on both sides of the abdominal flanks of mice and allow them to grow into tumors. When the tumor volume reaches a certain level, the mice are treated with RT and immunization. The tumor that is not directly irradiated is defined as the secondary tumor and is observed for distant effects. Furthermore, to observing the changes in the tumor volume, tumor tissues have also been extensively evaluated[38,40,44,51,58,60,64,68,79,317–325].

All the experiments were designed based on the previous researcher. The wild-type mice were chosen for tumor-bearing mice because the complex immune environment was more convincing in the experimental results. After all, the use of nude mice does not allow rigorous research on some neo-antigens. In addition, I did not select the rectal cancer cell line with highly immunogenic because although the NSCLC is not highly immunogenic, it is the predominant form of lung cancer. The tumorigenicity of the KP cell line used in this research work has been verified in multiple investigations. The expression of EpCAM and PD-1 in the KP cell line was also tested in vitro by flow cytometry detection (data not shown). I have also conducted many tests to adjust the concentration of inoculated cells. This study needs to be designed so that the tumors do not progress too rapidly to prevent massive necrosis in the tumor tissue. The final concentration of KP cells inoculated mice was $1x10^6$ cells/ 100 µL per side.

Therefore, the wild-type mice were inoculated with NSCLC cell line (KP) that is mutant for Kras (KrasG12D) and have lost P53 ($Tp53^{-/-}$) in my experiments. After tumor formation, the health status of mice and tumor volume were recorded. RT with or without immunization was initiated after the tumor volume reached a specific average value. In this part of the experimental design, I need to solve the following problems: measurement of mouse tumor volume and

determination of tumor volume to start treatment, choice of RT dose and schedule, and choice of immunotherapy.

Based on the literature review[326], the tumor volume was calculated as: $\mathbf{Tumor\ volume} = \frac{\mathbf{length} * (\mathbf{width})^{\mathbf{2}}}{\mathbf{2}}$. In earlier experiments, we tested the conventional fractionation scheme of RT 2Gyx5F. In addition to the safety assessment, the primary consideration was to find the appropriate tumor volume to start the treatment. The treatment was started with a tumor volume of 200mm³ in consultation with a professional medical physicist. However, direct irradiation of tumors at 200 mm³ volume did not induce regression, as expected, and the progression was uncontrollable (data not shown). Therefore, in subsequent experiments, the starting tumor volume was 100 mm³. This experimental design also considered that implementing RT is very difficult if the tumor volume is too small. It is difficult to fix the tumor in actual operation, which also increases the difficulty of setting the RT plan. Simultaneously, skin damage was observed in the mice that received direct irradiation. In consultation with PI and a professional medical physicist, the Bolus used during RT was removed to reduce the amount of skin exposure and discomfort of the mice. The appropriate skincare was administered to mice, under the guidance of a veterinarian, after RT.

The next focus is on the choice of RT regimen. There is no standard treatment plan to decide the RT dose of flank tumors in mice; however, 8Gyx3F RT plans are more frequently reported in the literature. At this point, I'm still skeptical. In comparison of different RT regimens, the RT plan as a variable factor should be strictly controlled. It is worth noting that calculating of the prescribed dose of RT is not a simple mathematical operation, and the choice of RT scheme needs to be calculated according to the calculation formula of BED.

In contrast, in the published studies, the RT fractionation scheme of 8Gyx3F was often compared with the plan of 10Gyx1F[174,327,328,328–335]. After the BED calculation, we found that the BED value was 43.2 of 8Gyx3F, and the BED value was 20 of 10Gyx1F. It was clear that the BED of the two treatment regimens was different, and the difference was not slight. Of course, the status of BED in RT is clear, and its importance has been confirmed[336]. Therefore, in my experimental design, the BED calculation was carried out to design the RT segmentation plan, referring to the RT doses used by previous researchers and after confirmation by clinical medical physicians and medical physicists.

After the preliminary RT experimental protocol was determined, the next question was about the choice of the immunotherapy dosage form. In the context of previous research and clinical practice, my experimental protocol uses anti-PD-1 for immunotherapy. Similarly, the reference

of dose and cycle is also implemented in the existing research conclusions. The immunotherapy was administered intraperitoneally three times a week based on the small body weight of the mice as a dose of 150 μl. Regarding the timing of immunotherapy, although I also chose the plan of radiotherapy and then immunotherapy according to the experiments that have been completed in the past, this point is worth thinking about. The immune consolidation model of the PACIFIC study was indeed successful. However, from some real-world researches have revealed a high incidence of pneumonia in patients treated with sequential therapy. The timing of starting immunotherapy after RT may also be related to efficacy of the treatment[337].

After determining the framework of the trial protocol, direction, and some details, I selected the most commonly used 8Gyx3F radiotherapy protocol based on the published research results and designed another set of 5Gyx5F radiotherapy protocols based on the BED formula. At the beginning of the experiment, the same batch of mice was divided into treatment and control groups. The treatment group was further divided into subgroups according to RT and immunotherapy regimens. When the tumor volume increased to approximately 100 mm^3, RT was initiated according to the treatment plans; the anti-PD-1 antibodies were administered to the designated group 6 hours after RT. Notably, the frequency of 8Gyx3F RT was every other day for 3 sessions. The frequency of 5Gyx5F RT was once a day. After RT was completed, 3 weekly doses of anti-PD-1 were continued injected intraperitoneally in mice of designated groups according to the experimental plan until the tumor volume reached the end point of the study, or the experiment was terminated according to the evaluation of the status of the mice. The time from tumor inoculation to the end of the experiment was approximately 30-40 days. Unfortunately, the collected data did not yield the expected results from the analysis of tumor volume and growth rate alone (data not shown). The possible reasons may be the lack of an adequate number of mice in the groups and the mice leaving the group due to the state of the experimental mice during the intermediate and advanced phases of therapy. However, this group of experiments is not meaningless. The tumor volume analysis revealed that the simple tumor volume did not decrease significantly with the progression of the disease; it even further increased after treatment. Notably, the tumor became relatively soft to the touch, suggesting that our treatment had an effect. The control groups were refined considering that the treatment plan included combination of RT and immunotherapy. Therefore, in addition to the untreated control group, only RT and anti-PD-1 monotherapy groups were added to the experimental setup.

Based on the above reasons, the experimental plan was optimized again. In selecting the RT plan, I chose the 24Gyx1F program with the same dose as the mathematical calculation of

8Gyx3F. The high-dose single fractionation was based on the 20Gyx1F dose setting mentioned in the existing research literature and was evaluated by a professional radiation physicist. Similarly, according to the calculation of BED, the 8.7Gyx5F RT plan was formulated as a control with different segmentation methods of 24Gyx1F. A higher number of mice (n = 5–8) were included in each group in this setup. Further, the secondary tumor was evaluated for the abscopal effect. The comparison of tumor volume data showed that the tumor development was best in the 8.7Gyx5F RT combined with the immunotherapy group. The tumor growth rate was also assessed to assess the tumor growth. Notably, the results showed that the increase in tumor volume growth was accelerated in the 24Gyx1F RT only group. Therefore, the study of the abscopal effect should not only stop at the changes of the general tumor but also need to analyze the cellular and molecular level of tissues such as tumor samples.

Therefore, I performed single-cell sample preparation, and flow cytometry-based analysis of tumors and other tissues was conducted. Digestion of tumor tissue and preparation of single-cell samples have also been challenged and adjusted. Because the obtained tumor samples are from mice that have been treated and survived for a long time, necrosis occurs in the tumor samples, so it is essential to remove the necrosis and purify the sample. Further, challenges were experienced in flow cytometry gating, and the removal of adhesions once became a significant problem that hindered data analysis. The Percoll purification resolved the problems, and relatively precise gating and data analysis were performed appropriately.

Multiple researches have demonstrated that RT combined with immunotherapy has advantages in inducing systemic antitumor effects with increased immune cells in tumor tissue in comparison to that in the tissues of unirradiated mice. These observations suggest that the activation of systemic immunity is key to the abscopal effect. Therefore, white blood cell counts were analyzed in the secondary tumor tissues. Higher leukocyte counts were observed in the 8.7Gyx5F RT+anti-PD-1 immunotherapy group, suggesting activation of systemic immunity in mice. However, In the group that received the 24Gyx1F RT, the white blood cell counts were similar with and without immunotherapy groups, which possibly confirmed the conclusion of the tumor volume curve. However, 8.7Gyx5F RT-only and anti-PD-1 monotherapy groups showed much lower white blood cell counts than the other groups. Still, the curve of tumor volume showed a tumor control effect. Furthermore, CD4 and CD8 antibodies were used to differentiate the leukocytes of tumor cells, and the cytometric analysis of CD4+ T cells also supported their role in suppressing tumors.

CD4+ T cells are a highly heterogeneous group of cells. In 1986, Mosmann et al.[338] published a seminal article describing the CD4+ Th cell population as a heterogeneous subpopulation that produces cytokine classes and their functions according to CD4+ Th clones divided into two subgroups, Th1 and Th2. The homeostasis is preserved by the ratio of Th1 to Th2. An unbalanced proportion indicates the presence and progression of diverse ailments. Th1 cells have an essential role in the antitumor process, while Th2 cells significantly affect the promotion of tumors. In clinical case studies, Th2 cells predominate in tumor growth. Among them, the spite of NSCLC was positively correlated with Th2[339]. Many studies have reported that tumor tissues secrete Th2 cytokines, which is one of the mechanisms of tumor immune escape when the body is in a state of Th2 cytokine predominance. The drift between Th1 and Th2 has an essential impact on tumor immunity, and it is one of the means of tumor immunotherapy to promote the reversal of Th2 to Th1[340]. This is also reflected in the fact that there is indeed a Th2 drift in the group with poor tumor growth control in the treatment group.

To illustrate these issues further, I contrasted the expression of EpCAM, PD-L1, and PD-L2 in tumor tissues. Among the CD28 family, PD-1 is the second T-cell co-inhibitory receptor-stimulated on T cells in response to TCR activation or specific cytokines[341]. Two ligands expressed on antigen-presenting cells, PD-L1/B7-H1 and PD-L2/B7-DC, are bound to PD-1. Besides impairing early TCR/CD28 signaling, PD-1 binding to PD-L1 or PD-L2 also reduces IL-2 synthesis, T-cell proliferation, T-cell effector function, and T-cell survival. Tumor cells usually upregulate PD-L1 expression and, by binding to PD-1, inhibit antitumor T cell responses and evade immune system attack[342]. Upregulation of PD-1 expression is associated with T cell exhaustion in cancer and has been shown in multiple human tumor cells. Blocking PD-1 or PD-L1 using antagonistic monoclonal antibodies enhances antitumor activity immune response. One of the critical ligands of the PD-1 signaling pathway, PD-L2 binds to PD-1 second in importance after PD-L1. In immunotherapy, when PD-L2 and PD-L1 coexist, PD-1 preferentially binds to PD-L2. Previous studies have also confirmed that the combined analysis of PD-L2 and PD-L1 can better predict the efficacy of immunotherapy. According to my research, PD-L2 has an advantage when combining PD-1 and anti-PD-1, which supports the impact of immunotherapy. This is supported by the expression outcomes of PD-L1 and PD-L2 on the surfaces of cancerous cells. Further, EpCAM expression on tumor cells was also analyzed. The EpCAM is only expressed on tumors derived from epithelial cells, its high expression is related to tumor advancement and poor outcomes. However, in my case, there is no way to get full support from the results. Further research is needed to obtain full support for these results.

In the follow-up data analysis and literature review, another point that caught my attention: the sex of the animals. Beery and Zuker analyzed more than 2000 animal experiments and found that most researchers prefer to choose male animals for experiments, the ratio of males to females is as high as 1:5.5[343]. Because, in the past, researchers believed that male animals were used in animal experiments to avoid the interference of female estrus cycles. Compared with males, females have more obvious changes in estrogen and progesterone cycles, so it is believed that the use of male animals can yield more stable data. Recent studies have shown that the variation of various physiological indicators in female mice during the entire hormonal cycle is not more significant than that in male mice[344]. Even the individual variation of some sex-differential phenotypes in male animals is more evident than in females. Individual differences in hormone levels have implications for cancer treatment[345]. In some experiments, using a large number of male animals, will cause additional casualties, because of the possibility of biting and causing wounds/injuries. Further, it can also lead to biased experimental results by ignoring gender differences. Considering the possibility of bias, NIH recommends that all experiments currently performed on male animals can also be performed on females. Therefore, the selected animals should contain both males and females, except in some extraordinary experiments with specific requirements. Taking into account the differences in drug toxicity in different genders, an equal number of male and female animals should be included in the experimental design. If there is a significant difference in drug toxicities, the LD50 value should be determined separately for each group[346].

The analysis of lymphocytes in different strains of mice revealed sex-specific significant differences in the concentration of mouse immune cells[347]. In C57BL/6NCr mice, the results indicate that gender may affect the distribution of immune cell subpopulations in C57BL/6NCr mice. This includes significant increases in neutrophils and splenic macrophages and sex differences in changes in bone marrow B cell levels. These findings carry significant ramifications for comprehending sex-related differences in the mouse immune system and designing sex-sensitive experimental studies. Gender has long been recognized as a critical factor affecting cancer incidence, prognosis, and response to treatment[348]. In clinical cases, we can observe differences in treatment outcomes by cancer type and gender[349–353].

In summary, mice with a C57BL background were used in this study, the sex ratio of experimental mice should be controlled at 1:1, or a detailed grouping of different genders should be performed in the data analysis. This may lead to more convincing results to support the experimental hypothesis.

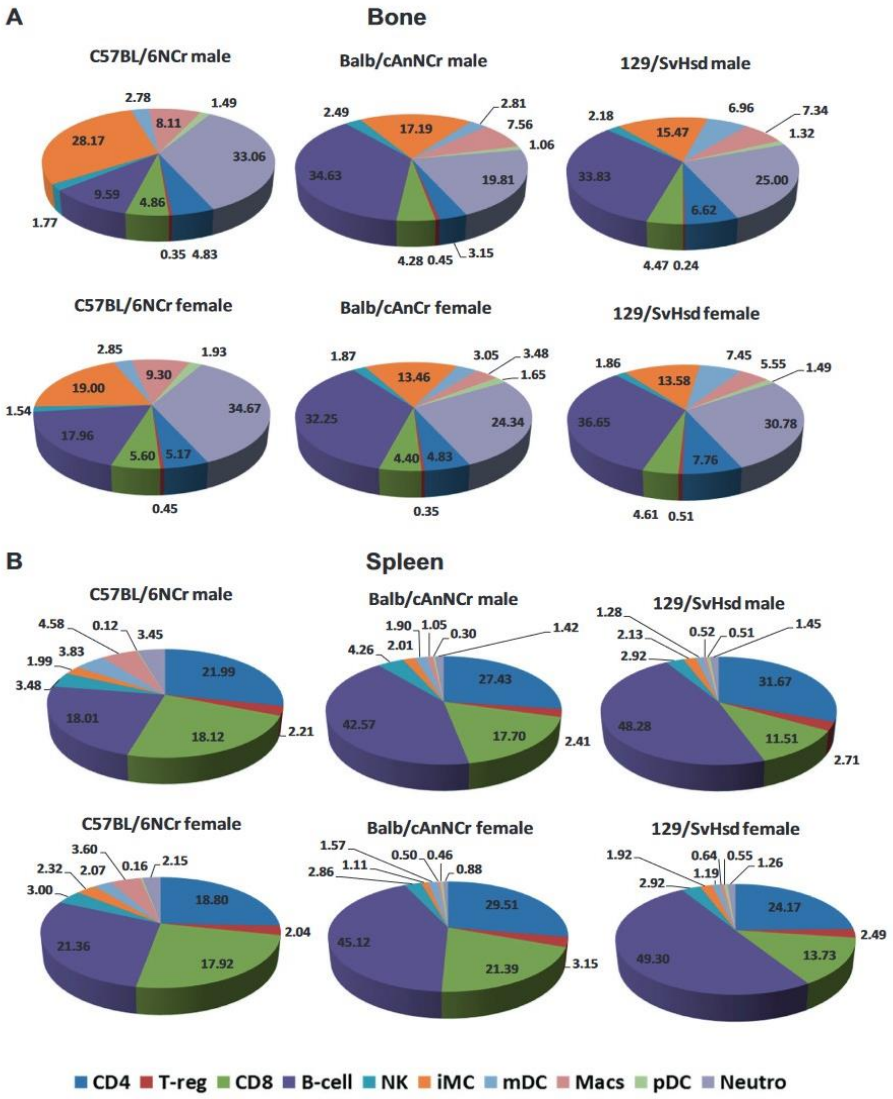

Figure 19. Strain- and gender-specific immune cell distribution of critical cell types in three mouse strains commonly used in preclinical research

Taken from Jonathan A. Hensel et al., 2019[347].

6.2 Outlook

This study validated the protocol for introducing the concept of BED in the observational study of the abscopal effects. Further, tumor samples were evaluated using different staining strategies. However, the data needs to be further optimized. For example, comparing the activation and depletion signals of B, NK, and T cells may provide more reliable evidence for the abscopal effects. The experimental protocol used in the study can be further optimized by sampling and analysis at different time points after the completion of RT because the homing and transformation time of T cells may change due to different RT regimens. Therefore, when the tumor volume reached the experimental endpoint, it may be possible that most of the T cells were already in a depleted state, resulting in the unexpected results in the parameter table of tumor volume. Moreover, it is worth noting that the observation endpoint of the tumor

volume in the published studies is set at 1500 mm^3, leaving a more extended time window to observe the treatment effect. Further, considering the possible bias because of the sex of the experiment mice, the results may be more convincing if the subgroups of genders will be compared for different parameters.

7. Literaturverzeichnis

1 Cancer statistics for the year 2020 An overview.

2 Siegel RL, Miller KD, Wagle NS, Jemal A. Cancer statistics, 2023. *CA Cancer J Clin* 2023; **73**: 17–48.

3 Cancer Facts & Figures 2022. 1930; : 80.

4 What Are the Risk Factors for Lung Cancer? | CDC. 2023; published online Aug 2. https://www.cdc.gov/cancer/lung/basic_info/risk_factors.htm (accessed Dec 8, 2023).

5 Lung cancer - Symptoms and causes. Mayo Clin. https://www.mayoclinic.org/diseases-conditions/lung-cancer/symptoms-causes/syc-20374620 (accessed Dec 8, 2023).

6 Ettinger DS, Wood DE, Aisner DL, *et al.* Non–Small Cell Lung Cancer, Version 3.2022, NCCN Clinical Practice Guidelines in Oncology. *J Natl Compr Canc Netw* 2022; **20**: 497–530.

7 Lung Cancer Signs & Symptoms | Common Symptoms of Lung Cancer. https://www.cancer.org/cancer/types/lung-cancer/detection-diagnosis-staging/signs-symptoms.html (accessed Dec 8, 2023).

8 Daniel Humberto Pozza, Ramon Bezerra Andrade de Mello. Treatment Sequencing Strategies in Lung Cancer. *Chin J Lung Cancer* 2022; **25**: 323–36.

9 Nicholson AG, Tsao MS, Beasley MB, *et al.* The 2021 WHO Classification of Lung Tumors: Impact of Advances Since 2015. *J Thorac Oncol Off Publ Int Assoc Study Lung Cancer* 2022; **17**: 362–87.

10 Amin MB, Greene FL, Edge SB, *et al.* The Eighth Edition AJCC Cancer Staging Manual: Continuing to build a bridge from a population-based to a more ‘personalized’ approach to cancer staging. *CA Cancer J Clin* 2017; **67**: 93–9.

11 Goldstraw P, Chansky K, Crowley J, *et al.* The IASLC Lung Cancer Staging Project: Proposals for Revision of the TNM Stage Groupings in the Forthcoming (Eighth) Edition of the TNM Classification for Lung Cancer. *J Thorac Oncol Off Publ Int Assoc Study Lung Cancer* 2016; **11**: 39–51.

12 Detterbeck FC. The eighth edition TNM stage classification for lung cancer: What does it mean on main street? *J Thorac Cardiovasc Surg* 2018; **155**: 356–9.

13 Lababede O, Meziane MA. The Eighth Edition of TNM Staging of Lung Cancer: Reference Chart and Diagrams. *The Oncologist* 2018; **23**: 844–8.

14 Howington JA, Blum MG, Chang AC, Balekian AA, Murthy SC. Treatment of stage I and II non-small cell lung cancer: Diagnosis and management of lung cancer, 3rd ed: American College of Chest Physicians evidence-based clinical practice guidelines. *Chest* 2013; **143**: e278S-e313S.

15 Orlowski TM, Szczesny TJ. Surgical treatment of stage III non-small cell lung cancer. *Lung Cancer Amst Neth* 2001; **34 Suppl 2**: S137-143.

16 Daly ME, Singh N, Ismaila N, *et al.* Management of Stage III Non–Small-Cell Lung Cancer: ASCO Guideline. *J Clin Oncol* 2022; **40**: 1356–84.

17 Yang C-FJ, Gu L, Shah SA, *et al.* Long-term outcomes of surgical resection for stage IV non-small-cell lung cancer: A national analysis. *Lung Cancer Amst Neth* 2018; **115**: 75–83.

18 Giaj-Levra N, Borghetti P, Bruni A, *et al.* Current radiotherapy techniques in NSCLC: challenges and potential solutions. *Expert Rev Anticancer Ther* 2020; **20**: 387–402.

19 Ma Y, Pitt JM, Li Q, Yang H. The renaissance of anti-neoplastic immunity from tumor cell demise. *Immunol Rev* 2017; **280**: 194–206.

20 Shinde A, Li R, Kim J, Salgia R, Hurria A, Amini A. Stereotactic body radiation therapy (SBRT) for early-stage lung cancer in the elderly. *Semin Oncol* 2018; **45**: 210–9.

21 Singh S, Gupta R, Singh TP, Jakhar SL, Sharma N, Kumar HS. A Comparative Study Of Concurrent Chemo-Radiotherapy With or Without Neoadjuvant Chemotherapy in Treatment of Locally Advanced Non Small Cell Lung Cancer. *Gulf J Oncolog* 2021; **1**: 62–9.

22 Iyengar P, Wardak Z, Gerber DE, *et al.* Consolidative Radiotherapy for Limited Metastatic Non-Small-Cell Lung Cancer: A Phase 2 Randomized Clinical Trial. *JAMA Oncol* 2018; **4**: e173501.

23 Herrera FG, Bourhis J, Coukos G. Radiotherapy combination opportunities leveraging immunity for the next oncology practice. *CA Cancer J Clin* 2017; **67**: 65–85.

24 Gomez DR, Blumenschein GR, Lee JJ, *et al.* Local consolidative therapy versus maintenance therapy or observation for patients with oligometastatic non-small-cell lung cancer without progression after first-line systemic therapy: a multicentre, randomised, controlled, phase 2 study. *Lancet Oncol* 2016; **17**: 1672–82.

25 Postmus PE, Kerr KM, Oudkerk M, *et al.* Early and locally advanced non-small-cell lung cancer (NSCLC): ESMO Clinical Practice Guidelines for diagnosis, treatment and follow-up. *Ann Oncol Off J Eur Soc Med Oncol* 2017; **28**: iv1–21.

26 Campisi A, Catelli C, Gabryel P, *et al.* Upfront surgery for N2 NSCLC: a large retrospective multicenter cohort study. *Gen Thorac Cardiovasc Surg* 2023; **71**: 715–22.

27 Majem M, Juan O, Insa A, *et al.* SEOM clinical guidelines for the treatment of non-small cell lung cancer (2018). *Clin Transl Oncol Off Publ Fed Span Oncol Soc Natl Cancer Inst Mex* 2019; **21**: 3–17.

28 Yoon SM, Shaikh T, Hallman M. Therapeutic management options for stage III non-small cell lung cancer. *World J Clin Oncol* 2017; **8**: 1–20.

29 Postoperative radiotherapy in non-small-cell lung cancer: systematic review and meta-analysis of individual patient data from nine randomised controlled trials. PORT Meta-analysis Trialists Group. *Lancet Lond Engl* 1998; **352**: 257–63.

30 van Meerbeeck JP, Kramer GWPM, Van Schil PEY, *et al.* Randomized controlled trial of resection versus radiotherapy after induction chemotherapy in stage IIIA-N2 non-small-cell lung cancer. *J Natl Cancer Inst* 2007; **99**: 442–50.

31 Koury J, Lucero M, Cato C, *et al.* Immunotherapies: Exploiting the Immune System for Cancer Treatment. *J Immunol Res* 2018; **2018**: 9585614.

32 Dhar R, Seethy A, Singh S, *et al.* Cancer immunotherapy: Recent advances and challenges. *J Cancer Res Ther* 2021; **17**: 834–44.

33 Islam MK, Stanslas J. Peptide-based and small molecule PD-1 and PD-L1 pharmacological modulators in the treatment of cancer. *Pharmacol Ther* 2021; **227**: 107870.

34 de Jong D, Das JP, Ma H, *et al.* Novel Targets, Novel Treatments: The Changing Landscape of Non-Small Cell Lung Cancer. *Cancers* 2023; **15**: 2855.

35 West H (Jack), Jin JO. Performance Status in Patients With Cancer. *JAMA Oncol* 2015; **1**: 998.

36 Wu Y-L, Planchard D, Lu S, *et al.* Pan-Asian adapted Clinical Practice Guidelines for the management of patients with metastatic non-small-cell lung cancer: a CSCO-ESMO initiative endorsed by JSMO, KSMO, MOS, SSO and TOS. *Ann Oncol Off J Eur Soc Med Oncol* 2019; **30**: 171–210.

37 Mole RH. Whole body irradiation; radiobiology or medicine? *Br J Radiol* 1953; **26**: 234–41.

38 Chen AC, Butler EB, Lo SS, Teh BS. Radiotherapy and the abscopal effect: insight from the past, present, and future. *J Radiat Oncol* 2015; **4**: 321–30.

39 Seiwert TY, Kiess AP. Time to Debunk an Urban Myth? The 'Abscopal Effect' With Radiation and Anti-PD-1. *J Clin Oncol Off J Am Soc Clin Oncol* 2021; **39**: 1–3.

40 Vilinovszki O, Andratschke N, Huellner M, Curioni-Fontecedro A, Kroeze SGC. True abscopal effect in a patient with metastatic non-small cell lung cancer. *Radiat Oncol* 2021; **16**: 194.

41 Nobler MP. The abscopal effect in malignant lymphoma and its relationship to lymphocyte circulation. *Radiology* 1969; **93**: 410–2.

42 Postow MA, Callahan MK, Barker CA, *et al.* Immunologic correlates of the abscopal effect in a patient with melanoma. *N Engl J Med* 2012; **366**: 925–31.

43 Wersäll PJ, Blomgren H, Pisa P, Lax I, Kälkner K-M, Svedman C. Regression of non-irradiated metastases after extracranial stereotactic radiotherapy in metastatic renal cell carcinoma. *Acta Oncol Stockh Swed* 2006; **45**: 493–7.

44 Hu ZI, McArthur HL, Ho AY. The Abscopal Effect of Radiation Therapy: What Is It and How Can We Use It in Breast Cancer? *Curr Breast Cancer Rep* 2017; **9**: 45–51.

45 Ohba K, Omagari K, Nakamura T, *et al.* Abscopal regression of hepatocellular carcinoma after radiotherapy for bone metastasis. *Gut* 1998; **43**: 575–7.

46 Golden EB, Chhabra A, Chachoua A, *et al.* Local radiotherapy and granulocyte-macrophage colony-stimulating factor to generate abscopal responses in patients with metastatic solid tumours: a proof-of-principle trial. *Lancet Oncol* 2015; **16**: 795–803.

47 Ali Mohammad S, Hak A, Pogu SV, Rengan AK. Radiotherapy, photodynamic therapy, and cryoablation-induced abscopal effect: Challenges and future prospects. *Cancer Innov* 2023; **2**: 323–45.

48 Ashrafizadeh M, Farhood B, Eleojo Musa A, Taeb S, Rezaeyan A, Najafi M. Abscopal effect in radioimmunotherapy. *Int Immunopharmacol* 2020; **85**: 106663.

49 Chi M-S, Mehta MP, Yang K-L, *et al.* Putative Abscopal Effect in Three Patients Treated by Combined Radiotherapy and Modulated Electrohyperthermia. *Front Oncol* 2020; **10**: 254.

50 Farias V de A, Tovar I, Del Moral R, *et al.* Enhancing the Bystander and Abscopal Effects to Improve Radiotherapy Outcomes. *Front Oncol* 2019; **9**: 1381.

51 Xing D, Siva S, Hanna GG. The Abscopal Effect of Stereotactic Radiotherapy and Immunotherapy: Fool's Gold or El Dorado? *Clin Oncol* 2019; **31**: 432–43.

52 Palumbo MO, Kavan P, Miller WH, *et al.* Systemic cancer therapy: achievements and challenges that lie ahead. *Front Pharmacol* 2013; **4**: 57.

53 Pucci C, Martinelli C, Ciofani G. Innovative approaches for cancer treatment: current perspectives and new challenges. *ecancermedicalscience* 2019; **13**: 961.

54 Jairam V, Lee V, Park HS, *et al.* Treatment-Related Complications of Systemic Therapy and Radiotherapy. *JAMA Oncol* 2019; **5**: 1028–35.

55 Niedzwiedz CL, Knifton L, Robb KA, Katikireddi SV, Smith DJ. Depression and anxiety among people living with and beyond cancer: a growing clinical and research priority. *BMC Cancer* 2019; **19**: 943.

56 Naughton MJ, Weaver KE. Physical and Mental Health Among Cancer Survivors. *N C Med J* 2014; **75**: 283–6.

57 Lai J-Z, Zhu Y-Y, Liu Y, *et al.* Abscopal Effects of Local Radiotherapy Are Dependent on Tumor Immunogenicity. *Front Oncol* 2021; **11**: 690188.

58 Reynders K, Illidge T, Siva S, Chang JY, De Ruysscher D. The abscopal effect of local radiotherapy: using immunotherapy to make a rare event clinically relevant. *Cancer Treat Rev* 2015; **41**: 503–10.

59 Ngwa W, Ouyang Z. Following the Preclinical Data: Leveraging the Abscopal Effect More Efficaciously. *Front Oncol* 2017; **7**: 66.

60 Ngwa W, Irabor OC, Schoenfeld JD, Hesser J, Demaria S, Formenti SC. Using immunotherapy to boost the abscopal effect. *Nat Rev Cancer* 2018; **18**: 313–22.

61 Romine PE, Harkins SK, Gray SW. Quality in the Age of Precision Medicine: The Clinician Perspective. *J Oncol Pract* 2016; **12**: 839–43.

62 Demaria S, Coleman CN, Formenti SC. Radiotherapy: Changing the Game in Immunotherapy. *Trends Cancer* 2016; **2**: 286–94.

63 Aliru ML, Schoenhals JE, Venkatesulu BP, *et al.* Radiation therapy and immunotherapy: what is the optimal timing or sequencing? *Immunotherapy* 2018; **10**: 299–316.

64 Demaria S, Formenti SC. The abscopal effect 67 years later: from a side story to center stage. *Br J Radiol* 2020; **93**: 20200042.

65 Azami A, Suzuki N, Azami Y, *et al.* Abscopal effect following radiation monotherapy in breast cancer: A case report. *Mol Clin Oncol* 2018; **9**: 283–6.

66 Franzese O, Torino F, Giannetti E, *et al.* Abscopal Effect and Drug-Induced Xenogenization: A Strategic Alliance in Cancer Treatment? *Int J Mol Sci* 2021; **22**: 10672.

67 Rodríguez-Ruiz ME, Vanpouille-Box C, Melero I, Formenti SC, Demaria S. Immunological Mechanisms Responsible for Radiation-Induced Abscopal Effect. *Trends Immunol* 2018; **39**: 644–55.

68 Muto M, Nakata H, Ishigaki K, *et al.* Successful Treatment of Advanced Gastric Cancer with Brain Metastases through an Abscopal Effect by Radiation and Immune Checkpoint Inhibitor Therapy. *J Gastric Cancer* 2021; **21**: 319–24.

69 Martinez-Zubiaurre I, Chalmers AJ, Hellevik T. Radiation-Induced Transformation of Immunoregulatory Networks in the Tumor Stroma. *Front Immunol* 2018; **9**: 1679.

70 Vanpouille-Box C, Pilones KA, Wennerberg E, Formenti SC, Demaria S. In situ vaccination by radiotherapy to improve responses to anti-CTLA-4 treatment. *Vaccine* 2015; **33**: 7415–22.

71 Golden EB, Apetoh L. Radiotherapy and Immunogenic Cell Death. *Semin Radiat Oncol* 2015; **25**: 11–7.

72 Zhu M, Yang M, Zhang J, *et al.* Immunogenic Cell Death Induction by Ionizing Radiation. *Front Immunol* 2021; **12**. DOI:10.3389/fimmu.2021.705361.

73 Xiong X, Zhao J, Su R, Liu C, Guo X, Zhou S. Double enhancement of immunogenic cell death and antigen presentation for cancer immunotherapy. *Nano Today* 2021; **39**: 101225.

74 Fucikova J, Kasikova L, Truxova I, *et al.* Relevance of the chaperone-like protein calreticulin for the biological behavior and clinical outcome of cancer. *Immunol Lett* 2018; **193**: 25–34.

75 Li X. The inducers of immunogenic cell death for tumor immunotherapy. *Tumori J* 2018; **104**: 1–8.

76 Vaes RDW, Hendriks LEL, Vooijs M, De Ruysscher D. Biomarkers of Radiotherapy-Induced Immunogenic Cell Death. *Cells* 2021; **10**: 930.

77 Ahmed A, Tait SWG. Targeting immunogenic cell death in cancer. *Mol Oncol* 2020; **14**: 2994–3006.

78 Chen DS, Mellman I. Oncology Meets Immunology: The Cancer-Immunity Cycle. *Immunity* 2013; **39**: 1–10.

79 Zhu X, Li S. The combination timing of radio-immunotherapy determines immune microenvironment remodeling and abscopal effect through eosinophils. *J Clin Oncol* 2022; published online June 2. DOI:10.1200/JCO.2022.40.16_suppl.e14566.

80 Charpentier M, Spada S, Van Nest SJ, Demaria S. Radiation therapy-induced remodeling of the tumor immune microenvironment. *Semin Cancer Biol* 2022; published online April 9. DOI:10.1016/j.semcancer.2022.04.003.

81 Walle T, Martinez Monge R, Cerwenka A, Ajona D, Melero I, Lecanda F. Radiation effects on antitumor immune responses: current perspectives and challenges. *Ther Adv Med Oncol* 2018; **10**: 1758834017742575.

82 Jarosz-Biej M, Smolarczyk R, Cichoń T, Kułach N. Tumor Microenvironment as A "Game Changer" in Cancer Radiotherapy. *Int J Mol Sci* 2019; **20**: 3212.

83 Baskar R, Lee KA, Yeo R, Yeoh K-W. Cancer and Radiation Therapy: Current Advances and Future Directions. *Int J Med Sci* 2012; **9**: 193–9.

84 Kassick M, Abdel-Wahab M. Efforts to improve radiation oncology collaboration worldwide. *Lancet Oncol* 2021; **22**: 751–3.

85 Gospodarowicz M. Global Access to Radiotherapy—Work in Progress. *JCO Glob Oncol* 2021; : 144–5.

86 Falcke SE, Rühle PF, Deloch L, Fietkau R, Frey B, Gaipl US. Clinically Relevant Radiation Exposure Differentially Impacts Forms of Cell Death in Human Cells of the Innate and Adaptive Immune System. *Int J Mol Sci* 2018; **19**: E3574.

87 Atun R, Jaffray DA, Barton MB, *et al.* Expanding global access to radiotherapy. *Lancet Oncol* 2015; **16**: 1153–86.

88 Formenti SC, Demaria S. Combining radiotherapy and cancer immunotherapy: a paradigm shift. *J Natl Cancer Inst* 2013; **105**: 256–65.

89 Delaney G, Jacob S, Featherstone C, Barton M. The role of radiotherapy in cancer treatment: estimating optimal utilization from a review of evidence-based clinical guidelines. *Cancer* 2005; **104**: 1129–37.

90 Ozpiskin OM, Zhang L, Li JJ. Immune targets in the tumor microenvironment treated by radiotherapy. *Theranostics* 2019; **9**: 1215–31.

91 Chajon E, Castelli J, Marsiglia H, De Crevoisier R. The synergistic effect of radiotherapy and immunotherapy: A promising but not simple partnership. *Crit Rev Oncol Hematol* 2017; **111**: 124–32.

92 Lauber K, Ernst A, Orth M, Herrmann M, Belka C. Dying cell clearance and its impact on the outcome of tumor radiotherapy. *Front Oncol* 2012; **2**: 116.

93 Deloch L, Derer A, Hartmann J, Frey B, Fietkau R, Gaipl US. Modern Radiotherapy Concepts and the Impact of Radiation on Immune Activation. *Front Oncol* 2016; **6**: 141.

94 Maier P, Hartmann L, Wenz F, Herskind C. Cellular Pathways in Response to Ionizing Radiation and Their Targetability for Tumor Radiosensitization. *Int J Mol Sci* 2016; **17**: E102.

95 Gupta K, Burns TC. Radiation-Induced Alterations in the Recurrent Glioblastoma Microenvironment: Therapeutic Implications. *Front Oncol* 2018; **8**: 503.

96 Bortfeld T, Jeraj R. The physical basis and future of radiation therapy. *Br J Radiol* 2011; **84**: 485–98.

97 Toulany M. Targeting DNA Double-Strand Break Repair Pathways to Improve Radiotherapy Response. *Genes* 2019; **10**: E25.

98 Baskar R, Dai J, Wenlong N, Yeo R, Yeoh K-W. Biological response of cancer cells to radiation treatment. *Front Mol Biosci* 2014; **1**: 24.

99 Schaue D, McBride WH. Opportunities and challenges of radiotherapy for treating cancer. *Nat Rev Clin Oncol* 2015; **12**: 527–40.

100 Watanabe Y, Dahlman EL, Leder KZ, Hui SK. A mathematical model of tumor growth and its response to single irradiation. *Theor Biol Med Model* 2016; **13**: 6.

101 Cui Y, Guo G. Immunomodulatory Function of the Tumor Suppressor p53 in Host Immune Response and the Tumor Microenvironment. *Int J Mol Sci* 2016; **17**: 1942.

102 Tubin S, Khan MK, Gupta S, Jeremic B. Biology of NSCLC: Interplay between Cancer Cells, Radiation and Tumor Immune Microenvironment. *Cancers* 2021; **13**: 775.

103 Tubin S, Gupta S, Grusch M, *et al.* Shifting the Immune-Suppressive to Predominant Immune-Stimulatory Radiation Effects by SBRT-PArtial Tumor Irradiation Targeting HYpoxic Segment (SBRT-PATHY). *Cancers* 2020; **13**: E50.

104 Menon H, Ramapriyan R, Cushman TR, *et al.* Role of Radiation Therapy in Modulation of the Tumor Stroma and Microenvironment. *Front Immunol* 2019; **10**: 193.

105 Shaul ME, Fridlender ZG. Tumour-associated neutrophils in patients with cancer. *Nat Rev Clin Oncol* 2019; **16**: 601–20.

106 Lin EW, Karakasheva TA, Hicks PD, Bass AJ, Rustgi AK. The tumor microenvironment in esophageal cancer. *Oncogene* 2016; **35**: 5337–49.

107 Wu T, Dai Y. Tumor microenvironment and therapeutic response. *Cancer Lett* 2017; **387**: 61–8.

108 Jin M-Z, Jin W-L. The updated landscape of tumor microenvironment and drug repurposing. *Signal Transduct Target Ther* 2020; **5**: 166.

109 Arnold KM, Flynn NJ, Raben A, *et al.* The Impact of Radiation on the Tumor Microenvironment: Effect of Dose and Fractionation Schedules. *Cancer Growth Metastasis* 2018; **11**: 1179064418761639.

110 Barker HE, Paget JTE, Khan AA, Harrington KJ. The tumour microenvironment after radiotherapy: mechanisms of resistance and recurrence. *Nat Rev Cancer* 2015; **15**: 409–25.

111 Wang R, Zhou T, Liu W, Zuo L. Molecular mechanism of bystander effects and related abscopal/cohort effects in cancer therapy. *Oncotarget* 2018; **9**: 18637–47.

112 Mukherjee S, Chakraborty A. Radiation-induced bystander phenomenon: insight and implications in radiotherapy. *Int J Radiat Biol* 2019; **95**: 243–63.

113 Marín A, Martín M, Liñán O, *et al.* Bystander effects and radiotherapy. *Rep Pract Oncol Radiother J Gt Cancer Cent Poznan Pol Soc Radiat Oncol* 2015; **20**: 12–21.

114 Kabiljo J, Harpain F, Carotta S, Bergmann M. Radiotherapy as a Backbone for Novel Concepts in Cancer Immunotherapy. *Cancers* 2020; **12**: 79.

115 Yuan Z, Fromm A, Ahmed KA, *et al.* Radiotherapy Rescue of a Nivolumab-Refractory Immune Response in a Patient with PD-L1-Negative Metastatic Squamous Cell Carcinoma of the Lung. *J Thorac Oncol Off Publ Int Assoc Study Lung Cancer* 2017; **12**: e135–6.

116 Xu J, editor. Regulation of Cancer Immune Checkpoints: Molecular and Cellular Mechanisms and Therapy. Singapore: Springer, 2020 DOI:10.1007/978-981-15-3266-5.

117 Kang J, Demaria S, Formenti S. Current clinical trials testing the combination of immunotherapy with radiotherapy. *J Immunother Cancer* 2016; **4**: 51.

118 Abuodeh Y, Venkat P, Kim S. Systematic review of case reports on the abscopal effect. *Curr Probl Cancer* 2016; **40**: 25–37.

119 Prainsack B. Personalized Medicine: Empowered Patients in the 21st Century? New York University Press, 2017 DOI:10.18574/9781479838943.

120 Topper MJ, Vaz M, Marrone KA, Brahmer JR, Baylin SB. The emerging role of epigenetic therapeutics in immuno-oncology. *Nat Rev Clin Oncol* 2020; **17**: 75–90.

121 Mahdavi Sharif P, Pastaki Khoshbin A, Nasrollahzadeh E, Keshavarz-Fathi M, Rezaei N. Chapter 4 - Tumor immunology. In: Rezaei N, ed. Clinical Immunology. Academic Press, 2023: 245–452.

122 Smith SM, Wachter K, Burris HA, *et al.* Clinical Cancer Advances 2021: ASCO's Report on Progress Against Cancer. *J Clin Oncol Off J Am Soc Clin Oncol* 2021; **39**: 1165–84.

123 Barbari C, Fontaine T, Parajuli P, *et al.* Immunotherapies and Combination Strategies for Immuno-Oncology. *Int J Mol Sci* 2020; **21**: E5009.

124 Liao L, Xu H, Zhao Y, Zheng X. Metabolic interventions combined with CTLA-4 and PD-1/PD-L1 blockade for the treatment of tumors: mechanisms and strategies. *Front Med* 2023; **17**: 805–22.

125 He M, Yang T, Wang Y, *et al.* Immune Checkpoint Inhibitor-Based Strategies for Synergistic Cancer Therapy. *Adv Healthc Mater* 2021; **10**: 2002104.

126 Vaddepally RK, Kharel P, Pandey R, Garje R, Chandra AB. Review of Indications of FDA-Approved Immune Checkpoint Inhibitors per NCCN Guidelines with the Level of Evidence. *Cancers* 2020; **12**: 738.

127 Johnson DB, Nebhan CA, Moslehi JJ, Balko JM. Immune-checkpoint inhibitors: long-term implications of toxicity. *Nat Rev Clin Oncol* 2022; **19**: 254–67.

128 Marei HE, Hasan A, Pozzoli G, Cenciarelli C. Cancer immunotherapy with immune checkpoint inhibitors (ICIs): potential, mechanisms of resistance, and strategies for reinvigorating T cell responsiveness when resistance is acquired. *Cancer Cell Int* 2023; **23**: 64.

129 Meng L, Wu H, Wu J, *et al.* Mechanisms of immune checkpoint inhibitors: insights into the regulation of circular RNAS involved in cancer hallmarks. *Cell Death Dis* 2024; **15**: 3.

130 Wojtukiewicz MZ, Rek MM, Karpowicz K, *et al.* Inhibitors of immune checkpoints—PD-1, PD-L1, CTLA-4—new opportunities for cancer patients and a new challenge for internists and general practitioners. *Cancer Metastasis Rev* 2021; **40**: 949–82.

131 Qin S, Xu L, Yi M, Yu S, Wu K, Luo S. Novel immune checkpoint targets: moving beyond PD-1 and CTLA-4. *Mol Cancer* 2019; **18**: 155.

132 Twomey JD, Zhang B. Cancer Immunotherapy Update: FDA-Approved Checkpoint Inhibitors and Companion Diagnostics. *AAPS J* 2021; **23**: 39.

133 Patsoukis N, Wang Q, Strauss L, Boussiotis VA. Revisiting the PD-1 pathway. *Sci Adv* 2020; **6**: eabd2712.

134 E H, J C, J Z, *et al.* T cell costimulatory receptor CD28 is a primary target for PD-1-mediated inhibition. *Science* 2017; **355**. DOI:10.1126/science.aaf1292.

135 Mj K, Sj H. Differential Role of PD-1 Expressed by Various Immune and Tumor Cells in the Tumor Immune Microenvironment: Expression, Function, Therapeutic Efficacy, and Resistance to Cancer Immunotherapy. *Front Cell Dev Biol* 2021; **9**. DOI:10.3389/fcell.2021.767466.

136 Zak KM, Grudnik P, Magiera K, Dömling A, Dubin G, Holak TA. Structural Biology of the Immune Checkpoint Receptor PD-1 and Its Ligands PD-L1/PD-L2. *Struct Lond Engl 1993* 2017; **25**: 1163–74.

137 Zhang X, Huang Y, Yang X. The complex role of PD-L1 in antitumor immunity: a recent update. *Cell Mol Immunol* 2021; **18**: 2067–8.

138 Abaza A, Sid Idris F, Anis Shaikh H, *et al.* Programmed Cell Death Protein 1 (PD-1) and Programmed Cell Death Ligand 1 (PD-L1) Immunotherapy: A Promising Breakthrough in Cancer Therapeutics. *Cureus*; **15**: e44582.

139 Diskin B, Adam S, Cassini MF, *et al.* PD-L1 engagement on T cells promotes self-tolerance and suppression of neighboring macrophages and effector T cells in cancer. *Nat Immunol* 2020; **21**: 442–54.

140 Munari E, Mariotti FR, Quatrini L, *et al.* PD-1/PD-L1 in Cancer: Pathophysiological, Diagnostic and Therapeutic Aspects. *Int J Mol Sci* 2021; **22**: 5123.

141 Gou Q, Dong C, Xu H, *et al.* PD-L1 degradation pathway and immunotherapy for cancer. *Cell Death Dis* 2020; **11**: 1–7.

142 Shiravand Y, Khodadadi F, Kashani SMA, *et al.* Immune Checkpoint Inhibitors in Cancer Therapy. *Curr Oncol Tor Ont* 2022; **29**: 3044–60.

143 Zhang J, Wu D, Zhang Z, *et al.* Pembrolizumab or Bevacizumab Plus Chemotherapy as First-Line Treatment of Advanced Nonsquamous Nonsmall Cell Lung Cancer: A Retrospective Cohort Study. *Technol Cancer Res Treat* 2021; **20**: 15330338211039676.

144 Wang D-R, Wu X-L, Sun Y-L. Therapeutic targets and biomarkers of tumor immunotherapy: response versus non-response. *Signal Transduct Target Ther* 2022; **7**: 1–27.

145 Kraehenbuehl L, Weng C-H, Eghbali S, Wolchok JD, Merghoub T. Enhancing immunotherapy in cancer by targeting emerging immunomodulatory pathways. *Nat Rev Clin Oncol* 2022; **19**: 37–50.

146 Liu J, Chen Z, Li Y, Zhao W, Wu J, Zhang Z. PD-1/PD-L1 Checkpoint Inhibitors in Tumor Immunotherapy. *Front Pharmacol* 2021; **12**: 731798.

147 Migden MR, Rischin D, Schmults CD, *et al.* PD-1 Blockade with Cemiplimab in Advanced Cutaneous Squamous-Cell Carcinoma. *N Engl J Med* 2018; **379**: 341–51.

148 Dal Bello MG, Alama A, Coco S, Vanni I, Grossi F. Understanding the checkpoint blockade in lung cancer immunotherapy. *Drug Discov Today* 2017; **22**: 1266–73.

149 Rossi J-F, Céballos P, Lu Z-Y. Immune precision medicine for cancer: a novel insight based on the efficiency of immune effector cells. *Cancer Commun Lond Engl* 2019; **39**: 34.

150 Yan L, Zhang W. Precision medicine becomes reality-tumor type-agnostic therapy. *Cancer Commun Lond Engl* 2018; **38**: 6.

151 Robert C, Schachter J, Long GV, *et al.* Pembrolizumab versus Ipilimumab in Advanced Melanoma. *N Engl J Med* 2015; **372**: 2521–32.

152 Gandhi L, Rodríguez-Abreu D, Gadgeel S, *et al.* Pembrolizumab plus Chemotherapy in Metastatic Non-Small-Cell Lung Cancer. *N Engl J Med* 2018; **378**: 2078–92.

153 Garon EB, Rizvi NA, Hui R, *et al.* Pembrolizumab for the treatment of non-small-cell lung cancer. *N Engl J Med* 2015; **372**: 2018–28.

154 Burtness B, Harrington KJ, Greil R, *et al.* Pembrolizumab alone or with chemotherapy versus cetuximab with chemotherapy for recurrent or metastatic squamous cell carcinoma of the head and neck (KEYNOTE-048): a randomised, open-label, phase 3 study. *Lancet Lond Engl* 2019; **394**: 1915–28.

155 Balar AV, Castellano DE, Grivas P, *et al.* Efficacy and safety of pembrolizumab in metastatic urothelial carcinoma: results from KEYNOTE-045 and KEYNOTE-052 after up to 5 years of follow-up. *Ann Oncol Off J Eur Soc Med Oncol* 2023; **34**: 289–99.

156 Powles T, Csőszi T, Özgüroğlu M, *et al.* Pembrolizumab alone or combined with chemotherapy versus chemotherapy as first-line therapy for advanced urothelial carcinoma (KEYNOTE-361): a randomised, open-label, phase 3 trial. *Lancet Oncol* 2021; **22**: 931–45.

157 Liu W, Huo G, Chen P. Clinical benefit of pembrolizumab in treatment of first line non-small cell lung cancer: a systematic review and meta-analysis of clinical characteristics. *BMC Cancer* 2023; **23**: 458.

158 Wang N, Zheng L, Li M, *et al.* Clinical efficacy and safety of individualized pembrolizumab administration based on pharmacokinetic in advanced non-small cell lung cancer: A prospective exploratory clinical trial. *Lung Cancer* 2023; **178**: 183–90.

159 A S, S K, M G, *et al.* Cemiplimab monotherapy for first-line treatment of advanced non-small-cell lung cancer with PD-L1 of at least 50%: a multicentre, open-label, global, phase 3, randomised, controlled trial. *Lancet Lond Engl* 2021; **397**. DOI:10.1016/S0140-6736(21)00228-2.

160 Gümüş M, Chen C-I, Ivanescu C, *et al.* Patient-reported outcomes with cemiplimab monotherapy for first-line treatment of advanced non-small cell lung cancer with PD-L1 of ≥50%: The EMPOWER-Lung 1 study. *Cancer* 2023; **129**: 118–29.

161 T M, Rgw Q, T M, *et al.* Quality of life with cemiplimab plus chemotherapy for first-line treatment of advanced non-small cell lung cancer: Patient-reported outcomes from phase 3 EMPOWER-Lung 3. *Cancer* 2023; **129**. DOI:10.1002/cncr.34687.

162 Hober C, Fredeau L, Pham-Ledard A, *et al.* Cemiplimab for Locally Advanced and Metastatic Cutaneous Squamous-Cell Carcinomas: Real-Life Experience from the French CAREPI Study Group. *Cancers* 2021; **13**: 3547.

163 Deng R, Bumbaca D, Pastuskovas CV, *et al.* Preclinical pharmacokinetics, pharmacodynamics, tissue distribution, and tumor penetration of anti-PD-L1 monoclonal antibody, an immune checkpoint inhibitor. *mAbs* 2016; **8**: 593–603.

164 Mathieu LN, Larkins E, Sinha AK, *et al.* FDA Approval Summary: Atezolizumab as Adjuvant Treatment following Surgical Resection and Platinum-Based Chemotherapy for Stage II to IIIA NSCLC. *Clin Cancer Res* 2023; **29**: 2973–8.

165 Herbst RS, Giaccone G, de Marinis F, *et al.* Atezolizumab for First-Line Treatment of PD-L1-Selected Patients with NSCLC. *N Engl J Med* 2020; **383**: 1328–39.

166 Kim ES, Velcheti V, Mekhail T, *et al.* Blood-based tumor mutational burden as a biomarker for atezolizumab in non-small cell lung cancer: the phase 2 B-F1RST trial. *Nat Med* 2022; **28**: 939–45.

167 Rittmeyer A, Barlesi F, Waterkamp D, *et al.* Atezolizumab versus docetaxel in patients with previously treated non-small-cell lung cancer (OAK): a phase 3, open-label, multicentre randomised controlled trial. *Lancet Lond Engl* 2017; **389**: 255–65.

168 Chin K, Chand VK, Nuyten DSA. Avelumab: clinical trial innovation and collaboration to advance anti-PD-L1 immunotherapy. *Ann Oncol* 2017; **28**: 1658–66.

169 Wu Y-L, Cheng Y, Chen H, *et al.* Phase I/Ib dose-escalation study of avelumab in Chinese patients with advanced solid tumors. *Future Oncol Lond Engl* 2022; **18**: 2053–62.

170 PD-L1/CD80 cis Interactions Disrupt PD-L1–PD-1 Binding and Promote T-cell Function. *Cancer Discov* 2019; **9**: OF10.

171 Antonia SJ, Villegas A, Daniel D, *et al.* Durvalumab after Chemoradiotherapy in Stage III Non–Small-Cell Lung Cancer. *N Engl J Med* 2017; **377**: 1919–29.

172 Kim R, Kwon M, An M, *et al.* Phase II study of ceralasertib (AZD6738) in combination with durvalumab in patients with advanced/metastatic melanoma who have failed prior anti-PD-1 therapy. *Ann Oncol Off J Eur Soc Med Oncol* 2022; **33**: 193–203.

173 Rizvi NA, Cho BC, Reinmuth N, *et al.* Durvalumab With or Without Tremelimumab vs Standard Chemotherapy in First-line Treatment of Metastatic Non-Small Cell Lung Cancer: The MYSTIC Phase 3 Randomized Clinical Trial. *JAMA Oncol* 2020; **6**: 661–74.

174 Brix N, Tiefenthaller A, Anders H, Belka C, Lauber K. Abscopal, immunological effects of radiotherapy: Narrowing the gap between clinical and preclinical experiences. *Immunol Rev* 2017; **280**: 249–79.

175 Liu Y, Dong Y, Kong L, Shi F, Zhu H, Yu J. Abscopal effect of radiotherapy combined with immune checkpoint inhibitors. *J Hematol OncolJ Hematol Oncol* 2018; **11**: 104.

176 Hodge JW, Sharp HJ, Gameiro SR. Abscopal regression of antigen disparate tumors by antigen cascade after systemic tumor vaccination in combination with local tumor radiation. *Cancer Biother Radiopharm* 2012; **27**: 12–22.

177 Vatner RE, Cooper BT, Vanpouille-Box C, Demaria S, Formenti SC. Combinations of immunotherapy and radiation in cancer therapy. *Front Oncol* 2014; **4**: 325.

178 Theelen WSME, Peulen HMU, Lalezari F, *et al.* Effect of Pembrolizumab After Stereotactic Body Radiotherapy vs Pembrolizumab Alone on Tumor Response in Patients With Advanced Non-Small Cell Lung Cancer: Results of the PEMBRO-RT Phase 2 Randomized Clinical Trial. *JAMA Oncol* 2019; **5**: 1276–82.

179 Theelen WSME, Chen D, Verma V, *et al.* Pembrolizumab with or without radiotherapy for metastatic non-small-cell lung cancer: a pooled analysis of two randomised trials. *Lancet Respir Med* 2021; **9**: 467–75.

180 Folkert MR, Timmerman RD. Stereotactic ablative body radiosurgery (SABR) or Stereotactic body radiation therapy (SBRT). *Adv Drug Deliv Rev* 2017; **109**: 3–14.

181 Hiniker SM, Chen DS, Reddy S, *et al.* A systemic complete response of metastatic melanoma to local radiation and immunotherapy. *Transl Oncol* 2012; **5**: 404–7.

182 Brenneman RJ, Sharifai N, Fischer-Valuck B, *et al.* Abscopal Effect Following Proton Beam Radiotherapy in a Patient With Inoperable Metastatic Retroperitoneal Sarcoma. *Front Oncol* 2019; **9**: 922.

183 Choi JS, Sansoni ER, Lovin BD, *et al.* Abscopal Effect Following Immunotherapy and Combined Stereotactic Body Radiation Therapy in Recurrent Metastatic Head and Neck Squamous Cell Carcinoma: A Report of Two Cases and Literature Review. *Ann Otol Rhinol Laryngol* 2020; **129**: 517–22.

184 Garelli E, Rittmeyer A, Putora PM, Glatzer M, Dressel R, Andreas S. Abscopal effect in lung cancer: three case reports and a concise review. *Immunotherapy* 2019; **11**: 1445–61.

185 Trommer M, Yeo SY, Persigehl T, *et al.* Abscopal Effects in Radio-Immunotherapy-Response Analysis of Metastatic Cancer Patients With Progressive Disease Under Anti-PD-1 Immune Checkpoint Inhibition. *Front Pharmacol* 2019; **10**: 511.

186 Dong H, Zhu G, Tamada K, Chen L. B7-H1, a third member of the B7 family, co-stimulates T-cell proliferation and interleukin-10 secretion. *Nat Med* 1999; **5**: 1365–9.

187 Callahan MK, Wolchok JD. At the bedside: CTLA-4- and PD-1-blocking antibodies in cancer immunotherapy. *J Leukoc Biol* 2013; **94**: 41–53.

188 Zhuang H. Abscopal effect of stereotactic radiotherapy combined with anti-PD-1/PD-L1 immunotherapy: Mechanisms, clinical efficacy, and issues. *Cancer Commun Lond Engl* 2020; **40**: 649–54.

189 Leary R, Gardner RB, Mockbee C, Roychowdhury DF. Boosting Abscopal Response to Radiotherapy with Sargramostim: A Review of Data and Ongoing Studies. *Cureus* 2019; **11**: e4276.

190 Wang M, Zhao J, Zhang L, *et al.* Role of tumor microenvironment in tumorigenesis. *J Cancer* 2017; **8**: 761–73.

191 Anderson NM, Simon MC. The tumor microenvironment. *Curr Biol CB* 2020; **30**: R921–5.

192 Bolon B, Aeffner F. A Primer for Oncoimmunology (Immunooncology). *Toxicol Pathol* 2017; **45**: 584–8.

193 Lei X, Lei Y, Li J-K, *et al.* Immune cells within the tumor microenvironment: Biological functions and roles in cancer immunotherapy. *Cancer Lett* 2020; **470**: 126–33.

194 Zhan J, Zhou L, Zhang H, *et al.* A comprehensive analysis of the expression, immune infiltration, prognosis and partial experimental validation of CHST family genes in gastric cancer. *Transl Oncol* 2024; **40**: 101843.

195 Peña-Romero AC, Orenes-Piñero E. Dual Effect of Immune Cells within Tumour Microenvironment: Pro- and Anti-Tumour Effects and Their Triggers. *Cancers* 2022; **14**: 1681.

196 Uhl LFK, Gérard A. Modes of Communication between T Cells and Relevance for Immune Responses. *Int J Mol Sci* 2020; **21**: 2674.

197 Overview of T Cell Subsets | Immunopaedia. Immunopaedia Adv. Glob. Immunol. Educ. 2016; published online June 27. https://www.immunopaedia.org.za/immunology/basics/5-overview-of-t-cell-subsets/ (accessed June 7, 2022).

198 Sundberg EJ, Deng L, Mariuzza RA. TCR recognition of peptide/MHC class II complexes and superantigens. *Semin Immunol* 2007; **19**: 262–71.

199 Heath WR. T Lymphocytes. In: Delves PJ, ed. Encyclopedia of Immunology (Second Edition). Oxford: Elsevier, 1998: 2341–3.

200 Busch DH, Fräßle SP, Sommermeyer D, Buchholz VR, Riddell SR. Role of memory T cell subsets for adoptive immunotherapy. *Semin Immunol* 2016; **28**: 28–34.

201 Sauls RS, McCausland C, Taylor BN. Histology, T-Cell Lymphocyte. In: StatPearls [Internet]. StatPearls Publishing, 2023. https://www.ncbi.nlm.nih.gov/books/NBK535433/ (accessed Dec 20, 2023).

202 Cossarizza A, Ortolani C, Paganelli R, *et al.* CD45 isoforms expression on CD4+ and CD8+ T cells throughout life, from newborns to centenarians: implications for T cell memory. *Mech Ageing Dev* 1996; **86**: 173–95.

203 Sun T, Li Y, Wu J, *et al.* Downregulation of exosomal MHC-I promotes glioma cells escaping from systemic immunosurveillance. *Nanomedicine Nanotechnol Biol Med* 2022; **46**: 102605.

204 Ascierto PA, Lewis KD, Giacomo AMD, *et al.* Prognostic impact of baseline tumour immune infiltrate on disease-free survival in patients with completely resected, BRAFv600 mutation–positive melanoma receiving adjuvant vemurafenib. *Ann Oncol* 2020; **31**: 153–9.

205 Viret C, Wong FS, Janeway CA. Designing and maintaining the mature TCR repertoire: the continuum of self-peptide:self-MHC complex recognition. *Immunity* 1999; **10**: 559–68.

206 Zhang N, Bevan MJ. CD8+ T Cells: Foot Soldiers of the Immune System. *Immunity* 2011; **35**: 161–8.

207 Xie Q, Ding J, Chen Y. Role of CD8+ T lymphocyte cells: Interplay with stromal cells in tumor microenvironment. *Acta Pharm Sin B* 2021; **11**: 1365–78.

208 Raskov H, Orhan A, Christensen JP, Gögenur I. Cytotoxic CD8+ T cells in cancer and cancer immunotherapy. *Br J Cancer* 2021; **124**: 359–67.

209 Kim JM, Chen DS. Immune escape to PD-L1/PD-1 blockade: seven steps to success (or failure). *Ann Oncol Off J Eur Soc Med Oncol* 2016; **27**: 1492–504.

210 Sade-Feldman M, Yizhak K, Bjorgaard SL, *et al.* Defining T Cell States Associated with Response to Checkpoint Immunotherapy in Melanoma. *Cell* 2018; **175**: 998-1013.e20.

211 Guo X, Zhang Y, Zheng L, *et al.* Global characterization of T cells in non-small-cell lung cancer by single-cell sequencing. *Nat Med* 2018; **24**: 978–85.

212 Desai S, Meza-Perez S, Liu M, Randall TD. Characterizing the role of IL-33/ST2 axis in regulating anti-tumor function by CD8 T cells during tumor metastasis in the omentum. *J Immunol* 2023; **210**: 86.07.

213 He Q-F, Xu Y, Li J, Huang Z-M, Li X-H, Wang X. CD8+ T-cell exhaustion in cancer: mechanisms and new area for cancer immunotherapy. *Brief Funct Genomics* 2019; **18**: 99–106.

214 St. Paul M, Ohashi PS. The Roles of CD8+ T Cell Subsets in Antitumor Immunity. *Trends Cell Biol* 2020; **30**: 695–704.

215 Wang W, Green M, Choi JE, *et al.* CD8+ T cells regulate tumour ferroptosis during cancer immunotherapy. *Nature* 2019; **569**: 270–4.

216 Lopez-Yrigoyen M, Cassetta L, Pollard JW. Macrophage targeting in cancer. *Ann N Y Acad Sci* 2021; **1499**: 18–41.

217 Martinez RJ, Andargachew R, Martinez HA, Evavold BD. Low-affinity CD4+ T cells are major responders in the primary immune response. *Nat Commun* 2016; **7**: 13848.

218 Davis MM, Bjorkman PJ. T-cell antigen receptor genes and T-cell recognition. *Nature* 1988; **334**: 395–402.

219 Cachot A, Bilous M, Liu Y-C, *et al.* Tumor-specific cytolytic CD4 T cells mediate immunity against human cancer. *Sci Adv* 2021; **7**: eabe3348.

220 Tay RE, Richardson EK, Toh HC. Revisiting the role of CD4+ T cells in cancer immunotherapy—new insights into old paradigms. *Cancer Gene Ther* 2021; **28**: 5–17.

221 Belikov AV. The role of reactive oxygen species and mitochondria in T-cell activation. .

222 Pradeep Yeola A, Akbar I, Baillargeon J, Mercy Ignatius Arokia Doss P, Paavilainen VO, Rangachari M. Protein translocation and retro-translocation across the endoplasmic reticulum are crucial to inflammatory effector CD4+ T cell function. *Cytokine* 2020; **129**: 154944.

223 Nonaka K, Saio M, Umemura N, *et al.* Th1 polarization in the tumor microenvironment upregulates the myeloid-derived suppressor-like function of macrophages. *Cell Immunol* 2021; **369**: 104437.

224 Viallard JF, Pellegrin JL, Ranchin V, *et al.* Th1 (IL-2, interferon-gamma (IFN-γ)) and Th2 (IL-10, IL-4) cytokine production by peripheral blood mononuclear cells (PBMC) from patients with systemic lupus erythematosus (SLE). *Clin Exp Immunol* 1999; **115**: 189–95.

225 Espinosa Gonzalez M, Volk-Draper L, Bhattarai N, Wilber A, Ran S. Th2 Cytokines IL-4, IL-13, and IL-10 Promote Differentiation of Pro-Lymphatic Progenitors Derived from Bone Marrow Myeloid Precursors. *Stem Cells Dev* 2022; **31**: 322–33.

226 Raphael I, Nalawade S, Eagar TN, Forsthuber TG. T cell subsets and their signature cytokines in autoimmune and inflammatory diseases. *Cytokine* 2015; **74**: 5–17.

227 Sakaguchi S, Yamaguchi T, Nomura T, Ono M. Regulatory T cells and immune tolerance. *Cell* 2008; **133**: 775–87.

228 Leclerc M, Voilin E, Gros G, *et al.* Regulation of antitumour CD8 T-cell immunity and checkpoint blockade immunotherapy by Neuropilin-1. *Nat Commun* 2019; **10**: 3345.

229 Pellerin L, Jenks JA, Bégin P, Bacchetta R, Nadeau KC. Regulatory T cells and their roles in immune dysregulation and allergy. *Immunol Res* 2014; **58**: 358–68.

230 Rocamora-Reverte L, Melzer FL, Würzner R, Weinberger B. The Complex Role of Regulatory T Cells in Immunity and Aging. *Front Immunol* 2021; **11**: 616949.

231 Ankathatti Munegowda M, Deng Y, Mulligan SJ, Xiang J. Th17 and Th17-stimulated CD8+ T cells play a distinct role in Th17-induced preventive and therapeutic antitumor immunity. *Cancer Immunol Immunother* 2011; **60**: 1473–84.

232 Ye J, Su X, Hsueh EC, *et al.* Human tumor-infiltrating Th17 cells have the capacity to differentiate into IFN-γ+ and FOXP3+ T cells with potent suppressive function. *Eur J Immunol* 2011; **41**: 936–51.

233 He S, Fei M, Wu Y, *et al.* Distribution and clinical significance of Th17 cells in the tumor microenvironment and peripheral blood of pancreatic cancer patients. *Int J Mol Sci* 2011; **12**: 7424–37.

234 Bailey SR, Nelson MH, Himes RA, Li Z, Mehrotra S, Paulos CM. Th17 Cells in Cancer: The Ultimate Identity Crisis. *Front Immunol* 2014; **5**. DOI:10.3389/fimmu.2014.00276.

235 Chen T, Guo J, Cai Z, *et al.* Th9 Cell Differentiation and Its Dual Effects in Tumor Development. *Front Immunol* 2020; **11**. https://www.frontiersin.org/articles/10.3389/fimmu.2020.01026 (accessed Sept 12, 2022).

236 Purwar R, Schlapbach C, Xiao S, *et al.* Robust tumor immunity to melanoma mediated by interleukin-9-producing T cells. *Nat Med* 2012; **18**: 1248–53.

237 Lu Y, Hong B, Li H, *et al.* Tumor-specific IL-9-producing CD8+ Tc9 cells are superior effector than type-I cytotoxic Tc1 cells for adoptive immunotherapy of cancers. *Proc Natl Acad Sci U S A* 2014; **111**: 2265–70.

238 Shen Y, Song Z, Lu X, *et al.* Fas signaling-mediated TH9 cell differentiation favors bowel inflammation and antitumor functions. *Nat Commun* 2019; **10**: 2924.

239 Kim I-K, Kim B-S, Koh C-H, *et al.* Glucocorticoid-induced tumor necrosis factor receptor-related protein co-stimulation facilitates tumor regression by inducing IL-9-producing helper T cells. *Nat Med* 2015; **21**: 1010–7.

240 Abdul-Wahid A, Cydzik M, Prodeus A, *et al.* Induction of antigen-specific TH 9 immunity accompanied by mast cell activation blocks tumor cell engraftment. *Int J Cancer* 2016; **139**: 841–53.

241 You F-P, Zhang J, Cui T, *et al.* Th9 cells promote antitumor immunity via IL-9 and IL-21 and demonstrate atypical cytokine expression in breast cancer. *Int Immunopharmacol* 2017; **52**: 163–7.

242 Rivera Vargas T, Cai Z, Shen Y, *et al.* Selective degradation of PU.1 during autophagy represses the differentiation and antitumour activity of TH9 cells. *Nat Commun* 2017; **8**: 559.

243 Kim I-K, Koh C-H, Jeon I, *et al.* GM-CSF Promotes Antitumor Immunity by Inducing Th9 Cell Responses. *Cancer Immunol Res* 2019; **7**: 498–509.

244 Salazar Y, Zheng X, Brunn D, *et al.* Microenvironmental Th9 and Th17 lymphocytes induce metastatic spreading in lung cancer. *J Clin Invest* 2020; **130**: 3560–75.

245 Doulabi H, Masoumi E, Rastin M, Foolady Azarnaminy A, Esmaeili S-A, Mahmoudi M. The role of Th22 cells, from tissue repair to cancer progression. *Cytokine* 2022; **149**: 155749.

246 Kim HJ, Ji YR, Lee YM. Crosstalk between angiogenesis and immune regulation in the tumor microenvironment. *Arch Pharm Res* 2022; **45**: 401–16.

247 Nowosad CR, Spillane KM, Tolar P. Germinal center B cells recognize antigen through a specialized immune synapse architecture. *Nat Immunol* 2016; **17**: 870–7.

248 Roghanian A, Fraser C, Kleyman M, Chen J. B Cells Promote Pancreatic Tumorigenesis. *Cancer Discov* 2016; **6**: 230–2.

249 Downs-Canner SM, Meier J, Vincent BG, Serody JS. B Cell Function in the Tumor Microenvironment. *Annu Rev Immunol* 2022; **40**: 169–93.

250 Willsmore ZN, Harris RJ, Crescioli S, *et al.* B Cells in Patients With Melanoma: Implications for Treatment With Checkpoint Inhibitor Antibodies. *Front Immunol* 2021; **11**. DOI:10.3389/fimmu.2020.622442.

251 Zhao K, Yang X, Jin H, Zhao L, Hu J, Qin W. Double-edge Role of B Cells in Tumor Immunity: Potential Molecular Mechanism. *Curr Med Sci* 2019; **39**: 685–9.

252 Yuen GJ, Demissie E, Pillai S. B lymphocytes and cancer: a love-hate relationship. *Trends Cancer* 2016; **2**: 747–57.

253 Shah S, Divekar AA, Hilchey SP, *et al.* Increased rejection of primary tumors in mice lacking B cells: inhibition of anti-tumor CTL and TH1 cytokine responses by B cells. *Int J Cancer* 2005; **117**: 574–86.

254 Tadmor T, Zhang Y, Cho H-M, Podack ER, Rosenblatt JD. The absence of B lymphocytes reduces the number and function of T-regulatory cells and enhances the anti-tumor response in a murine tumor model. *Cancer Immunol Immunother CII* 2011; **60**: 609–19.

255 Zirakzadeh AA, Sherif A, Rosenblatt R, *et al.* Tumour-associated B cells in urothelial urinary bladder cancer. *Scand J Immunol* 2020; **91**: e12830.

256 Guo FF, Cui JW. The Role of Tumor-Infiltrating B Cells in Tumor Immunity. *J Oncol* 2019; **2019**: 2592419.

257 Catalán D, Mansilla MA, Ferrier A, *et al.* Immunosuppressive Mechanisms of Regulatory B Cells. *Front Immunol* 2021; **12**. DOI:10.3389/fimmu.2021.611795.

258 Schwartz M, Zhang Y, Rosenblatt JD. B cell regulation of the anti-tumor response and role in carcinogenesis. *J Immunother Cancer* 2016; **4**: 40.

259 Wang J-Z, Zhang Y-H, Guo X-H, Zhang H-Y, Zhang Y. The double-edge role of B cells in mediating antitumor T-cell immunity: Pharmacological strategies for cancer immunotherapy. *Int Immunopharmacol* 2016; **36**: 73–85.

260 Wouters MCA, Nelson BH. Prognostic Significance of Tumor-Infiltrating B Cells and Plasma Cells in Human Cancer. *Clin Cancer Res* 2018; **24**: 6125–35.

261 Rodriguez AB, Engelhard VH. Insights into Tumor-Associated Tertiary Lymphoid Structures: Novel Targets for Antitumor Immunity and Cancer Immunotherapy. *Cancer Immunol Res* 2020; **8**: 1338–45.

262 Cui C, Wang J, Fagerberg E, *et al.* Neoantigen-driven B cell and CD4 T follicular helper cell collaboration promotes anti-tumor CD8 T cell responses. *Cell* 2021; **184**: 6101-6118.e13.

263 Jia W, Zhang T, Yao Q, *et al.* Tertiary Lymphatic Structures in Primary Hepatic Carcinoma: Controversy Cannot Overshadow Hope. *Front Immunol* 2022; **13**. https://www.frontiersin.org/articles/10.3389/fimmu.2022.870458 (accessed Sept 12, 2022).

264 Lynch KT, Young SJ, Meneveau MO, *et al.* Heterogeneity in tertiary lymphoid structure B-cells correlates with patient survival in metastatic melanoma. *J Immunother Cancer* 2021; **9**: e002273.

265 Kinker GS, Vitiello GAF, Ferreira WAS, Chaves AS, Cordeiro de Lima VC, Medina T da S. B Cell Orchestration of Anti-tumor Immune Responses: A Matter of Cell Localization and Communication. *Front Cell Dev Biol* 2021; **9**. DOI:10.3389/fcell.2021.678127.

266 Ayasoufi K, Fan R, Fairchild RL, Valujskikh A. CD4 T Cell Help via B Cells Is Required for Lymphopenia-Induced CD8 T Cell Proliferation. *J Immunol* 2016; **196**: 3180–90.

267 Delvecchio FR, Goulart MR, Fincham REA, Bombadieri M, Kocher HM. B cells in pancreatic cancer stroma. *World J Gastroenterol* 2022; **28**: 1088–101.

268 Aizik L, Dror Y, Taussig D, Barzel A, Carmi Y, Wine Y. Antibody Repertoire Analysis of Tumor-Infiltrating B Cells Reveals Distinct Signatures and Distributions Across Tissues. *Front Immunol* 2021; **12**. DOI:10.3389/fimmu.2021.705381.

269 Healy JI, Dolmetsch RE, Timmerman LA, *et al.* Different Nuclear Signals Are Activated by the B Cell Receptor during Positive Versus Negative Signaling. *Immunity* 1997; **6**: 419–28.

270 Hansen JE, Chan G, Liu Y, *et al.* Targeting cancer with a lupus autoantibody. *Sci Transl Med* 2012; **4**: 157ra142.

271 Greenberg AH, Hudson L, Shen L, Roitt IM. Antibody-dependent cell-mediated cytotoxicity due to a 'null' lymphoid cell. *Nature New Biol* 1973; **242**: 111–3.

272 Du N, Guo F, Wang Y, Cui J. NK Cell Therapy: A Rising Star in Cancer Treatment. *Cancers* 2021; **13**: 4129.

273 Smyth MJ, Crowe NY, Godfrey DI. NK cells and NKT cells collaborate in host protection from methylcholanthrene-induced fibrosarcoma. *Int Immunol* 2001; **13**: 459–63.

274 Campos C, Pera A, Pita-López ML, *et al.* Natural Killer Cells in Human Aging. In: Fulop T, Franceschi C, Hirokawa K, Pawelec G, eds. Handbook of Immunosenescence: Basic Understanding and Clinical Implications. Cham: Springer International Publishing, 2019: 945–65.

275 Wang M, Zhou Z, Wang X, Zhang C, Jiang X. Natural killer cell awakening: unleash cancer-immunity cycle against glioblastoma. *Cell Death Dis* 2022; **13**: 1–10.

276 Quatrini L, Della Chiesa M, Sivori S, Mingari MC, Pende D, Moretta L. Human NK cells, their receptors and function. *Eur J Immunol* 2021; **51**: 1566–79.

277 Street SEA, Zerafa N, Iezzi M, *et al.* Host perforin reduces tumor number but does not increase survival in oncogene-driven mammary adenocarcinoma. *Cancer Res* 2007; **67**: 5454–60.

278 Imai K, Matsuyama S, Miyake S, Suga K, Nakachi K. Natural cytotoxic activity of peripheral-blood lymphocytes and cancer incidence: an 11-year follow-up study of a general population. *Lancet Lond Engl* 2000; **356**: 1795–9.

279 Eckl J, Buchner A, Prinz PU, *et al.* Transcript signature predicts tissue NK cell content and defines renal cell carcinoma subgroups independent of TNM staging. *J Mol Med Berl Ger* 2012; **90**: 55–66.

280 Carrega P, Morandi B, Costa R, *et al.* Natural killer cells infiltrating human nonsmall-cell lung cancer are enriched in CD56 bright CD16(-) cells and display an impaired capability to kill tumor cells. *Cancer* 2008; **112**: 863–75.

281 Jin WJ, Jagodinsky JC, Vera JM, *et al.* NK cells propagate T cell immunity following in situ tumor vaccination. *Cell Rep* 2023; **42**. DOI:10.1016/j.celrep.2023.113556.

282 Fauriat C, Long EO, Ljunggren H-G, Bryceson YT. Regulation of human NK-cell cytokine and chemokine production by target cell recognition. *Blood* 2010; **115**: 2167–76.

283 Lee H, Da Silva IP, Palendira U, Scolyer RA, Long GV, Wilmott JS. Targeting NK Cells to Enhance Melanoma Response to Immunotherapies. *Cancers* 2021; **13**: 1363.

284 Whiteside TL. Chapter 10 - Natural killer (NK) cells. In: Fink G, ed. Stress: Immunology and Inflammation. Academic Press, 2024: 83–90.

285 Chiossone L, Vivier E. NK Cell-Based Therapies. In: Zitvogel L, Kroemer G, eds. Oncoimmunology: A Practical Guide for Cancer Immunotherapy. Cham: Springer International Publishing, 2018: 275–88.

286 Stringaris K, Sekine T, Khoder A, *et al.* Leukemia-induced phenotypic and functional defects in natural killer cells predict failure to achieve remission in acute myeloid leukemia. *Haematologica* 2014; **99**: 836–47.

287 Zhang Q, Bi J, Zheng X, *et al.* Blockade of the checkpoint receptor TIGIT prevents NK cell exhaustion and elicits potent anti-tumor immunity. *Nat Immunol* 2018; **19**: 723–32.

288 Benson DM, Bakan CE, Mishra A, *et al.* The PD-1/PD-L1 axis modulates the natural killer cell versus multiple myeloma effect: a therapeutic target for CT-011, a novel monoclonal anti-PD-1 antibody. *Blood* 2010; **116**: 2286–94.

289 Chretien A-S, Devillier R, Fauriat C, *et al.* NKp46 expression on NK cells as a prognostic and predictive biomarker for response to allo-SCT in patients with AML. *Oncoimmunology* 2017; **6**: e1307491.

290 Chretien A-S, Fauriat C, Orlanducci F, *et al.* NKp30 expression is a prognostic immune biomarker for stratification of patients with intermediate-risk acute myeloid leukemia. *Oncotarget* 2017; **8**: 49548–63.

291 Epling-Burnette PK, Bai F, Painter JS, *et al.* Reduced natural killer (NK) function associated with high-risk myelodysplastic syndrome (MDS) and reduced expression of activating NK receptors. *Blood* 2007; **109**: 4816–24.

292 Augugliaro R, Parolini S, Castriconi R, *et al.* Selective cross-talk among natural cytotoxicity receptors in human natural killer cells. *Eur J Immunol* 2003; **33**: 1235–41.

293 Zhao Y, Bai Y, Shen M, Li Y. Therapeutic strategies for gastric cancer targeting immune cells: Future directions. *Front Immunol* 2022; **13**. https://www.frontiersin.org/articles/10.3389/fimmu.2022.992762 (accessed Jan 14, 2024).

294 Hilpert J, Grosse-Hovest L, Grünebach F, *et al.* Comprehensive analysis of NKG2D ligand expression and release in leukemia: implications for NKG2D-mediated NK cell responses. *J Immunol Baltim Md 1950* 2012; **189**: 1360–71.

295 Ferrari de Andrade L, Tay RE, Pan D, *et al.* Antibody-mediated inhibition of MICA and MICB shedding promotes NK cell-driven tumor immunity. *Science* 2018; **359**: 1537–42.

296 Reiners KS, Topolar D, Henke A, *et al.* Soluble ligands for NK cell receptors promote evasion of chronic lymphocytic leukemia cells from NK cell anti-tumor activity. *Blood* 2013; **121**: 3658–65.

297 Shimasaki N, Jain A, Campana D. NK cells for cancer immunotherapy. *Nat Rev Drug Discov* 2020; **19**: 200–18.

298 Blumenreich MS. The White Blood Cell and Differential Count. Butterworths, 1990 https://www.ncbi.nlm.nih.gov/books/NBK261/ (accessed Sept 13, 2022).

299 Segal AW. How Neutrophils Kill Microbes. *Annu Rev Immunol* 2005; **23**: 197–223.

300 Lewis TJ, Trempe CL. Chapter 11 - Differential Diagnosis Toward a Cure for Alzheimer's. In: Lewis TJ, Trempe CL, eds. The End of Alzheimer's (Second Edition). Academic Press, 2017: 346–92.

301 Salvatore V, Teti G, Focaroli S, Mazzotti MC, Mazzotti A, Falconi M. The tumor microenvironment promotes cancer progression and cell migration. *Oncotarget* 2016; **8**: 9608–16.

302 Kaltenmeier C, Simmons RL, Tohme S, Yazdani HO. Neutrophil Extracellular Traps (NETs) in Cancer Metastasis. *Cancers* 2021; **13**: 6131.

303 Baghban R, Roshangar L, Jahanban-Esfahlan R, *et al.* Tumor microenvironment complexity and therapeutic implications at a glance. *Cell Commun Signal* 2020; **18**: 59.

304 Shaul ME, Levy L, Sun J, *et al.* Tumor-associated neutrophils display a distinct N1 profile following TGFβ modulation: A transcriptomics analysis of pro- vs. antitumor TANs. *Oncoimmunology* 2016; **5**: e1232221.

305 Sionov RV, Fridlender ZG, Granot Z. The Multifaceted Roles Neutrophils Play in the Tumor Microenvironment. *Cancer Microenviron* 2014; **8**: 125–58.

306 Xia J, Zhang Z, Huang Y, Wang Y, Liu G. Regulation of neutrophil extracellular traps in cancer. *Int J Cancer* 2024; **154**: 773–85.

307 Shiao SL, Ganesan AP, Rugo HS, Coussens LM. Immune microenvironments in solid tumors: new targets for therapy. *Genes Dev* 2011; **25**: 2559–72.

308 Spiegel A, Brooks MW, Houshyar S, *et al.* Neutrophils suppress intraluminal NK-mediated tumor cell clearance and enhance extravasation of disseminated carcinoma cells. *Cancer Discov* 2016; **6**: 630–49.

309 Ozga AJ, Chow MT, Luster AD. Chemokines and the immune response to cancer. *Immunity* 2021; **54**: 859–74.

310 Tecchio C, Cassatella MA. Neutrophil-derived chemokines on the road to immunity. *Semin Immunol* 2016; **28**: 119–28.

311 Giese MA, Hind LE, Huttenlocher A. Neutrophil plasticity in the tumor microenvironment. *Blood* 2019; **133**: 2159–67.

312 Galdiero MR, Varricchi G, Loffredo S, Mantovani A, Marone G. Roles of neutrophils in cancer growth and progression. *J Leukoc Biol* 2018; **103**: 457–64.

313 Takeshima T, Pop LM, Laine A, Iyengar P, Vitetta ES, Hannan R. Key role for neutrophils in radiation-induced antitumor immune responses: Potentiation with G-CSF. *Proc Natl Acad Sci U S A* 2016; **113**: 11300–5.

314 Faraoni EY, O'Brien BJ, Strickland LN, *et al.* Radiofrequency Ablation Remodels the Tumor Microenvironment and Promotes Neutrophil-Mediated Abscopal Immunomodulation in Pancreatic Cancer. *Cancer Immunol Res* 2023; **11**: 4–12.

315 Kim R, Hashimoto A, Markosyan N, *et al.* Ferroptosis of tumour neutrophils causes immune suppression in cancer. *Nature* 2022; **612**: 338–46.

316 Sobottka B, Nowak M, Frei AL, *et al.* Establishing standardized immune phenotyping of metastatic melanoma by digital pathology. *Lab Invest* 2021; **101**: 1561–70.

317 Wang H, Lin X, Luo Y, *et al.* α-PD-L1 mAb enhances the abscopal effect of hypo-fractionated radiation by attenuating PD-L1 expression and inducing CD8+ T-cell infiltration. *Immunotherapy* 2019; **11**: 101–18.

318 Khan SY, Melkus MW, Rasha F, *et al.* Tumor-Infiltrating Lymphocytes (TILs) as a Biomarker of Abscopal Effect of Cryoablation in Breast Cancer: A Pilot Study. *Ann Surg Oncol* 2022; **29**: 2914–25.

319 Buchwald ZS, Nasti TH, Lee J, *et al.* Tumor-draining lymph node is important for a robust abscopal effect stimulated by radiotherapy. *J Immunother Cancer* 2020; **8**: e000867.

320 Mihaylov IB, Totiger TM, Giret TM, Wang D, Spieler B, Welford S. Toward prediction of abscopal effect in radioimmunotherapy: Pre-clinical investigation. *PloS One* 2021; **16**: e0255923.

321 Grass GD, Krishna N, Kim S. The immune mechanisms of abscopal effect in radiation therapy. *Curr Probl Cancer* 2016; **40**: 10–24.

322 Janopaul-Naylor JR, Shen Y, Qian DC, Buchwald ZS. The Abscopal Effect: A Review of Pre-Clinical and Clinical Advances. *Int J Mol Sci* 2021; **22**: 11061.

323 Daniel J Craig, Nisha S Nanavaty, Monika Devanaboyina, *et al.* The abscopal effect of radiation therapy | Future Oncology. *Future Oncol* 2021; : 1683–94.

324 Zhao X, Shao C. Radiotherapy-Mediated Immunomodulation and Anti-Tumor Abscopal Effect Combining Immune Checkpoint Blockade. *Cancers* 2020; **12**: E2762.

325 Wang D, Zhang X, Gao Y, *et al.* Research Progress and Existing Problems for Abscopal Effect. *Cancer Manag Res* 2020; **12**: 6695–706.

326 Naito S, von Eschenbach AC, Giavazzi R, Fidler IJ. Growth and metastasis of tumor cells isolated from a human renal cell carcinoma implanted into different organs of nude mice. *Cancer Res* 1986; **46**: 4109–15.

327 Strigari L, Mancuso M, Ubertini V, *et al.* Abscopal effect of radiation therapy: Interplay between radiation dose and p53 status. *Int J Radiat Biol* 2014; **90**: 248–55.

328 Buchwald ZS, Wynne J, Nasti TH, *et al.* Radiation, Immune Checkpoint Blockade and the Abscopal Effect: A Critical Review on Timing, Dose and Fractionation. *Front Oncol* 2018; **8**: 612.

329 Baba K, Nomura M, Ohashi S, *et al.* Experimental model for the irradiation-mediated abscopal effect and factors influencing this effect. *Am J Cancer Res* 2020; **10**: 440–53.

330 Burnette BC, Liang H, Lee Y, *et al.* The efficacy of radiotherapy relies upon induction of type i interferon-dependent innate and adaptive immunity. *Cancer Res* 2011; **71**: 2488–96.

331 Rodriguez-Ruiz ME, Rodriguez I, Garasa S, *et al.* Abscopal Effects of Radiotherapy Are Enhanced by Combined Immunostimulatory mAbs and Are Dependent on CD8 T Cells and Crosspriming. *Cancer Res* 2016; **76**: 5994–6005.

332 Habets THPM, Oth T, Houben AW, *et al.* Fractionated Radiotherapy with 3 x 8 Gy Induces Systemic Anti-Tumour Responses and Abscopal Tumour Inhibition without Modulating the Humoral Anti-Tumour Response. *PloS One* 2016; **11**: e0159515.

333 Dewan MZ, Galloway AE, Kawashima N, *et al.* Fractionated but not single-dose radiotherapy induces an immune-mediated abscopal effect when combined with anti-CTLA-4 antibody. *Clin Cancer Res Off J Am Assoc Cancer Res* 2009; **15**: 5379–88.

334 Dewan MZ, Vanpouille-Box C, Kawashima N, *et al.* Synergy of topical toll-like receptor 7 agonist with radiation and low-dose cyclophosphamide in a mouse model of cutaneous breast cancer. *Clin Cancer Res Off J Am Assoc Cancer Res* 2012; **18**: 6668–78.

335 Dovedi SJ, Cheadle EJ, Popple AL, *et al.* Fractionated Radiation Therapy Stimulates Antitumor Immunity Mediated by Both Resident and Infiltrating Polyclonal T-cell Populations when Combined with PD-1 Blockade. *Clin Cancer Res Off J Am Assoc Cancer Res* 2017; **23**: 5514–26.

336 Millar WT, Hopewell JW, Paddick I, *et al.* The role of the concept of biologically effective dose (BED) in treatment planning in radiosurgery. *Phys Medica PM Int J Devoted Appl Phys Med Biol Off J Ital Assoc Biomed Phys AIFB* 2015; **31**: 627–33.

337 Zhang Z, Liu X, Chen D, Yu J. Radiotherapy combined with immunotherapy: the dawn of cancer treatment. *Signal Transduct Target Ther* 2022; **7**: 258.

338 Mosmann TR, Cherwinski H, Bond MW, Giedlin MA, Coffman RL. Two types of murine helper T cell clone. I. Definition according to profiles of lymphokine activities and secreted proteins. *J Immunol Baltim Md 1950* 1986; **136**: 2348–57.

339 Chen B, Hou Q, Liu L, *et al.* A Comprehensive Exploration of Metabolism and Tumor Microenvironment and Immunotherapy Response: Evidence From Large Populations in Non-small Cell Lung Cancer. *Curr Cancer Drug Targets*; **24**: 46–58.

340 Shang Q, Yu X, Sun Q, Li H, Sun C, Liu L. Polysaccharides regulate Th1/Th2 balance: A new strategy for tumor immunotherapy. *Biomed Pharmacother* 2024; **170**: 115976.

341 Hui E, Cheung J, Zhu J, *et al.* T cell costimulatory receptor CD28 is a primary target for PD-1–mediated inhibition. *Science* 2017; **355**: 1428–33.

342 Ji W, Zhang B, Sun X, *et al.* Inhibition of tumor immune escape by blocking PD-1/PD-L1 engagement with dual-targeting molecularly imprinted polymer layer. *Cancer Nanotechnol* 2023; **14**: 51.

343 Beery AK, Zucker I. Sex bias in neuroscience and biomedical research. *Neurosci Biobehav Rev* 2011; **35**: 565–72.

344 Dayton A, Exner EC, Bukowy JD, *et al.* Breaking the Cycle: Estrous Variation Does Not Require Increased Sample Size in the Study of Female Rats. *Hypertens Dallas Tex 1979* 2016; **68**: 1139–44.

345 Yang C, Jin J, Yang Y, *et al.* Androgen receptor-mediated CD8+ T cell stemness programs drive sex differences in antitumor immunity. *Immunity* 2022; **55**: 1268-1283.e9.

346 Clayton JA, Collins FS. NIH to balance sex in cell and animal studies. *Nature* 2014; **509**: 282–3.

347 Hensel JA, Khattar V, Ashton R, Ponnazhagan S. Characterization of immune cell subtypes in three commonly used mouse strains reveals gender and strain-specific variations. *Lab Invest* 2019; **99**: 93–106.

348 Yuan Y, Liu L, Chen H, *et al.* Comprehensive Characterization of Molecular Differences in Cancer between Male and Female Patients. *Cancer Cell* 2016; **29**: 711–22.

349 Yang W, Warrington NM, Taylor SJ, *et al.* Sex differences in GBM revealed by analysis of patient imaging, transcriptome, and survival data. *Sci Transl Med* 2019; **11**: eaao5253.

350 Haupt S, Caramia F, Klein SL, Rubin JB, Haupt Y. Sex disparities matter in cancer development and therapy. *Nat Rev Cancer* 2021; **21**: 393–407.

351 Özdemir BC, Gerard CL, Espinosa da Silva C. Sex and Gender Differences in Anticancer Treatment Toxicity: A Call for Revisiting Drug Dosing in Oncology. *Endocrinology* 2022; **163**: bqac058.

352 Yu Y, Li A, Chen Y, *et al.* 1036P Patients' sex and PD-L1 expression jointly associated with overall survival benefits of immune checkpoint inhibitors in cancer. *Ann Oncol* 2020; **31**: S713.

353 Zheng S-Y, Cui H-J. 1041P Explore the efficacy of immune checkpoint inhibitors in non-small cell lung cancer patients of different gender. *Ann Oncol* 2020; **31**: S715.

8. Appendix

8.1 List of Figures

8.2 List of Tables